Role of extracellular zinc in the regulation of ion transport in airway and intestinal epithelium

Dissertation

Tamás Dankó M.D.

Semmelweis University, Ph.D. School
Basic Medical Science

Supervisor: Ákos Zsembery M.D., Ph.D.

Reviewers: János Magyar M.D., DSc.
László Köles M.D., Ph.D.

Exam board chair: Ildikó Horváth M.D., DSc.
Exam board members: Gábor Petheő M.D., Ph.D.
László Fodor Ph.D.

Budapest
2011

Table of contents

Abbreviations

$1,25(OH)_2D_3$	Vitamin D_3
ABC	ATP-binding cassette
ADA	Adenosine desaminase
ADO	Adenosine
AMP-PNP	5′-adenylyl-β,γ-imidodiphosphate
ASL	Airway surface liquid
ATP	Adenosine triphosphate
BAPTA	1,2-bis(o-aminophenoxy)ethane-N,N,N',N'-tetraacetic acid
CaCC	Calcium-activated chloride channels
CaMKII	Calmodulin kinase II
cAMP	Cyclic adenosine monophosphate
CAP	Channel activating protease
CaT1	Calcium transporter 1
CF	Cystic fibrosis
CFTR	Cystic fibrosis transmembrane conductance regulator
cGMP	Cyclic guanosine monophosphate
ClC	Voltage-gated Cl^- channel family
DIDS	4,4'-Diisothiocyano-2,2'-stilbenedisulfonic acid
DMEM	Dulbecco’s modified MEM medium
DMSO	Dimethyl-sulfoxide
DNA	Desoxyribonucleic acid
EDTA	Ethylene diamine tetraacetic acid
EGTA	Ethylene glycol tetraacetic acid
ENaC	Amiloride-sensitive epithelial sodium channel
FBS	Foetal bovine serum
*Fr*ECaC	Epithelial calcium channel from *Fugu rubripes*
GABA	γ-aminobutyric acid
GI	Gastrointestinal
HEK293	Human embryonic kidney cells
HEPES	4-(2-hydroxyethyl)-1-piperazineethanesulfonic acid

HRP	Horseradish peroxidase
hTRPV6	Human transient receptor potential channel vanilloid type 6
IB3-1	CF human bronchial epithelial cell line
IP_3	Inositol trisphosphate
MCC	Mucociliary clearance
NBD	Nucleotide binding domain
NCX1	Na^+/Ca^{2+}-exchanger
NFA	Niflumic acid
NHE	Na^+/H^+-exchanger
NKCC1	Na^+-K^+-$2Cl^-$-cotransporter
NMDA	N-Methyl-D-aspartate
NMDG	N-methyl-D-glucamine
NPPB	5-Nitro-2-(3-phenylpropylamino) benzoic acid
NSP4	Rotavirus enterotoxin
*Om*ECaC	Epithelial calcium channel from rainbow trout gill
*Om*SLC39A1	Epithelial zinc transporter from rainbow trout gill
PBS	Phosphate buffered saline
PCL	Periciliary layer
PIP_2	Phosphatidylinositol-4,5-bisphosphate
PIV	Parainfluenza virus
PKA	Protein kinase A
PKC	Protein kinase C
PMCA1b	Plasma membrane Ca^{2+}-ATPase
PNGase F	Native glycoaminidase from *Flavobacterium meningosepticum*
RD	Regulatory domain
RFP	Red fluorescence protein
RNA	Ribonucleic acid
ROC	Receptor-operated channels
ROI	Region of interest
ROMK1	Inwardly rectifying K^+ channel
RSV	Respiratory syncytial virus
SDS	Sodium dodecyl sulfate

SGLT1	Na^+-glucose-cotransporter
SOC	Store-operated channels
TM	Transmembrane domain
TRIS	Tris(hydroxymethyl)aminomethane
TRPA	Transient receptor potential channel ankyrin type
TRPM	Transient receptor potential channel melastatin type
TX-100	Triton-X 100
VIP	Vasoactive intestinal peptide
VRAC	Volume-regulated anion channels
YFP	Yellow fluorescence protein
ZIP4	Zrt- and Irt-like protein 4, SLC39 family
ZnT1	Zinc transporter 1, SLC30 family
ΔF508	Mutation with a phenylalanine missing at position 508

1. Introduction

1.1. Zinc: a trace element with versatile functions

Zinc is an important trace element that belongs to the IIb transition metal group. It is one of the most widely utilized biometal in the human body because of its physical and chemical properties that enables it to interact with a variety of proteins and enzymes. Zn^{2+} is an important component of the catalytic site of several metalloenzymes such as alkaline phosphatase and alcohol dehydrogenase. Also, it is a crucial structural component of hundreds of "zinc finger"-containing proteins. Accordingly, Zn^{2+} plays a fundamental role in a number of physiological processes, including growth and development, inflammation and tissue repair [1]. Zn^{2+} is also important for cell proliferation because it stabilizes the structure of DNA and RNA, and also acts as a vital cofactor of many enzymes required for DNA and RNA synthesis. Additionally, some of the zinc-finger proteins enhance gene transcription, such as transcription factor IIIa [2].
Furthermore, Zn^{2+} is an allosteric modulator of a wide variety of ion channels, potentiating or inhibiting their activity [3, 4]. Channels that are affected by extracellular Zn^{2+} include voltage-dependent Na^+ [5, 6], K^+ [7, 8] and Ca^{2+} [9, 10] channels, as well as two-pore K^+ channels [11, 12], acid-sensitive ion channels [13], epithelial Na^+ channels [14], transient receptor potential melastatin type 1 (TRPM1) [15] and type 2 (TRPM2) [16] channels. Zn^{2+} is also a potent modulator of ionotropic receptors for γ-aminobutyric acid (GABA) [17, 18], glycine [19], 5-hydroxytryptamine [20], glutamate [21, 22] and ATP [23-26]. Zn^{2+} may inhibit different chloride channels, such as voltage-gated and calcium-activated chloride channels [4, 27-31]. Voltage-gated, highly selective H^+ channels are also inhibited by extracellular Zn^{2+} [32-34].
On the other hand, extracellular Zn^{2+} activates the transient receptor potential vanilloid type 1 (TRPV1) channels, which represents a mechanism underlying metallic taste [35]. It is noteworthy that intracellular Zn^{2+} can also influence ion channel activity. As such, large conductance Ca^{2+}-activated K^+ channels are activated by cytosolic Zn^{2+} [36]. Pancreatic K_{ATP} channels might be opened by Zn^{2+} from both the extracellular and intracellular side [37].

Furthermore, Zn^{2+} has been shown to permeate the ionotropic receptors for glutamate [38] and the nicotinic acetylcholine receptor [39, 40]. Zn^{2+} is also permeable for voltage-dependent Ca^{2+} [40-42], TRPM3 [43] and TRPM7 channels [44, 45]. Consequently, TRPM7 channels play a role in mediating Zn^{2+} neurotoxicity [44].

In the blood, Zn^{2+} is transported by albumin (70%) and α_2-macroglobulin (30%) [1]. About 99% of total body Zn^{2+} is intracellular, and exists in two main states: a bound form associated with metalloproteins and zinc-finger proteins, and a labile form that is only loosely bound to proteins [46]. Approximately 30-40% of the total cellular Zn^{2+} resides in the nucleus, 50% in the cytoplasm and its organelles, whereas the remainder is localized in the cell membrane. Zn^{2+} is excreted from the body through different organs including GI tract, pancreas, kidneys, liver and skin. Since Zn^{2+} homeostasis is tightly regulated, chronic disorders due to excessive accumulation of Zn^{2+} rarely occurs. In contrast, acute Zn^{2+} toxicity is manifested by nausea, vomiting, diarrhea, headache, and abdominal cramps [1].

1.2. Physiology of transepithelial ion transport

Epithelial cells form dynamic interfaces between different physiological compartments. Despite the wide range of specific functions that epithelial cells perform in different tissues, they share common characteristics as covering and protecting surfaces exposed to injury by providing a physical barrier. Furthermore, they maintain tissue homeostasis by allowing the regulated transport of solutes, electrolytes and water across them. Concerning the latter function, there is a remarkable consistency in the mechanisms used by the cells. Epithelial tissue is built up of polarized cells, with apical surface facing the lumen or external world while the basolateral membrane faces the internal environment. This structure is achieved by uneven distribution of membrane proteins along the apico-basal axis. The net transport of solutes, ions and water across the epithelial layer is then accomplished by the coordinated action of ion channels, transporters and pumps in the apical or basolateral membrane.

Bidirectional transport of Na^+ and Cl^- is one of the main functions of epithelial tissue in the gastrointestinal (GI) system and kidney to achieve proper body fluid homeostasis and is also essential for the maintenance of airway surface liquid (ASL) that represents the primary protective mechanism against infections in the airways. Epithelial transport

processes are governed by a large number of hormones, neurotransmitters and local factors, e.g. acetylcholine, epinephrine, aldosterone, vitamin D_3, prostaglandin E_2, vasoactive intestinal peptide (VIP), secretin and elements of the recently established purinergic signaling cascade (ATP, adenosine). These regulatory pathways mainly utilize two types of intracellular messengers: cyclic adenosine monophosphate (cAMP) and calcium (Ca^{2+}) [47] (Fig. 1.).

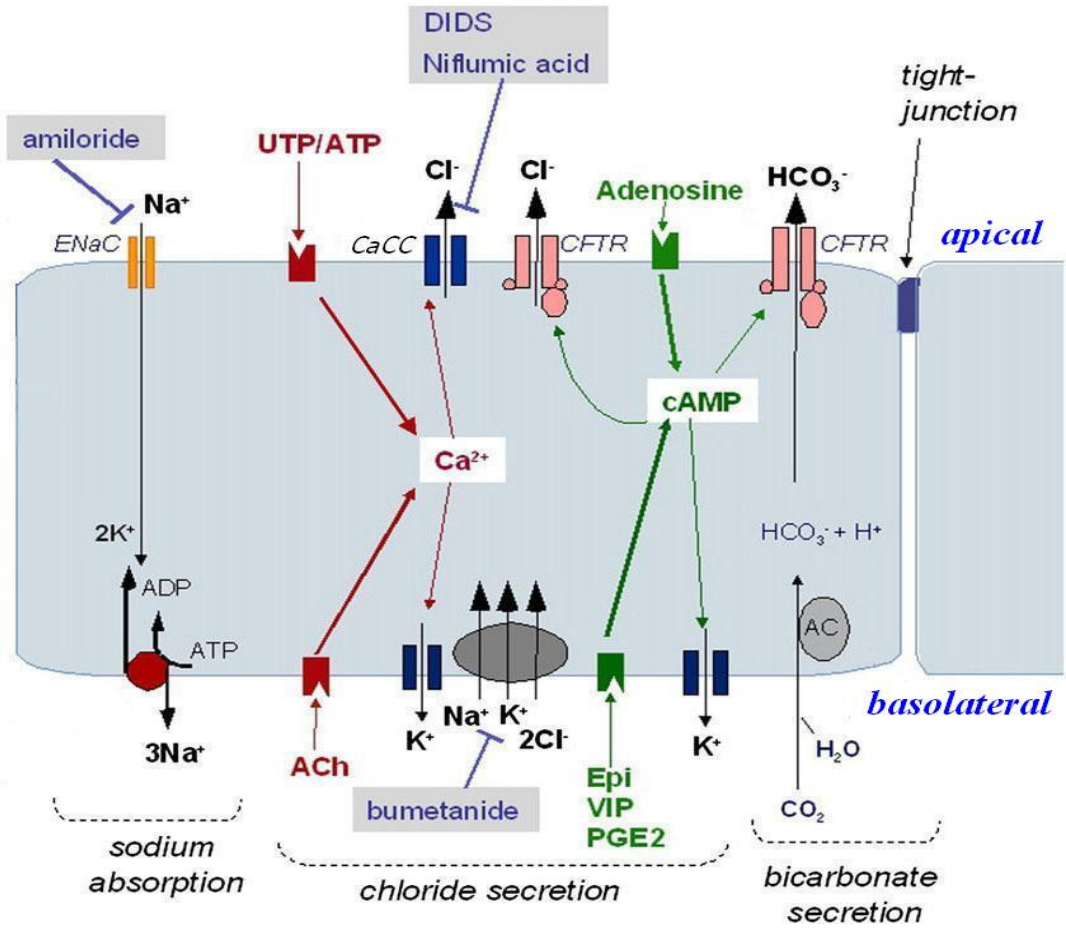

Figure 1. Summary of the most important epithelial Na^+ and Cl^- transport systems. Na^+ enters the cell through ENaC channel in the apical membrane of the epithelium and leaves the cell mainly through the Na^+-K^+-ATPase in the basolateral membrane. Cl^- enters the cell through the NKCC1-cotransporter in the basolateral membrane and leaves the cell at the apical membrane either through CFTR or through a Ca^{2+}-dependent Cl^- channel (CaCC). Consequently, Cl^- secretion can be divided into a Ca^{2+}-activated system (in red) and a cAMP-dependent system (in green). Ca^{2+} mobilizing agonists acting on apical or basolateral membrane receptors are shown, such as P2Y receptor activated by ATP or UTP and the muscarinic acetylcholine receptor activated by acetylcholine (ACh). Similarly, agonists that increase cAMP levels include adenosine, epinephrine (Epi), prostaglandin PGE_2, or vasoactive intestinal peptide (VIP). Additionally, bicarbonate permeates CFTR that is formed by carbonic anhydrase (AC). Parallel activation of basolateral Ca^{2+}- and/or cAMP-dependent K^+ channels provide the driving force required for Cl^- secretion. Grey boxes indicate inhibitors for some channels or transporters (Modified after Ref. [47]

1.3. cAMP-regulated epithelial ion transport mechanisms in the airways

1.3.1. The CFTR protein

Mammalian anion channels can be subdivided into five classes according to their gating mechanism: the phosphorylation-regulated Cystic Fibrosis Transmembrane conductance Regulator (CFTR) channel, Ca^{2+}-activated Cl^- channels (CaCCs), voltage-gated Cl^- channels (ClCs), ligand-gated Cl^- channels (GABA and glycine-activated) and volume-regulated anion channels (VRACs) [48]. The CFTR protein is the only known member of the ATP-Binding Cassette (ABC) transporter superfamily that acts as an ion channel. It is the most dominant anion channel in several epithelial tissues, including sweat ducts, small pancreatic ducts, epithelium in the reproductive tract, lung epithelia, intestinal crypts and the epithelia of kidney tubules. Localization of CFTR by immunological techniques has revealed that the protein appears to be restricted to the apical membrane. The cell and tissue distribution of the CFTR anion channel is consistent with a vectorial ion transport system across the epithelium [47]. CFTR is also expressed in the heart [49] and in the central nervous system [50], but its functional importance has not yet been fully elucidated.

As most members of the ABC superfamily, CFTR is composed of a motif containing a transmembrane domain (TMs) with 6 transmembrane segments and an intracellular nucleotide binding domain (NBD). This motif is repeated twice, with the first motif linked to the second by a regulatory domain (RD) in the large third intracytoplasmic loop that contains a considerable number of putative phosphorylation sites [51] (Fig. 2A).

CFTR is activated by phosphorylation at multiple sites located at the RD by protein kinase A (PKA), and probably also by protein kinase C (PKC) [52]. Consequently, CFTR channel is often referred to as a "cAMP-activated channel", because channel phosphorylation by PKA is obligatory for channel activity. Activation of adenylate cyclase enzyme by G-protein linked hormone pathways including glucagon, epinephrine, acetylcholine, secretin, VIP [53] or adenosine (ADO) [54] results in the cellular production of cAMP. Similar effect can be obtained directly by using forskolin or membrane permeable cAMP analogues. The most accepted model of CFTR gating

proposes that in phosphorylated channels and in the presence of ATP the two NBDs can dimerize and together form two binding sites for ATP [55, 56]. Binding of ATP at the two sites leads to a conformational change at the level of the TM domains that in turn leads to channel opening. Subsequently, hydrolysis of ATP by the enzymatic activity of the second NBD site terminates the transport cycle (Fig. 2B) [55-57].

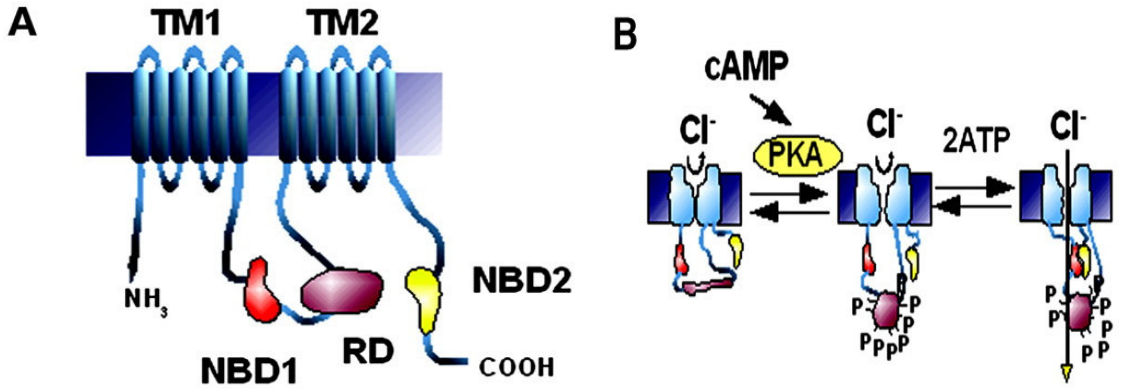

Figure 2. (A) Schema of CFTR topology in the cell membrane. TM1 and TM2: transmembrane domains; NBD1 and NBD2: nucleotide binding domains; RD: regulatory domain **(B)** Activation of CFTR channels. The cAMP-dependent activation of protein kinase A (PKA) phosphorylates the RD of inactive CFTR, causing a change in conformation. The binding of ATP to the NBDs induces a second conformational change that opens the channel pore [47].

Interestingly, the energy of ATP hydrolysis is not used up for transporting anions, since phosphorylated CFTR channels can be activated by non-hydrolysable ATP analogues, such as 5′-adenylyl-β,γ-imidodiphosphate (AMP-PNP) as well [57, 58]. Accordingly, when CFTR pore opens, the flux of anions across the cell membrane is predominantly determined by the electrochemical driving forces [59].

In addition to its channel function, there is growing evidence that CFTR also regulates other ion channels and transporters, such as outwardly rectifying Cl^- channels [60, 61], amiloride-sensitive Na^+ channels [62, 63], inwardly rectifying K^+ channels (ROMK1) [64, 65], the Cl^-/HCO_3^- exchanger [66] and the Na^+-HCO_3^--cotransporter [67, 68].

The mechanisms by which CFTR regulates other channels are still unclear. It may involve either a direct association of CFTR protein with other channel proteins [69], or via molecules that interact with CFTR's C-terminal PDZ (postsynaptic density protein, disc-large, ZO-1)-domain binding motif, such as the NHERF adaptor proteins [64, 70-72]. Additionally, an indirect relation is also presumable, as it is clearly suggested for CFTR's influence on outward rectifier Cl^- channels [73].

1.3.2. Liquid transport in normal airways

Normal airway surface liquid of conductive airways is thought to be organized into two compartments: a low-viscosity periciliary layer (PCL, approx. 7 μm in height) that permits ciliary beating, upon which rests a hydrated mucus layer (1% salt; 1% mucin; 98% water) that traps inhaled particles and pathogens. Mucus is produced by submucosal glands and superficial goblet cells in the proximal airways, whereas by Clara cells in distal airways. During the transport of mucus, both layers are conveyed in a cephalic direction at approximately equal velocities by the propulsive activity of cilia [74]. Additionally, the mucus layer serves as a passive liquid reservoir for ensuring optimal PCL height. This special structure maintains the normal mucociliary clearance (MCC) which is the primary line of defense against bacterial infections in the airways [75-77] (Fig. 3A).

The hydration of airway surface is principally determined by the mass of salt (NaCl) in the ASL [78]. Due to the fact that airway epithelium is highly permeable to water, the ionic composition of ASL is rigorously maintained in a near-isotonic state [79, 80]. The mass of salt on airway surfaces is regulated by passive mechanisms caused by the movement of liquid along airway surfaces as well as active ion transport located within the airway epithelia [81].

As it was previously mentioned, the volume of PCL is maintained at a physiologically relevant height, defined by the length of the outstretched cilia. In normal human airways, an “excess” PCL volume (that might mimic the volume found at the convergence point of two small airways to form one larger airway) is rapidly absorbed by the epithelia by active volume absorption processes until a steady state is reached. [82]. Studies using transepithelial potential difference (PD) measurements have revealed that the rapid absorption of excess PCL is mediated by amiloride-sensitive Na^+ channels (ENaC) [75]. The Na^+ that enters the cell exits via the basolateral Na^+-K^+-ATPase. Cl^- follows passively through the paracellular pathway. As PCL volume approaches the physiologic height, the amiloride-sensitive Na^+ absorption is reduced. This inhibition of ENaC enhances Cl^- secretion by hyperpolarizing the apical membrane that generates the necessary electrical driving force for Cl^- exit into the ASL. Chloride may be primarily secreted from the cell by the apical membrane CFTR Cl^- channel and partially by the

Ca^{2+}-activated Cl^- channel (CaCC) [83, 84]. Cl^- enters the cell principally via the Na^+-K^+-$2Cl^-$-cotransporter at the basolateral membrane (Fig. 1. and Fig. 3B).

The mechanism how ASL volume is sensed by airway epithelia is not yet fully understood. The possible role for surface cilia as a "mechanosensor" could be excluded, since both in cultured cells with immotile cilia or poorly differentiated cells with no cilia were still able to regulate ASL volume normally [54].

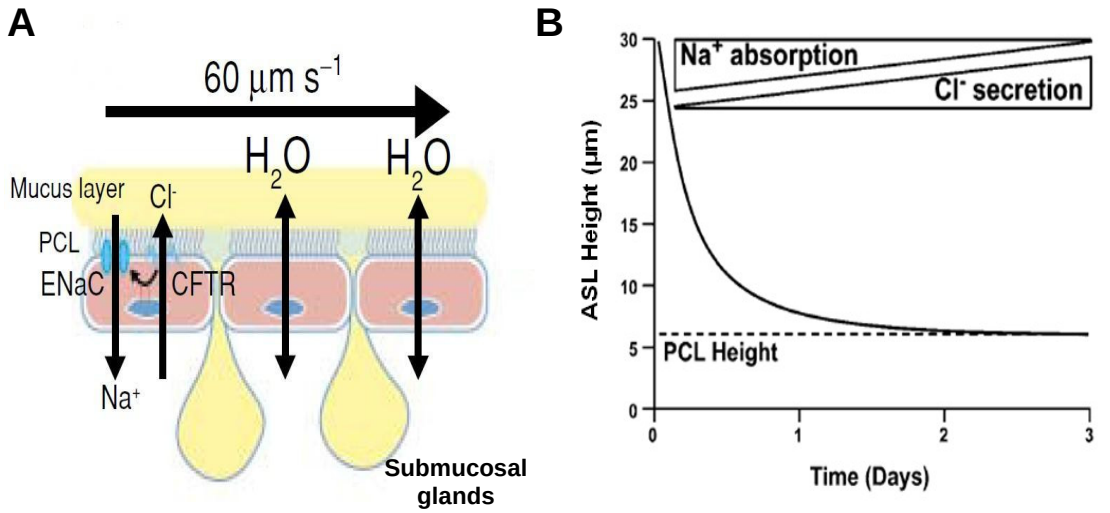

Figure 3. (A) Mucociliary clearance in normal airways [85]. **(B)** Regulation of PCL volume by active ion transport following a challenge with excess PCL volume. In this model system, all mucus was removed from the surface of the cultured cells to principally measure the PCL compartment of ASL by confocal microscopy. Horizontal bar represents relative magnitudes of Na^+ absorption vs. Cl^- secretion measured by transepithelial potential difference studies. Steady-state PCL height (7 µm, approximating the length of the outstretched cilia) is maintained by continuous Cl^- secretion through CFTR that is outweighed by a modest rate of Na^+ absorption through ENaC [86].

It is likely that the information that controls the activity of these apical channels is encoded within the PCL itself in the form of soluble "reporter molecules" that are sensed by "chemosensors" on the extracellular side of the apical membrane [54]. Possible candidates might include adenosine (ADO) that regulates CFTR via stimulation of the A_{2b} subtype of ADO receptors and cell attached channel activating proteases (CAPs) [87] and endogenous CAP inhibitors that regulate the activity of ENaC [88, 89]. In the presence of an excess PCL volume, any soluble regulatory molecules such as ADO or secreted CAP inhibitors are diluted. As a result, CFTR is inactive due to the lack of stimulation by ADO and anion secretion does not occur. On the other hand, ENaC activity is close to maximal due to activation by proteases in the absence of CAP inhibitors, leading to Na^+-driven isotonic PCL absorption with Cl^-

following passively through the paracellular pathway **(**Fig. 4A). As the excess liquid is absorbed over time, ADO and CAP inhibitors accumulate in the PCL sufficiently to activate CFTR and to inactivate ENaC via inhibition of CAPs. Furthermore, activated CFTR appears to exert an additional inhibitory effect on ENaC by either direct [69, 90] or indirect [64] molecular interactions (Fig. 4B). The role of active ion secretion is further supported by the addition of bumetanide, which blocks basolateral Cl^- uptake via Na^+-K^+-$2Cl^-$-cotransporter (see Fig. 1.) and causes PCL volume depletion (Fig. 4C). Similar result can be achieved with the cationophore nystatin that bypasses the inhibited ENaC and reestablishes Na^+-driven PCL absorption (Fig. 4D). This emphasizes that physiological inhibition of ENaC is also required for maintenance of a steady-state PCL height [54].

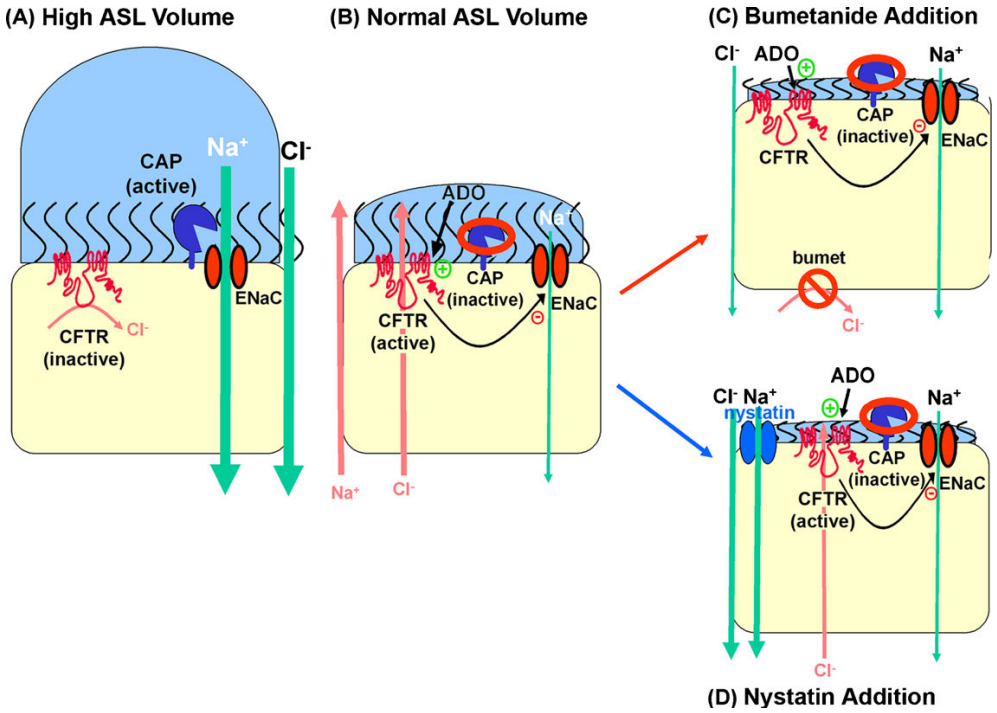

Figure 4. Normal ASL volume regulation under static conditions. **(A)** In normal airways under high volume conditions, CFTR is inactive and ENaC is near to fully active, leading to Na^+-led isotonic ASL absorption with Cl^- following through the paracellular pathway. **(B)** As ASL volume decreases, CFTR becomes activated due to stimulation of A_{2b} receptors by adenosine (ADO), whereas ENaC inactivates due to inhibition of channel-activating proteases (CAPs) by the accumulated protease inhibitors (red circles). This leads to a steady state ASL height (7µm). **(C)** To confirm pharmacologically the active ion transport in the maintenance of steady state ASL height, bumetanide can be applied serosally which results in ASL collapse to CF levels (i.e. 3–4 µm). **(D)** Similar result can be achieved by the addition of the cationophore nystatin that leads to uncontrolled Na^+-led ASL absorption and ASL collapse [91].

Data from novel *in vitro* techniques using well-differentiated airway cell culture models coupled to confocal microscope have revealed that there may be additional factors that regulate PCL height. These techniques have the advantage of being capable to study airway epithelial cells under near physiologic conditions, such as intact native ASL and intermittent shear stress mimicking tidal breathing, respectively [92].

Upon exposure to phasic shear stress, normal airway cultures increased PCL height to approximately 14 µm (Fig. 5.). This increase in PCL height was due to the appearance of an additional Cl^- secretory pathway which was absent under static conditions. In normal airway epithelia, phasic shear stress is able to stimulate relatively large increases in nucleotide release into the ASL [82]. The higher ATP concentration (from the low nanomolar range to the 30-50 nM range) in the ASL is sufficient to activate the $P2Y_2$ purinergic receptors which stimulate CaCC-mediated Cl^- secretion. Additionally, ATP is also degraded to ADO by ecto-nucleotidases and ecto-apyrases located in the apical membrane which further increases the activity of CFTR via activation of A_{2b} receptors [93]. Indeed, the importance of both Cl^- secretory pathways in the regulation of the ASL homeostasis has been confirmed in normal airway epithelia [82]. It is also known that phasic shear stress inactivates Na^+ absorption which is also favorable for the secretion of Cl^-. There are multiple explanations for this latter observation. First, activation of the $P2Y_2$ receptor results in the depletion of PIP_2, a molecule whose presence is necessary for ENaC activation [94]. Second, due to the interactions between ENaC and the intracellular domains of CFTR, the increased activity of CFTR may lead to increased inhibition of ENaC [69, 90]. Third, it is possible that shear stress induces the increased release of CAP inhibitors which prevent CAP-mediated activation of ENaC [91]. The importance of ATP and ADO signaling in the maintenance of ASL volume under phasic motion condition is underscored by the effects of sequential application of apyrase and adenosine desaminase (ADA, an enzyme that degrades ADO) (Fig. 5.).

Additionally, the excess volume of PCL achieved by ATP-dependent activation of liquid transport is presumably stored in the mucus layer, which serves as a liquid reservoir for the PCL in vivo [75].

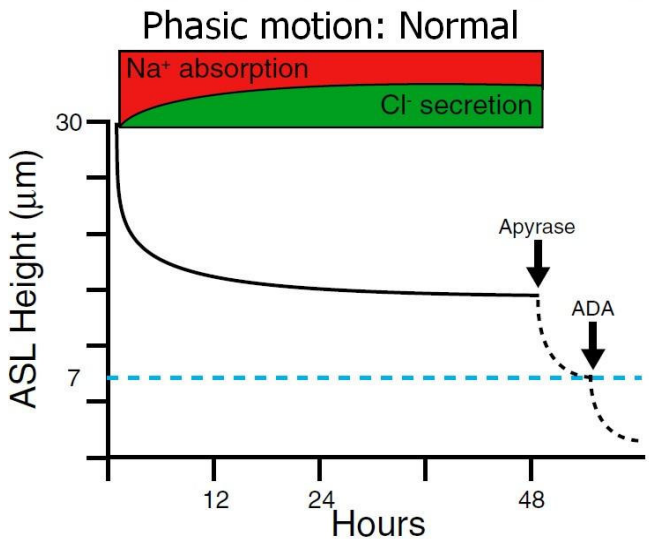

Figure 5. Regulation of airway surface liquid (ASL) volume by normal cultured bronchial epithelia under phasic motion culture conditions that reprise the periodicity and shear stresses observed with tidal breathing in vivo. Dashed line represents physiologically relevant ASL height, defined as the height (volume) consistent with normal mucus transport. Arrows depict luminal additions of pharmacologic probes. ADA: adenosine desaminase [85]

1.3.3. Cystic fibrosis

Cystic fibrosis (CF) is the most common lethal genetic disease in the Caucasian population. The CFTR gene is a large, ~250 kb gene that is located on the long arm (q) of chromosome 7 at position 31.2. [95]. Mutations in the CFTR gene are inherited by an autosomal recessive manner. To date, more than 1400 mutations in the CFTR gene [96] have been identified. The most common mutation, that accounts for more than 70% of all CF cases, is a three base pair deletion that leads to the absence of a phenylalanine at position 508 of the CFTR protein (designated as ΔF508). The ΔF508 CFTR protein lacks normal maturation and fails to traffic to the apical membrane that leads to the absence of functioning CFTR proteins in the apical plasma membrane and loss of ion transport activities. Other mutations may produce non-functioning CFTR channels at the apical membrane or a mutant CFTR with abnormal ion permeation characteristics. [97]. Consequently, the classic CF phenotype involves the functional failure of multiple organs (e.g. pancreas, lungs, sweat glands, GI tract and the reproductive system), although lung manifestations are still the prevailing source of both morbidity and mortality.

1.4. Ca^{2+}-regulated epithelial ion transport mechanisms in the airways

1.4.1. The Calcium-activated Chloride Channel

The calcium-activated chloride channels (CaCCs) are anion-selective channels that are activated by increases in cytosolic Ca^{2+} [48]. CaCCs were first described in *Xenopus* oocyte [98] and subsequently they have been identified in various cell types such as epithelial cells, vascular endothelial cells, neurons, smooth and cardiac muscle cells. Their broad expression in mammalian cells are related to the control of the most diverse physiological functions, including epithelial fluid secretion, oocyte fertilization, olfactory-, taste- and phototransduction, neuronal and cardiac excitability, smooth muscle contraction and endothelial function [99, 100].

Although CaCCs have been functionally well characterized in the last three decades, their molecular identity has remained to be elucidated. Based on data from electrophysiological measurements, at least four types of CaCCs have been suggested in different cell types. Until recently, the lacks of highly specific inhibitors or antibodies against CaCCs as well as an appropriate expression system have hampered the approaches to biochemically purify/identify the CaCC protein. At present, there are five molecular candidates that are proposed to be CaCCs: the calcium activated chloride channel ClCA family proteins [84], the ClC3 channel [101], the bestrophin family (BEST1–BEST4) [102-104], Tweety (a Ca^{2+}-regulated maxi Cl^- channel) [105]and most recently, TMEM16A or anoctamin-1 [106-108]. To date, bestrophins were the most promising candidates for Ca^{2+}-activated Cl^- channels. However, currently available data are contradictory in relation to their involvement in Ca^{2+}-dependent chloride channel activity [109-111]. As it was recently highlighted, bestrophins are likely to be multifunctional proteins, just as the CFTR, and exert their functions not only as a Cl^- channel but also as a regulator of other ion channels, such as voltage-gated Ca^{2+} channels [112, 113]. Furthermore, impaired chloride conductance appears to play only a minor role in the pathophysiology of bestrophin disorders [114].

In contrast, TMEM16A is a membrane localized protein that has been proposed as the major component of the CaCCs. TMEM16A (anoctamin 1, ANO1) belongs to a family of 10 TMEM16-proteins (TMEM16A-K, ANO 1–10). TMEM16A has eight

transmembrane domains (TMs) with a putative pore forming region between TM5 and TM6. Importantly, it is not clear how TMEM16A is regulated by intracellular Ca^{2+}, as the cytosolic parts do not possess any obvious binding sites for Ca^{2+}. Nevertheless, they carry several consensus sites for different kinases [106, 108]. TMEM16A is broadly expressed in mammalian tissues, including airway, intestinal and glandular epithelia, smooth muscle cells as well as interstitial cells of Cajal in the GI tract [115-117]. Data from a recently developed animal model emphasized the importance of TMEM16A-mediated Cl^- secretion in the maintenance of proper epithelial functions. In TMEM16A null mice, accumulated mucus was found in the lumen of their tracheas indicating impaired MCC [118]. Additionally, TMEM16A null animals died early in the postnatal period due to pronounced tracheomalacia which was believed to be the consequence of improper stratification of the embryonic tracheal epithelium [119]. Interestingly, in a very recent study the TMEM16A-mediated Cl^- conductance appeared to be only a minor contributor to total CaCC conductance in human airway and intestinal epithelium suggesting a role for an unidentified CaCC in these cells [120].

Apart from their possible molecular diversity, CaCCs share some common functional characteristics, including sensitivity to calcium, slow activation with depolarization, higher permeability to I^- than Cl^- as well as inhibition by DIDS, NPPB and niflumic acid (NFA). They also demonstrate a characteristic voltage dependence that is modulated by intracellular Ca^{2+}. As it was thoroughly analyzed in *Xenopus* oocytes [121], at subsaturating Ca^{2+} concentrations (< 1μM) the channels are inactivated at negative membrane potentials while activated at positive potentials resulting in an outwardly rectifying current-voltage relationship. On the other hand, at saturating Ca^{2+} concentrations, the channels are fully activated at all membrane potentials and the current-voltage relationship becomes linear.

Activation of CaCCs requires cytosolic Ca^{2+} concentrations ($[Ca^{2+}]_i$) in the range of 0.2-5μM. The increase in $[Ca^{2+}]_i$ that activates CaCCs can be a result of either Ca^{2+} influx or Ca^{2+}-release from IP_3-dependent intracellular stores [99]. CaCC activation may involve direct Ca^{2+}-binding as in *Xenopus* oocytes, vascular endothelial cells and parotid acinar cells [121-123]. Although this mechanism is still not fully understood, the observation that some CaCCs can be stably activated under experimental conditions by Ca^{2+} in the absence of ATP, further justifies the existence of a direct gating mechanism.

In other cell types, Ca^{2+}-dependent phosphorylation by calmodulin kinase II (CaMKII) is necessary to open the channel, as it is the case in intestinal epithelial cells [124]. These cell-type-dependent differences in the regulatory pathways also suggest the existence of more than one CaCC isoform.

Cl^- efflux through activated CaCCs mainly depends on two factors: the membrane potential and the Cl^- concentration gradient. Since the chemical gradient is usually unfavorable, therefore a facilitating change in the membrane potential is required to initiate Cl^- secretion. Following an increase in cytoplasmic calcium, the synchronous activation of Ca^{2+}-sensitive K^+ channels may lead to hyperpolarization of the cell providing the necessary electrical driving force for Cl^- efflux via CaCCs. If activation of CaCCs exceeds that of the K^+ channels, depolarization occurs. The final consequences are cell-type specific, including Cl^- secretion in epithelial cells or action potential generation in olfactory receptor neurons [48] (Fig. 6.).

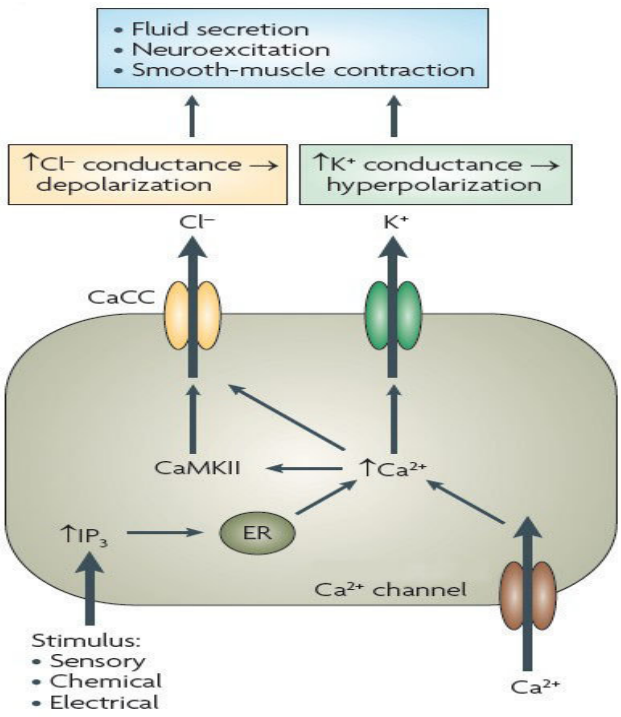

Figure 6. Cellular roles of CaCCs. Stimuli that elevate cytoplasmic calcium result in CaCC activation, either directly or through calcium/calmodulin kinase II (CaMKII)-mediated phosphorylation. Activation of CaCCs in a concerted way with K^+ channels leads to either depolarization or hyperpolarization of the plasma membrane which in turn modulates fluid secretion, neuroexcitation and smooth-muscle contraction. Modified after Ref. [48]

1.4.2. Liquid transport in CF airways

In humans, the CF airway epithelium fails to adequately hydrate the mucus layer on their surfaces, particularly in response to infectious challenges. The lack of mucus hydration leads to reduced MCC due to increased viscosity of the ASL [125], adhesion of mucus to airway surfaces, and chronic bacterial infections of the airways [77]. Due to the absence or dysfunction of the cAMP/PKA-regulated CFTR channels, CF airway epithelia exhibit reduced capacity to secrete Cl^- and/or HCO_3^- and also increased Na^+ absorption that contributes to the dehydration of the ASL above the airway epithelial cells [126]. The role of airway surface dehydration in CF-like lung disease was underscored in an *in vivo* animal model by overexpressing the β-subunits of the epithelial Na^+ channel in mice [127]. Data from these experiments demonstrated a threefold increase in Na^+ absorption compared to controls whereas the rate of Cl^- secretion was unchanged. Furthermore, neutrophilic inflammation and goblet cell hyperplasia could also be observed in the airways of these animals which are characteristic of CF lung disease. Accordingly, the imbalance between absorption and secretion resulted in the depletion of ASL volume followed by mucus stasis, inflammation of the airways and death prior to weaning in ~ 50% of transgenic animals. These results provided persuasive evidence that the disturbance in the balance between Na^+ absorption and Cl^- secretion could play pivotal role in causing dehydration of the airway surface and inducing inflammation that is typical of CF lung disease.

In contrast to normal epithelium, CF airway epithelium is unable to regulate PCL volume under static conditions, and it collapses to a height (approximately 3 μm) which is incompatible with efficient mucus transport [82, 128]. In CF airways, a challenge with an “excess” PCL volume leads to the dilution and inefficiency of the soluble regulatory molecules (ADO and/or secreted CAP inhibitors), just as in normal airways. Due to the lack of CFTR in the apical membrane, its inhibitory effects on ENaC are absent which result in increased rate of Na^+ absorption compared to that in normal airways, with Cl^- following paracellularly. As PCL volume diminishes, ADO accumulates sufficiently to activate A_{2b} receptors, but in the absence of CFTR the consequent rise in intracellular cAMP will further stimulate ENaC rather than inactivate it [82, 129]. Additionally, in CF, the CAP/CAP inhibitor system is also likely to be

defective despite the reduction in the PCL volume, which maintains ENaC in a proteolytically cleaved, and as such, in a constitutively active form [130]. Thus, the shift from Na^+ absorption to Cl^- secretion, that is characteristic for normal airway epithelia, is absent from CF airways and ASL volume depletion results [82] (Fig. 7.). These findings are further supported by the fact that the administration of bumetanide and/or nystatin (two agents that cause a collapse of ASL volume in normal airways, see earlier) is without effect in CF cultures, since these cells already lack the proper regulatory mechanisms necessary for the maintenance of normal ASL volume [54].

Data from *in vitro* studies proposed that in the CF lung, adequate MCC would disappear within 24-48 hours [128]. However, CF patients are born with sterile lungs and it takes months to years for the disease to develop in its typical form with mucus plugs and bacterial colonization (e.g. *Pseudomonas aeruginosa*). It is hypothesized that phasic motion, induced by tidal breathing is the missing regulatory factor *in vivo* that prevents CF epithelia from early development of pulmonary disease.

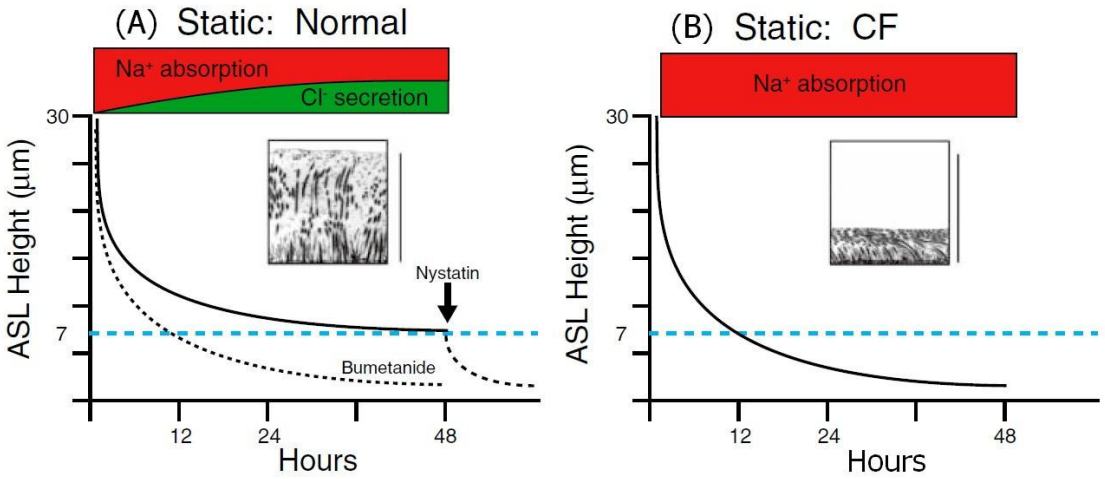

Figure 7. Regulation of airway surface liquid (ASL) volume by normal **(A)** and CF **(B)** cultured bronchial epithelia under static motion culture conditions. Dashed line represents normal ASL height. Insets illustrates perfluorocarbon-osmium fixed bronchial preparations 48 h after the addition of "excess" ASL volume (scale bar = 7 µm). Arrow depicts luminal addition of pharmacologic probe [85].

Indeed, in CF cultures phasic shear stress increases PCL volume to ~7 µm in contrast to the height of ~3 µm that is observed under static conditions. Although this height is approximately half the value that can be observed in normal airway cultures, it is now eligible to maintain sufficient mucus clearance [82]. This phenomenon indicates that shear stress activates a "salvage" pathway for Cl^- secretion and also suggests a

mechanism for the inhibition of Na^+ absorption in CF epithelium (Fig. 8.). Consequently, the mechanical stress that impacts airway epithelia during normal breathing leads to the release of large quantities of ATP in both normal and CF cultures [131-133]. Upon reaching the threshold concentration in the ASL, ATP interacts with mucosal $P2Y_2$ receptors leading to the activation of PLC and hydrolysis of phosphatidylinositol-4, 5-bisphosphate (PIP_2). The local depletion of PIP_2 inhibits Na^+ absorption through ENaC, whereas the IP_3-dependent release of Ca^{2+} from intracellular stores initiates CaCC-mediated Cl^- secretion [134]. In contrast, although the ADO-A_{2b} receptor system and cAMP-dependent activation of PKA are functional, in the absence of CFTR protein the effect of ADO signaling pathway on Cl^- secretion and Na^+ absorption is ineffective [91].

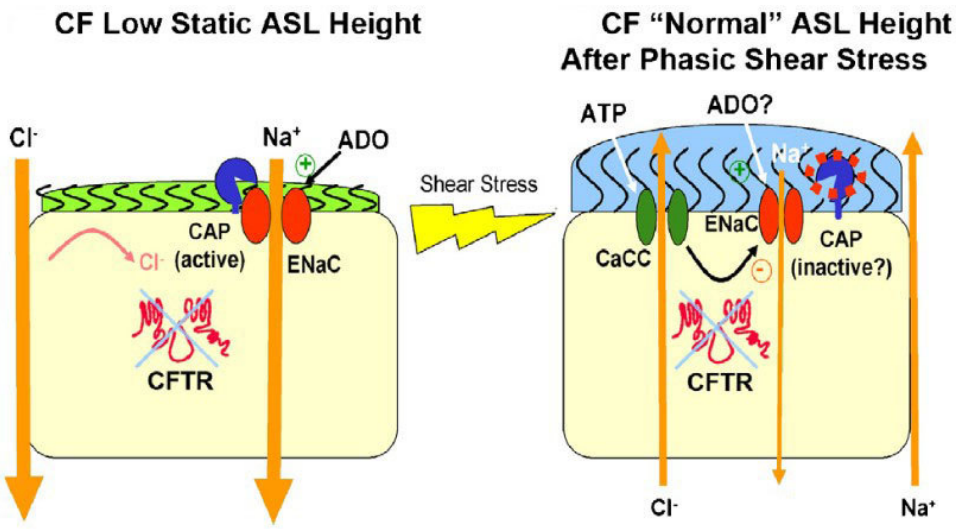

Figure 8. ASL height regulation by phasic shear stress in CF airways. In CF epithelia, the higher basal rate of Na^+ absorption and the failure to initiate Cl^- secretion under static conditions lead to PCL depletion ("flattened" cilia). Under phasic motion conditions, CF cultures release sufficient amount of ATP into the ASL to inhibit Na^+ absorption and initiate CaCC-mediated Cl^- secretion to restore ASL to a physiologically relevant height [91].

The functionality of the ATP-dependent $P2Y_2$ signaling system has been demonstrated experimentally by the addition of nucleotides to the mucosal surface of airway epithelia that induced liquid secretion in both normal and CF airways [135, 136]. However, the effects of nucleotides on airway epithelium are relatively transient and the height of the PCL diminishes to baseline value within 1 h that is in accordance with previous measurements of Ca^{2+}-mediated anion-secretion [137, 138]. The rationale of this transient action involves the rapid degradation (~30 s) [135] of even large doses of ATP

by ecto-nucleotidases that are active within the ASL [139] and also the desensitization of the $P2Y_2$ receptors or transient nature of the IP_3/Ca^{2+} signal [140].

Importantly, under circumstances that impair the efficiency of the ATP signaling system, CF airways fail to properly regulate mucus hydration and consequently, its clearance. These conditions involve infections of CF airway epithelium with paramyxoviruses, e.g. respiratory syncytial virus (RSV) or parainfluenza virus (PIV), which are known to induce the upregulation of a cell-surface ecto-ATPase expression with sufficient activity to reduce the amount of ATP in the ASL. The lack of $P2Y_2$-mediated inhibition of Na^+ absorption and stimulation of CaCC-mediated Cl^- secretion leads to the depletion of ASL volume with abolished mucus transport, even under phasic shear stress conditions [82] (Fig. 9.).

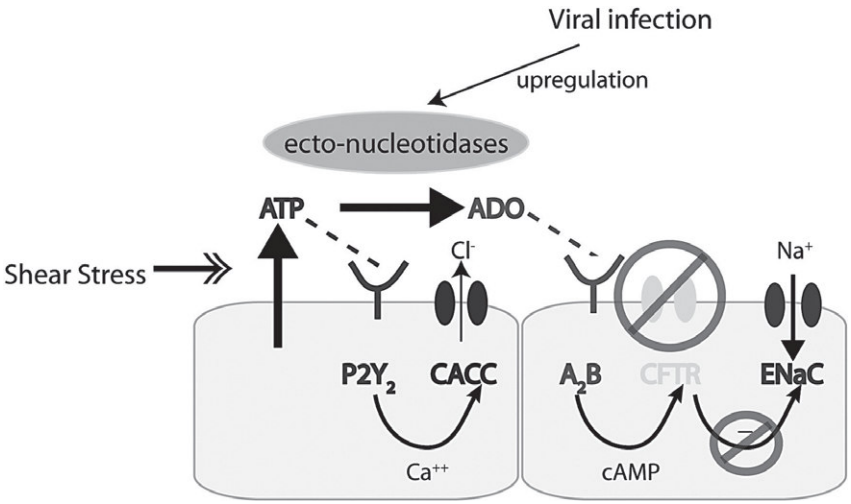

Figure 9. The importance of ATP-mediated chloride secretion in the ASL formation of CF epithelia. Shear stress, induced by airflow over airway surfaces, leads to the release of ATP, which activates $P2Y_2$ receptors and stimulates Cl^- secretion via CaCC. The effect of released ATP is limited by ectonucleotidase-mediated degradation. Viral infections or other inflammatory stimuli increase ectonucleotidase expression that impairs the ability to secrete Cl^- and water (via CaCC) in the CF airway. Due to the lack of CFTR, the formation of ADO is unable to stimulate Cl^-/water secretion in the CF airway. A_2B = A_2B adenosine receptor; ADO = adenosine [133]

It has been hypothesized that in CF patients, viral infections play the central role in initiating CF lung disease [85]. Virus infections produce “patchy” reductions in ASL volume leading to accumulation of dehydrated mucus in virus-infected areas followed by colonization with aspirated bacteria in that region. With subsequent events of viral infections, bacteria may spread as “metastases” from an already contaminated area of the lung to a previously normal region, resulting in acute exacerbations [141, 142].

1.4.3. The role of pH in the regulation of ASL

Additionally, the pH of ASL (pH_{ASL}) appears to play an important role in the maintenance of host defense in the lung. Despite the difficulties in sampling human ASL for pH measurements *in vivo*, data from previous studies using different methods uniformly indicated an acidic (from mild to more severe) pH_{ASL} in CF patients compared to healthy control subjects [143-146]. Furthermore, acidic pancreatic and seminal secretions have been observed in CF patients suggesting that the lack of CFTR function is somehow related to abnormally acidic luminal solutions [147-149]. This fact also proposes the role of CFTR in bicarbonate secretion into the ASL [150, 151]. It is yet unclear whether CFTR directly transports HCO_3^- or it regulates other transporters (e.g. an anion exchanger isoform) that secrete HCO_3^- in the apical membrane. Previous studies failed to detect the presence of an anion exchanger in the apical membrane of airway epithelium that might be regulated by CFTR. Instead, they provided firm evidence for an electrogenic HCO_3^- transport through the CFTR channel itself [152], an observation that is consistent with data from earlier studies [153, 154]. Previous investigations also revealed that the relative HCO_3^-:Cl^- permeability of CFTR is in the range of 0.13-0.25 [155].

pH_{ASL} may reflect an equilibrium between the electrogenic CFTR-dependent HCO_3^- transport and the acid (H^+) secreting mechanisms present in the apical membrane of airway epithelium, including a vacuolar type H^+-ATPase [156], a Zn^{2+}-sensitive H^+ channel [32, 33], but most importantly the H^+-K^+-ATPase [143]. To date, there is no evidence of a Na^+/H^+-exchanger in the apical membrane of pulmonary epithelia [155, 157, 158]. In CF, the ability to secrete HCO_3^- and compensate for the intact H^+-K^+-ATPase -mediated proton secretion into ASL is diminished, resulting in acidification of the ASL [143]. If indeed CFTR is the only path to transport HCO_3^- across the apical membrane, paracellular H^+ absorption and/or HCO_3^- secretion remains the only way to offset epithelial H^+ secretion but their capacity appears to be insufficient in CF [143].

Disturbances in epithelial HCO_3^- secretion and the resulting changes in pH_{ASL} could contribute to the pathophysiology of CF lung disease. In fact, some evidences indicate that the severity of CF disease may stronger correlate with defects in HCO_3^- transport than with the lack of Cl^- secretion [159].

Acidification of ASL may influence the function of cell surface ion channels and indirectly alter ASL height. CaCCs are known to play an important role in ASL homeostasis; however, there is little evidence about the direct regulation of CaCCs by external pH (pH_o) [99]. In contrast, acidic intracellular pH inhibited CaCCs in acinar cells from lachrymal and parotid glands [160, 161], but the exact mechanism of this effect is unknown. It is possible that pH regulation of CaCCs might be indirect, via alterations in intracellular Ca^{2+} levels. In an early study by Barnes and coworkers, it was reported that Ca^{2+}-activated Cl^- currents were reduced by extracellular acidification and enhanced by alkalinization in cone photoreceptors [162]. They proposed that this modulation was due to the pH sensitivity of Ca^{2+} channels in these cells which phenomenon had already been described in other cell types as well [163-165]. Based on these observations it was speculated that the gating mechanisms of Ca^{2+} permeable channels might function as sensors for changes in surface potential caused by the binding of H^+ to negative charges on the cell surface [163, 165].

Furthermore, low pH_{ASL} changes the net electrostatic charge of sulfated and sialated carbohydrate side chains of mucin molecules which essentially alters their hydration state, leading to increased ASL viscosity [166]. Additionally, an acidic surface pH may diminish the electrostatic repulsive forces between mucins in the mucus layer and membrane surface tethered mucins, producing adhesive mucus plaques on airway surfaces particularly when the PCL is depleted, as it is the case in CF [128]. At low pH_{ASL}, mucus clearance may also be diminished due to a reduction in ciliary beat frequency in airway epithelium when pH_o is acidic [167].

The abnormally low pH_{ASL} and the related tight biofilm formation that is characteristic in CF are also associated with attenuated immune responses. Phagocytic cells demonstrate less efficiency at ingesting and killing bacteria at acidic pH_o, thereby facilitating bacterial (e.g. *Pseudomonas aeruginosa*) survival in the airway lumen [168-170] (Fig. 10.).

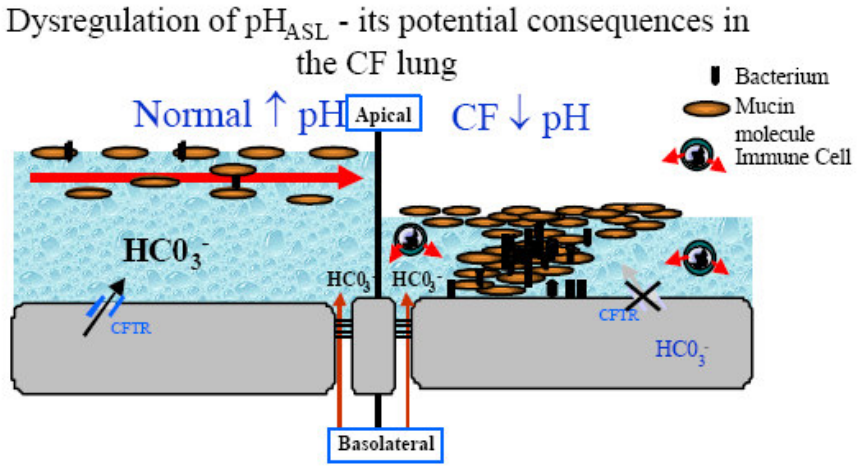

Figure 10. Effects of reduced pH_{ASL} on CF airway epithelium. In CF, lower pH results in a "low-volume" gel with increased viscosity and adherence of soluble mucins. This leads to the formation of mucous plaques with diminished clearance of bacteria [171].

Therefore, increasing the pH of the ASL in CF patients by inhalation of an alkaline solution might be beneficial. Importantly, it has been demonstrated that in contrast to acidic aerosols, alkaline aerosols do not trigger bronchoconstriction [172]. In fact, radioaerosol clearance was significantly improved in patients with chronic cough following the inhalation of an isotonic alkaline solution (pH: 8.0-9.0) with no side effects [173].

1.4.4. CaCC as a molecular target in CF

The basic defect in CF is the lack of functional CFTR protein in the apical membrane of secretory epithelia. The CF airways exhibit Cl^- and/or HCO_3^- hyposecretion and Na^+ hyperabsorption which lead to the depletion of ASL volume resulting in reduced MCC and chronic infections of the airways [77]. Since lung manifestations are the dominant source of morbidity in CF, several approaches have been considered with the potential to delay or arrest the development of CF lung disease. Most of these attempts focus on correction of the ion transport defects, with the particular aim to rehydrate airway surfaces. They include reintroduction of the wild-type CFTR gene, correctors/potentiators of the mutated CFTR protein, activation of Cl^- channels other than CFTR, inhibition of ENaC-mediated Na^+ transport and the application of osmotic agents on airway surfaces [174] (Fig. 11.).

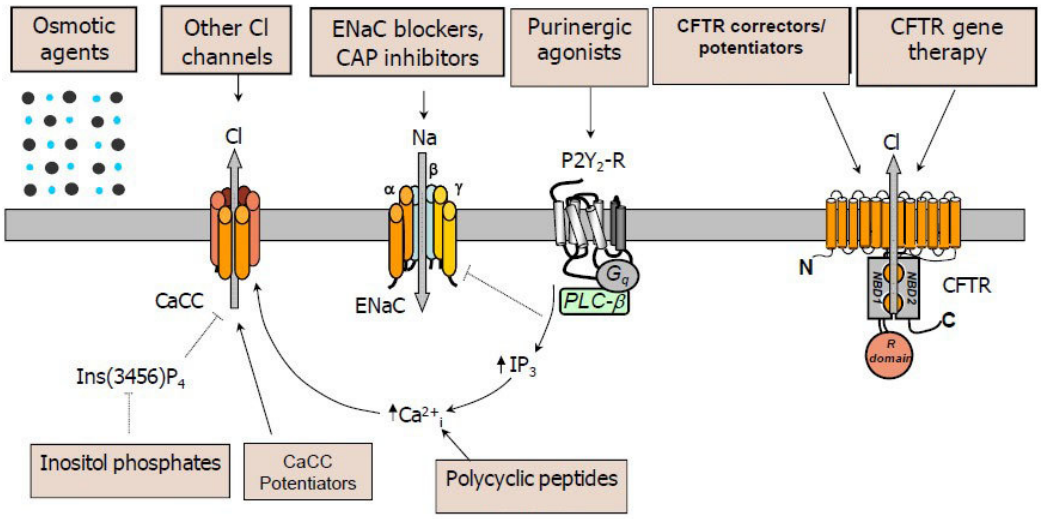

Figure 11. Novel CF therapies aimed to rehydrate airway surfaces by increasing ion and water secretion or blocking absorption. Pharmaceutical approaches that regulate ion channels directly or indirectly are shown. Airway secretion may be improved by replacing/potentiating dysfunctional CFTR or activating alternative Cl^- channels in the apical membrane such as CaCC or ClC-2. Furthermore, hyperosmotic agents draw water into the luminal space by providing a significant driving force. Alternatively, strategies that inhibit ENaC-mediated fluid absorption are predicted to increase the volume of ASL. $P2Y_2$-R: P2Y purinoceptor (Derek Paisley personal communication 2010).

The Ca^{2+}-activated Cl^- channel has often been referred to as the alternative Cl^- channel, because it may provide a parallel route for Cl^- secretion across the apical membrane in tissues that lack CFTR [137]. Although CaCC expression appears to be up-regulated in CF [175, 176], it is not able to compensate for the ion transport defects due to its relatively low basal activity [176].

Therefore, pharmacotherapeutic interventions aimed to stimulate alternative CaCCs are under development. It is noteworthy that the stable UTP analog Denufosol (INS37217) has been shown to stimulate purinergic $P2Y_2$ receptors, increasing the rate of PIP_2 hydrolysis that resulted in IP_3-dependent release of Ca^{2+} from intracellular stores. The increase in free $[Ca^{2+}]_i$ activated chloride secretion through CaCCs, while depletion in PIP_2 levels led to the decrease in ENaC activity. Consequently, aerosolized Denufosol appeared to be highly beneficial for CF patients during clinical Phase I and II studies and the completion of Phase III trials is underway [177]. Another drug, Moli-1901 (duramycin) - a 19-amino-acid residue bacterial polycyclic peptide - is currently in Phase II clinical trials in Europe. This peptide interacts with phospholipids present in plasma and organelle membranes, thereby elevating intracellular Ca^{2+} from both internal stores and the extracellular space which in turn leads to the activation of CaCCs

[178]. CaCC activators that target CaCCs directly without an elevation in cytoplasmic calcium have not yet been developed. Most recently, penetratin - a cationic 17-amino-acid peptide - has been shown to potentiate endogenous CaCC activity in *Xenopus* oocytes. This study suggested that penetratin acts, at least in part as a direct modulator of CaCCs, although the penetratin-mediated potentiation also required Ca^{2+} influx from the extracellular space [179].

Therapeutic interventions designed to activate CaCCs via Ca^{2+}-mobilizing agonists must face (at least) one serious problem. As it was already discussed in chapter 1.4.1., CaCC-mediated currents display time and voltage dependent profile. At intermedier (subsaturating) Ca^{2+} concentrations, the channels are closed at hyperpolarizing membrane potentials, because the voltage dependent channel inactivation exceeds the Ca^{2+}-dependent channel activation, thereby resulting in a lack of inward Cl^- currents (no Cl^- efflux). To induce Cl^- efflux via CaCCs, intracellular Ca^{2+} concentrations should reach saturating values (>1 μM) when the Ca^{2+}-dependent channel opening becomes voltage independent [100, 121]. However, it has been speculated that activation of CaCCs requires a saturating Ca^{2+} concentration only in the subplasmalemmal space [100]. Since rate of diffusion through the plasma membrane is much faster than diffusion rate towards the center of the cell, Ca^{2+} entry from the extracellular space leads to accumulation of Ca^{2+} near the plasma membrane. Furthermore, Cl^- currents show strong correlation with Ca^{2+} signals if Ca^{2+} derives from the extracellular space [180]. On the other hand, Ca^{2+} signals provided by the release of Ca^{2+} from internal stores must reach markedly higher levels in the bulk cytosol to induce Cl^- efflux. In fact, large and long-lasting increases of $[Ca^{2+}]_i$ could lead to undesirable side effects, such as apoptosis and/or activation of inflammatory processes. Consequently, controlled Ca^{2+} entry through the plasma membrane might be beneficial for therapeutic purposes in CF.

1.4.5. The role of zinc in the airways

Zinc has been shown to be essential as an anti-oxidant, microtubule-stabilizer, anti-apoptotic agent, growth cofactor and anti-inflammatory agent in several different tissues [181]. With respect to the respiratory tract, Zn^{2+} deficiency leads to increased susceptibility to infections and inflammation of airways [182]. Depletion of Zn^{2+} enhances nuclear translocation of NF-κB in both human and rat airways, providing a

mechanism for the pro-inflammatory effects of Zn^{2+} deficiency [183, 184]. Furthermore, it has been shown that the decreased intake of dietary anti-oxidants, such as Zn^{2+} strongly correlates with the increased incidence of asthma [185]. The loss of anti-oxidant function in Zn^{2+} deficiency causes oxidative/nitrosative damage and apoptosis, which might exacerbate allergen-induced hyperresponsiveness and inflammation in the airways [186, 187]. Zn^{2+} may also be beneficial in the treatment of the common cold. It has been suggested that Zn^{2+} prevents viral docking and replication in the respiratory epithelium [188]. However, direct application of Zn^{2+} into airways may result in a number of side effects. These include loss of olfactory sensation [189], as well as induction of acute respiratory tract inflammation [190].

Human airway epithelia express another subclass of nucleotide receptors, the P2X receptor channels [191-193]. P2X receptors are extracellular ATP-gated, Ca^{2+}-permeable, non-selective cation channels. Previously we have found that application of ATP caused a sustained increase in $[Ca^{2+}]_i$ via P2X receptor-mediated Ca^{2+} influx, that was able to induce Cl^- secretion in airway epithelial cells both *in vitro* and *in vivo* [191, 193, 194]. We also demonstrated that extracellular Zn^{2+} regulates purinergic Ca^{2+} influx in human CF and non-CF airway epithelial cells which ability is strongly dependent on the pH and Na^+ concentration of the extracellular environment [192, 194]. Furthermore, low micromolar Zn^{2+} (20μM) when applied to an alkaline, low Na^+-containing solution ("enhanced calcium transfer" solution) [193, 194] produced a Ca^{2+} signal and Cl^- secretion in CF airway epithelial cells comparable to that when Zn^{2+} was co-administered with ATP [194]. It is important to note that the effects were abolished by reducing pH or replacing external Na^+. This indicates that Ca^{2+} entry/Cl^- secretion in airway epithelial cells can be switched on/off by modifying the external ionic environment. Moreover, these findings suggested that P2X receptors are not simply ATP-gated receptors but might function as Zn^{2+} receptors and/or extracellular sensors of the local microenvironment [195]. A possible new therapeutic avenue has also been introduced by highlighting the beneficial effects of Ca^{2+} entry on rescuing anion transport in CF airway epithelium.

Thus, the administration of Zn^{2+} in a properly composed aerosol might be advantageous for CF patients by improving MCC function. The benefits of extracellular zinc and zinc-induced Ca^{2+}-entry are not limited to stimulation of epithelial Cl^- secretion. It may also

inhibit the ENaC-mediated Na^+ hyperabsorption [14], increase the frequency of ciliary beating [196], inhibit cell surface H^+ channels [32] and attenuate inflammatory responses in CF airways [181, 197]. Nonetheless, it is noteworthy that data are contradictory regarding the effects of Zn^{2+} on epithelial chloride channels. Ca^{2+}-activated Cl^- channels can be both stimulated and inhibited by extracellular Zn^{2+} [179, 198], while voltage-gated Cl^- channels (ClC-2) are inhibited [27]. On the other hand, the therapeutic application of Zn^{2+} may also be debatable, because overexposure to Zn^{2+} could lead to various side effects [189, 199, 200]. Interestingly, substituting Zn^{2+} with spiperone - a known anti-psychotic drug - in the "enhanced calcium transfer" solution elicits a similar response with a sustained increase in $[Ca^{2+}]_i$ and stimulation of CaCCs in both CF and non-CF airway epithelial cells [201]. These observations suggest that further experiments are needed to find the proper pharmacological tools for CF therapy.

1.5. cAMP-regulated epithelial ion transport mechanisms in the small intestine

Under normal conditions, the predominant function of small intestine is the absorption of luminal fluid, electrolytes and nutrients. Nevertheless, electrolyte secretion is of great importance by facilitating hydration of the intestinal mucosa and ensuring appropriate liquidity for intestinal contents during digestion and absorption.

Na^+ and Cl^- absorption is carried out by the coordinated operation of the apical membrane Na^+/H^+-exchangers (NHEs), mainly NHE-2 and NHE-3, and the anion exchangers SLC26A3 (DRA), SLC26A6 (PAT1) and SLC4A9 (AE4). In the postprandial period, coupled ion-solute transporters, such as the Na^+-glucose-cotransporter (SGLT1), are also important modes of Na^+ absorption. Fluid secretion is driven by active Cl^- transport in a transcellular manner. Cl^- is taken up via the Na^+-K^+-2 Cl^--cotransporter at the basolateral membrane of enterocytes whereas it is released via Cl^- channels in the apical membrane, primarily through the CFTR. Other apical Cl^- channels may also participate in Cl^- secretion, such as ClC-2, a member of the voltage-gated ClC family and Ca^{2+}-activated Cl^- channels. The secretion of both Na^+ and water follows Cl^- paracellularly. The driving force for net movement of Na^+ and Cl^- is produced by the Na^+-K^+-ATPase and K^+ channels in the basolateral membrane of enterocytes [202] (Fig. 12.). CFTR, in part by facilitating apical anion exchangers, is also essential for the regulation of HCO_3^- secretion. It is particularly important in the

duodenum where luminal pH is critical to protect the epithelium from damage caused by acid and pepsin [203, 204].

Fluid secretion can be activated by different neural, endocrine and paracrine mechanisms, including 5-hydroxytryptamine, acetylcholine and VIP. Prostaglandins and interleukins as inflammatory mediators may also be involved in initiating Cl^- secretion [205, 206]. Furthermore, there is growing body of evidence suggesting an important role for nucleotides and purinergic signaling in the physiology of the small intestines [207, 208]. These regulatory processes utilize different intracellular signaling cascades, involving second messengers (cAMP, cGMP, Ca^{2+}), serine/threonine and tyrosine kinases as well as phosphatases with plentiful cross talk and cellular specificity [202] (Fig. 12.).

The pivotal role of CFTR in intestinal Cl^- and fluid secretion is highlighted under some pathologic conditions, including CF and secretory diarrhea. In CF, due to the absence of CFTR-related anion secretion, constipation and intestinal obstruction occurs. In the intestine of newborns with CF, a thick, dehydrated mucoid plug is formed causing obstruction of the gut - a condition known as meconium ileus - that often requires urgent surgical intervention [209]. In addition, CFTR knock-out mice develop intestinal obstruction as well and die from intestinal obstruction by 5 weeks of age [210].

On the other hand, secretory diarrhea is caused by intestinal infections by various bacterial and viral pathogens. Bacterial enterotoxins, such as cholera toxin from V. cholerae and STa toxin from E. coli stimulates permanent production of cAMP and cGMP, respectively, resulting in CFTR-mediated continuous Cl^- and fluid secretion [211, 212].

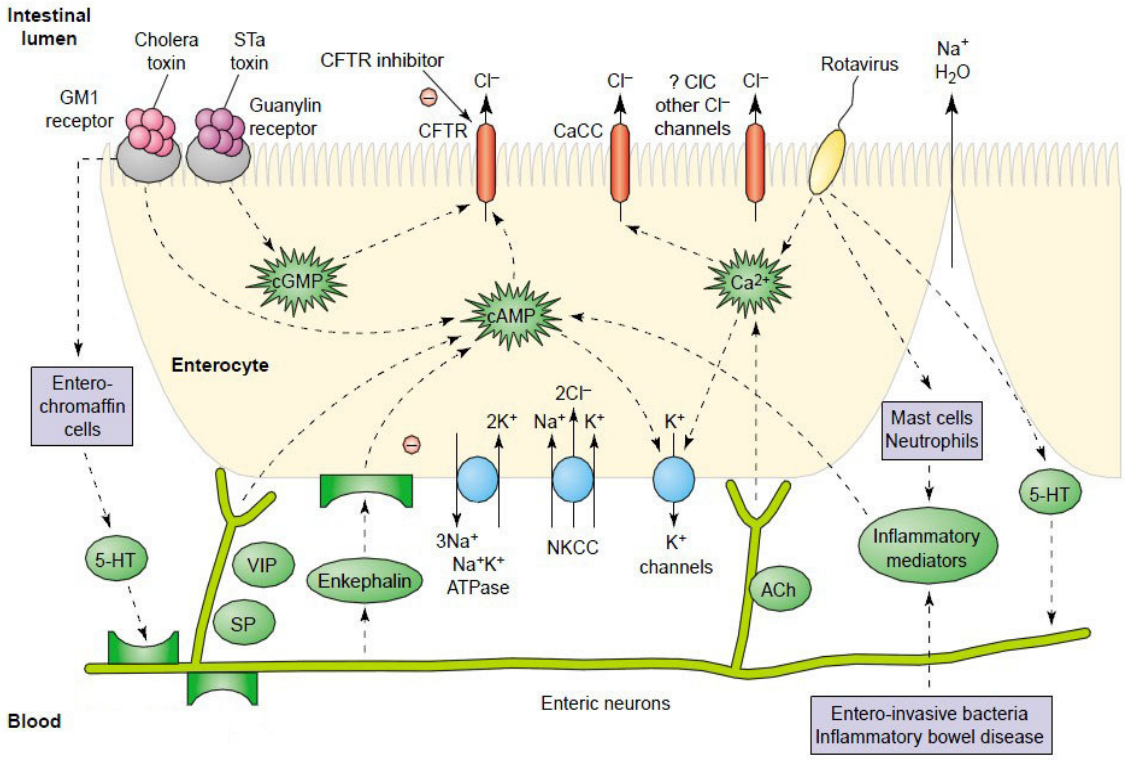

Figure 12. Summary of intestinal secretory pathways. Pathogens (cholera toxin, STa toxin and rotavirus) may initiate secretion by multiple pathways including the release of 5-hydroxytryptamine from enterochromaffin cells and inflammatory mediators from mast cells or neutrophils (e.g. prostaglandins and interleukins). Regulatory signals (neuronal, endocrine, paracrine) are transduced by second messengers (cAMP, cGMP, Ca^{2+}) to activate membrane ion channels. 5-HT: 5-hydroxytryptamine, VIP: vasoactive intestinal peptide, Ach: acetylcholine, SP: substance P; Modified after Ref. [213]

1.6. Ca^{2+}-regulated epithelial ion transport mechanisms in the small intestine

1.6.1. The role of Ca^{2+}-activated chloride channel in anion secretion in the intestines

Despite the fact that the presence of CaCCs is well established [214], there is only limited evidence that apical Cl^- channels, other than CFTR, participate in secretion of Cl^- and fluid in intestinal epithelium. Rotavirus, the major cause of gastroenteritis and diarrhea in childhood, releases the enterotoxin NSP4 which inhibits brush border disaccharidases and SGLT1 activity, thereby reducing solute and fluid absorption. In addition, it was found that NSP4 stimulates Ca^{2+}-activated Cl^- channels and elicits a transient Cl^- secretion [215], an observation that is consistent with previous studies performed in CF and non-CF infant mice [216]. Interestingly, the NSP4-induced Cl^-

secretion was substantially reduced in adult CF and non-CF mice, suggesting an age-dependent expression of CaCC. Agonists that increase $[Ca^{2+}]_{ic}$, including carbachol, histamine and nucleotides may lead to activation of CaCCs and initiation of a secretory response in the intestinal epithelium [217]. The finding that a residual cholinergic Cl^- secretion is preserved in CF patients with a mild phenotype has further strengthened the idea of an alternative, Ca^{2+}-activated Cl^- channel [218]. However, subsequent studies revealed that the Ca^{2+}-dependent activation of Cl- secretion required functional CFTR [219, 220]. This suggests that in intestinal epithelium CFTR is the predominant Cl^- channel that is responsible for both cAMP- and Ca^{2+}-regulated Cl^- secretion [221].

1.6.2. The transepithelial transport of Ca^{2+} in the intestines

The Ca^{2+} homeostasis is achieved by the concerted action of three organ systems including the gastrointestinal tract, bone, and kidney. Ca^{2+} is absorbed from the lumen of the intestines by both a Ca^{2+}-regulated and a hormonally regulated transcellular mechanism and by a passive, paracellular route [222] (Fig. 13.). Ca^{2+} enters the enterocytes via the apical epithelial calcium channel TRPV6 (and to a certain extent by TRPV5), facilitated by both chemical and electrical gradients. Inside the cell Ca^{2+} ions bind to calbindin D_{9K} protein, which maintains a low cytoplasmic $[Ca^{2+}]$, protecting the cells from the toxic effect of high intracellular calcium levels as well as maintaining the favorable lumen-to-enterocyte $[Ca^{2+}]$ gradient. Binding to calbindin also participates in the diffusion of Ca^{2+} from the apical to the basolateral membrane, where it is extruded against an electrochemical gradient by the plasma membrane Ca^{2+}-ATPase (PMCA1b) and the Na^+-Ca^{2+}-exchanger (NCX1). Paracellular Ca^{2+} transport takes place across the tight junctions and is driven by the electrochemical gradient for Ca^{2+}.

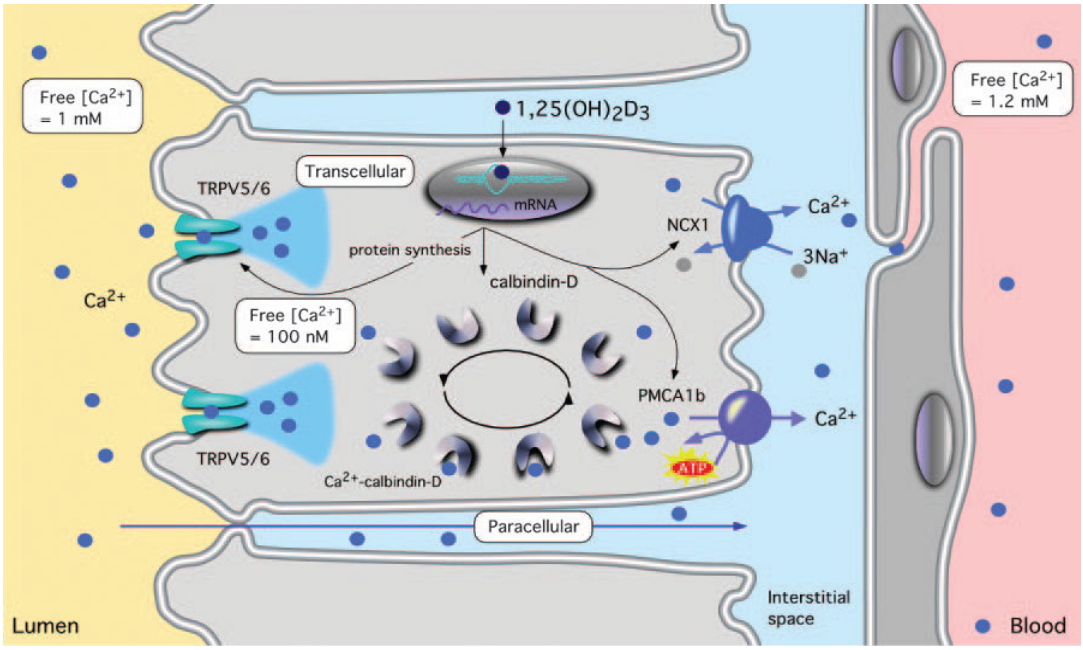

Figure 13. Mechanism of epithelial Ca^{2+} transport in the gut. Ca^{2+} is absorbed in the epithelium by paracellular and transcellular transport. The active form of vitamin D, 1,25-dihydroxyvitamin D_3 [1,25-$(OH)_2D_3$] regulates the distinct elements of transcellular Ca^{2+} transport by increasing the expression levels of the luminal Ca^{2+} channels (TRPV5/6), calbindin, and the extrusion systems (NCX1 and PMCA1b) [222].

The TRPV6 (CaT1) channel was first cloned from rat duodenum by Peng et al. in 1999 [223]. The TRPV6 gene is located on the chromosome 7 in humans. The encoded protein comprises 725 amino acids, has six transmembrane domains, and intracellular N- and C-termini like all the other TRPV family members. There are three ankyrin repeats on the N-terminal of the protein, whereas a calmodulin-binding site and a PKC phosphorylation site reside on the C-terminal. The putative pore region is localized between TM5 and TM6. TRPV6 shares relatively high sequence homology (75%-identity) with TRPV5 but significantly less with the other members of the TRPV family (30-35%) [224]. TRPV6 also shows greater functional similarity to TRPV5 than to other TRPV channels. Unlike TRPV1-4, TRPV5 and TRPV6 are highly Ca^{2+}-selective, and can form homo- or heteromultimer channels. Intracellular Mg^{2+} is required for the Ca^{2+} selectivity of TRPV5/6 channels [223, 225]. Both channels are ligand independent, they are not sensitive to capsaicin, heat or osmotic stress. Their pivotal role is to form constitutively active Ca^{2+} entry pathways in Ca^{2+} transporting epithelia including renal and intestinal epithelium. However, the channels are subject to Ca^{2+}-dependent feedback inactivation, which is believed to protect the cells from reaching toxic Ca^{2+} levels as well as limit epithelial calcium transport [226, 227] (Fig. 14.).

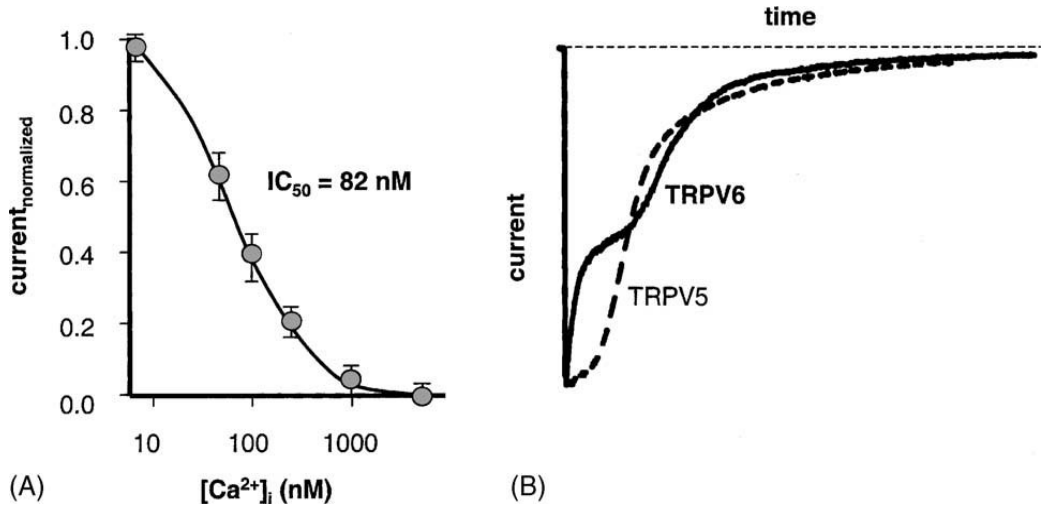

Figure 14. Role of intracellular Ca^{2+} in the regulation of TRPV5 and TRPV6 heterologously expressed in HEK293 cells. **(A)** normalized Ca^{2+} current decreases with increasing $[Ca^{2+}]_i$. **(B)** Ca^{2+}-dependent inactivation exhibit different patterns for TRPV5 (dotted line) and TRPV6 (solid line) [228].

There are several speculations for the explanation of this negative feedback inhibition. These include phosphorylation of the channels by Ca^{2+}-dependent kinases, such as CaMKII [229] and Ca^{2+}-induced depletion of PIP_2, a substrate that is otherwise necessary for the sustained operation of the channels [230, 231].

Since apical Ca^{2+} channels are the rate-limiting step for epithelial Ca^{2+} uptake, absorption of Ca^{2+} is also regulated on the level of gene transcription. To date, the most important regulators of TRPV5/6 expression are the biologically active form of Vitamin D_3 [$1,25(OH)_2D_3$], and estrogen. Dietary Ca^{2+} intake is an additional regulator of TRPV5/6 expression which effect appears to be independent of $1,25(OH)_2D_3$ [228, 232]. TRPV6 is mainly expressed in absorptive and secretory epithelia, including the gastrointestinal tract and the placenta [233]. TRPV6 is involved in transplacental Ca^{2+} transport. It was shown that the serum and amniotic Ca^{2+} concentrations as well as the growth rate of murine TRPV6-knockout fetuses were significantly lower [234], suggesting that TRPV6 is essential for Ca^{2+} supplementation and optimal development of the fetus. In the gastrointestinal tract, TRPV6 is expressed in the duodenum, proximal jejunum, and in the colon [223, 235]. Under Ca^{2+}-restricted conditions, a lack of TRPV6 in adult animals exerts a significant effect on Ca^{2+} homeostasis, suggesting that duodenal TRPV6 is a major Ca^{2+} absorptive mechanism in the gut [236, 237]. In

addition to the placenta and gut, TRPV6 is also expressed in the pancreas, salivary gland, mammary gland, and prostate but its function is still unclear in these organs.

1.6.3. The role of zinc in the intestines

Normal adults require approximately 10-15 mg/day Zn^{2+} intake, which mostly vary as a function of age and excretion. Zn^{2+} is absorbed in the small intestines, mainly in the jejunum and ileum. Absorption is accomplished by both passive diffusion and through different zinc-specific transporters [1]. ZIP4 (Zrt- and Irt-like protein 4, SLC39 family) seems to be the most important transporter, which mediates Zn^{2+} uptake into enterocytes across their apical membrane [238]. ZIP4 mRNA is expressed throughout the small intestines in both human and mice, while the protein appears to be localized to the apical membrane of enterocytes. The expression of ZIP4 accurately follows dietary Zn^{2+}, with up-regulation under Zn^{2+} deficiency and down-regulation under zinc-replete conditions at the mRNA level [239, 240]. Acrodermatitis enteropathica, an autosomal recessive disorder causing Zn^{2+} deficiency, develops as a result of a mutation in the gene encoding ZIP4. Accordingly, the classic symptoms of Zn^{2+} deficiency include dermatitis, diarrhea, growth retardation, immune dysfunctions and neurological disturbances [240]. Zn^{2+} is released from the enterocytes into the circulation mostly via basolateral ZnT1 (SLC30 family) transporter, which is also abundantly expressed in the small intestines [241].

Recently, the TRPV5/6 transporter proteins have been proposed to be involved in zinc absorption. There are a few studies reporting that the ancestral form of mammalian TRPV5/6 in fish also transports Zn^{2+}. The *Fr*ECaC (epithelial calcium channel from *Fugu rubripes*) was found to transport Zn^{2+} and to a smaller extent Fe^{2+} [242]. In freshwater rainbow trout gill, Ca^{2+} and Zn^{2+} were shown to use the same apical entry pathway, which had a much higher K_m value for Ca^{2+} than for Zn^{2+} [243]. In addition, 1α,25-$(OH)_2D_3$ increased Zn^{2+} uptake as well as *Om*ECaC and *Om*SLC39A1 expression [244]. In rat or pig brush border membrane vesicles from the small intestine, Zn^{2+}, Cd^{2+} and Ca^{2+} were reported to use the same channel-like pathway to enter the cells [245, 246]. Rat TRPV6 expressed in *Xenopus* oocytes was reported to transport Ca^{2+}, Ba^{2+}, Sr^{2+} but not Mg^{2+} or any of the other di- or trivalent cations examined [223]. When human TRPV6 (hTRPV6) was studied in the same system, similar results were obtained

[247]. To date, no studies are available investigating the permeability of human TRPV6 in mammalian expression systems, or of endogenous TRPV6 to different trace elements and toxic heavy metals.

In the GI tract, Zn^{2+} is directly involved in enterocyte proliferation and differentiation, gut-associated immune function, reduction of oxidative stress and inhibition of apoptosis [248]. Zn^{2+} deficiency is associated with severe diarrhea and generalized malabsorption in malnourished children [249]. Zn^{2+} is known to be beneficial in enterotoxin-induced diarrheas. The administration of Zn^{2+} to Caco-2 cells directly reduced Cl^- and fluid secretion by inhibiting cAMP- and Ca^{2+}-coupled transduction pathways [250, 251].

2. Specific Aims

The main purpose of the present work was to elucidate the effects of extracellular zinc on Ca^{2+} entry mechanisms in two different cellular models. The specific aims were as follows:

1. To investigate the role of zinc in different extracellular ionic milieu on the activity of Ca^{2+}-dependent Cl^- channels in CF airway epithelial cells.

2. To study the effect of extracellular zinc on human TRPV6, an intestinal Ca^{2+} transporter channel expressed in HEK293 cells.

3. Materials and methods

3.1. Cell culture protocols

IB3-1 is a CF human bronchial epithelial cell line carrying two different mutations of the CFTR gene (ΔF508/W1282X). Cells were grown in plastic tissue culture flasks in DMEM/F12 (1:1) medium supplemented with 10% FBS, 100 U/ml penicillin and 100 µg/ml streptomycin.

The human embryonic kidney 293 cell line (HEK293) was cultured in DMEM cell culture media. Media were supplemented with 10% FBS, 10 mM HEPES, 1 mM Na-pyruvate, and 1% penicillin/streptomycin. Both cell lines were maintained at 37^{o}C in a humidified cell culture incubator supplied with 5% CO_2. Cells were subcultivated when confluency reached 90-95%.

3.2. Transfection protocol for HEK293 cells

For ion imaging and electrophysiological experiments, cells were plated at 300,000 cells/well density on No. 00 coverslips coated with 100µg/ml poly-D-lysine in 35 mm dishes. For ^{45}Calcium uptake, 400,000 cells were placed into poly-D-lysine-coated 35 mm dishes. After 8-16 hours, cells were transfected with 2 µg pEYFP-C1-TRPV6 using 5 µl Lipofectamine 2000 per dish, as described in the manufacturer's protocol. For control experiments, cells were transfected with the pEYFP-C1 vector. In some experiments, cells were transfected with 2 µg pTagRFP-C1-hTRPV6 construct to avoid the interference of EYFP and fluorescence dyes with similar spectra. After 4 hours, transfection medium was replaced with antibiotic-free medium. Transfection efficiency was estimated to be 60-70% using fluorescence microscopy.

3.3. Cell surface biotinylation and Western blotting

All steps of cell surface biotinylation were carried out in a 4°C cold room using ice-cold solutions. First, HEK293 cells were rinsed once with PBS-Ca-Mg (PBS containing 0.1 mM $CaCl_2$ and 1 mM $MgCl_2$). Afterwards, surface proteins were biotinylated by incubating cells with 1.5 mg/ml sulfo-NHS-LC-biotin in 10 mM triethanolamine (pH

7.4), 1 mM $MgCl_2$, 2 mM $CaCl_2$, and 150 mM NaCl for 90 minutes with horizontal shaking at 4°C. After labeling, samples were washed with quenching buffer (PBS containing 1 mM $MgCl_2$, 0.1 mM $CaCl_2$, and 100 mM glycine) for 20 minutes at 4°C, and then rinsed three times with PBS. Cells were finally lysed in lysis buffer for 30 minutes according to Ref. [252] and lysates were cleared by centrifugation. Protein concentrations were determined by DC Protein Assay. Portion of cell lysates of equivalent amounts of protein were equilibrated overnight with streptavidin agarose beads at 4°C. Beads were washed sequentially with *solutions A* [50 mM Tris·HCl (pH 7.4), 100 mM NaCl, and 5 mM EDTA] three times, *B* [50 mM Tris·HCl (pH 7.4) and 500 mM NaCl] twice, and *C* (50 mM Tris·HCl, pH 7.4) once. Biotinylated surface proteins were then released by heating to 95°C with 4x Laemmli buffer. Proteins from the total lysate or intracellular fraction were also heated to 95°C for 5 minutes with 4x Laemmli buffer, after adjusting the protein concentration to 1 mg/ml.

Samples were run on a 6% SDS gel with 15 µg protein loaded into each lane. Using the semi-dry transfer method, samples were transferred onto a PVDF membrane in Dunn's buffer. Membranes were blocked overnight with PBS containing 5% milk, 0.5% BSA and 0.02% NaN_3. Afterwards, samples were incubated in blocking buffer containing the primary antibody (1:2000 for chicken anti-GFP (Abcam ab13970) or 1:200 for goat anti-rabbit TRPV6 (Biomol BML-SA567) at room temperature for 1.5 hours followed by three washes with PBS. HRP-conjugated donkey anti-chicken (1:8000) and HRP-conjugated goat anti-rabbit (1:20000) antibodies were used as secondary antibodies. After three consecutive washes with PBS, the enhanced chemiluminescence (ECL) method was used for detection.

3.4. Deglycosylation experiments in HEK293 cells

In these experiments, 50 µL of biotinylated, cell surface proteins were first denatured in 5 µL of 10X denaturing buffer (2% SDS and 10% 2-mercapto-ethanol) at 99ºC for 10 minutes. They were then digested for 3 hours at 37ºC with 4 µL PNGase F in 50 µL of 2X digestion buffer (100 mM Na_2HPO_4 and 2% NP40, pH adjusted to 7.5). The digestions were terminated by the administration of 100 µL 2X protein sample buffer. Samples were run, transferred and developed as described above.

3.5. Confocal microscopy

HEK293 cells transfected with pEYFP-C1-hTRPV6 were fixed with 4% paraformaldehyde at 37°C for 15 minutes after rinsing the cells thoroughly with PBS. After three washes with PBS, nuclei were counterstained with Hoechst33342 (1:1000) at room temperature for 5 minutes. After three final washes with PBS, cells were mounted, and imaged using a Nikon C1 confocal laser scanning microscopy system.

3.6. Live cell ion imaging

3.6.1. Cytosolic Ca^{2+} measurement in IB3-1 airway epithelial cells

For measurements of cytoplasmic Ca^{2+}-concentration, IB3-1 cells were plated at 10^6 cells/dish density on round glass coverslips (42 mm in diameter) in 60 mm dishes and were used for experiments within 24-48 hours. Cells were loaded with Fluo-3-acetoxymethyl ester (AM, 4 µM) in standard extracellular solution for 60 minutes at room temperature. Fluo-3-AM is the membrane-permeable derivative of the highly sensitive calcium indicator Fluo-3 (K_d (Ca^{2+}) = 0.39 µM), that allows rapid measurement of Ca^{2+} flux into cells. Fluorescence dye was dissolved in DMSO containing 20% Pluronic-F127. Additionally, the loading medium contained 1 mM probenecid to prevent dye leakage. Next, coverslips were mounted on the stage of an inverted microscope equipped with a perfusion chamber. At the beginning of each experiment, cells were superfused with standard extracellular solution.

Standard extracellular solution contained (in mM): 145 NaCl, 5 KCl, 3 $CaCl_2$, 1 $MgCl_2$, 10 D-glucose and 10 mM HEPES, pH 7.4 (with NaOH). Sodium-free solutions contained (in mM): 145 NMDG-Cl, 5 KCl, 3 $CaCl_2$, 1 $MgCl_2$, 10 D-glucose and 10 mM HEPES, varying pHs were adjusted by either NMDG or HCl. Nominally Ca^{2+}-free solutions were prepared by simply omitting $CaCl_2$. During recordings the pH_o was altered by changing the bath solution for a buffer with the same ionic composition except for the pH. Solutions were delivered by continuous perfusion at a rate of 3 ml/min. Recordings were made with a confocal laser scanning microscope, Axiovert 200M Zeiss LSM 510 Meta (Carl Zeiss, Jena, Germany) equipped with an 20x Plan Apochromat (NA = 0.80) DIC objective. For excitation, 488-nm argon-ion laser was used. The emitted light was collected by BP 505-570 band pass filter. Data were

obtained at a rate of 0.5 Hz. Changes in $[Ca^{2+}]_i$ are displayed as the percentage of fluorescence relative to the intensity at the beginning of each experiment. The baseline fluorescence (100 %) was calculated from the average fluorescence of ROIs during superfusion of cells with standard bathing solution. Background fluorescence was subtracted from readings by measuring a cell-free area on the same coverslip. All experiments were performed at room temperature.

3.6.2. Cytosolic divalent metal cation measurement in hTRPV6 expressing HEK293 cells

Cells were imaged after 48-72 hours. Non-transfected and transfected cells on the same piece of coverslip were loaded with 5 µg/ml Fura-2-AM (stock solution 5 µg/µl) for one hour in serum-free medium in a cell culture incubator at 37 °C. Fura-2-AM is the membrane-permeable derivative of the high affinity calcium indicator Fura-2 (K_d (Ca^{2+}) = 0.14 µM), that allows accurate, ratiometric measurements of intracellular calcium concentrations. Fura-2 is also suitable for the detection of other divalent cations, such as intracellular zinc (K_d (Zn^{2+}) = 3 nM) [253].

For high sensitivity Zn^{2+} measurements, cells were loaded with 6.8 µM Mag-Fura-2 for 10 minutes. The fluorescent dye Mag-Fura-2, previously used to measure intracellular Mg^{2+}, shows similarity in structure and spectral response to Fura-2. However, it has a much lower affinity to calcium (K_d (Ca^{2+}) =25 µM), while its affinity to zinc is not appreciably different (K_d (Zn^{2+}) = 20 nM), compared to Fura-2. Thus, Mag-Fura-2 is more suitable for intracellular Zn^{2+} measurements in the range of 1-100 nM [254]. To confirm that the change in fluorescence is due to an increase in intracellular Zn^{2+} levels rather than Ca^{2+} or Mg^{2+} levels, we loaded the cells with 5 µM NewPort Green DCF (stock solution 5 mM) for 45 minutes. NewPort Green DCF is a reliable tool for detecting Zn^{2+} influx into cells, because it is essentially insensitive to Ca^{2+} (K_d (Ca^{2+}) >100 µM), while it has a moderate affinity for zinc (K_d (Zn^{2+}) ≈ 1 µM) [255].

The fluorescence dyes were dissolved in DMSO containing 20% Pluronic-F127 and the loading medium contained 1 mM probenecid. Thereafter, cells were placed into modified Krebs-Ringer HEPES (KRH) (150 mM NaCl, 4.8 mM KCl, 1 mM $CaCl_2$, 1 mM $MgCl_2$, 10 mM D-glucose, and 10 mM HEPES, pH 7.4) for 20 minutes in order to achieve full de-esterification of the fluorescence dyes. Fura-2 as well as Mag-Fura-2

was alternatingly excited at 340 nm and 380 nm, and the F340/F380 ratio was monitored at the emission wavelength of 510 nm. The initial rate of the increase of the Fura-2 ratio was taken as the measure of the influx of the particular cation using the Felix software (Photon Technology International). NewPort Green DCF was excited at 500 nm, and the initial increase of the fluorescence intensity in response to the addition of the specific cation was measured. Fluorescence measurements were performed on a Nikon Eclipse TiU inverted microscope equipped with a polychrome V+ light source. Cells were visualized with a Nikon 40x S Fluor objective. Images were taken with a Hamamatsu Orca-EG cooled, monochrome CCD camera. Image acquisition and analysis were done with SimplePCI 6.2 from CImaging.

3.7. Electrophysiology

Voltage-clamp recordings were carried out in the standard whole-cell configuration using an Axopatch 200B amplifier (Axon Instruments) [256]. Micropipettes were pulled by a P-97 Flaming-Brown type micropipette puller (Sutter Instrument) from borosilicate glass capillary tubes (Harvard Apparatus) and had a tip resistance of 3–6 MΩ when filled with pipette solution. Command protocols and data acquisition were controlled by pClamp 6.03 software (Axon Instruments). Capacitative currents were compensated with analog compensation. Linear leak currents were not compensated. Series resistance was accepted if lower than five times the pipette tip resistance. Analog data were filtered at 1 kHz with a low-pass Bessel filter and digitized at 5 kHz using a Digidata 1200 interface board. Membrane potentials were corrected for liquid junction potential if greater than 2 mV values were detected. All experiments were performed at room temperature.

3.7.1. Whole cell experiments in IB3-1 airway epithelial cells

Currents were monitored at -80 mV using ramp commands (-100 mV to +100 mV in 200 ms, 1mV/ms) applied every 10 s. The holding potential was -50 mV between ramps. Stable recordings were maintained for 20-30 min. Once a steady-state current was obtained, I/V relationships were determined using a protocol that consisted of 300 ms square pulses of the test potential (-100 mV to +100 mV) from a holding potential of -50 mV in 20-mV increments, with 1-second intervals (polarity given for cell interior).

All reported currents were normalized by cell capacitance and expressed as current density (pA/pF). Standard pipette solution contained (in mM): 140 NMDG-Cl, 1 $MgCl_2$, 2 EGTA, 10 HEPES, pH 7.2 (with NMDG) and an appropriate concentration of $CaCl_2$, to give free $[Ca^{2+}]_i$ = 0.1 µM. In some experiments high free $[Ca^{2+}]_i$ = 1 µM was used. Free $[Ca^{2+}]_i$ was estimated using MaxChelator software (Stanford University). Low intracellular Cl^- solution contained (in mM): 90 NMDG-glutamate, 50 NMDG-Cl, 1 $MgCl_2$, 2 EGTA, 10 HEPES, pH 7.2 with NMDG (free $[Ca^{2+}]_i$ = 0.1 µM). Increased Ca^{2+}-buffering pipette solution contained (in mM): 140 NMDG-Cl, 1 $MgCl_2$, 20 EGTA, 10 HEPES, pH 7.2 (with NMDG). Standard extracellular solution contained (in mM): 145 NaCl, 2 $CaCl_2$, 1 $MgCl_2$, 10 D-glucose, 10 HEPES, pH 7.4 (with NaOH). Na^+-free control extracellular solution contained (in mM): 145 NMDG-Cl, 1 $MgCl_2$, 10 D-glucose, 10 HEPES, pH 7.4 (with NMDG) and 3 $CaCl_2$, unless stated otherwise. In some experiments, NaCl was equimolarly replaced by either TRIS-Cl or CsCl. After whole cell configuration was obtained in standard solution, bath solution was immediately switched to Na^+-free control solution. After 3-5 min (time for proper dialysis of the cell interior) experimental protocols were initiated. Niflumic acid (NFA) was added to the bath solution for 5 min before initiating any experimental protocol. All solutions were delivered by continuous perfusion with a gravity-fed delivery system.

3.7.2. Whole cell experiments in hTRPV6 expressing HEK293 cells

Patch pipette filling solution contained (in mM): 140 NMDG, 1 $MgCl_2$, 20 EGTA and 10 HEPES, adjusted to pH 7.2 with HCl. Normal extracellular solution contained (in mM): 147 NaCl, 3 KCl, 1 $CaCl_2$, 2 $MgCl_2$, 10 D-glucose, 10 HEPES, adjusted to pH 7.4 with NaOH. Control solution with no divalent cations contained (in mM): 147 NMDG, 15 D-glucose, 10 HEPES, adjusted to pH 7.4 with HCl. After whole-cell configuration was obtained in normal solution, cells were initially bathed in control solution without divalent cations for 5 minutes to allow proper dialysis of the cell interior. During recordings, the bath solution was changed to a control solution supplemented with 2 mM test divalent cation (XCl_2; X = Ca^{2+}, Zn^{2+}, Cd^{2+}). Solutions were delivered by continuous perfusion with a gravity-fed delivery system. TRPV6-expressing cells were selected using a Diaphot 300 inverted patch clamp microscope (Nikon) equipped with an epifluorescent attachment (Elektro-Optika). Electrophysiological measurements were

performed as described by Bödding et al. [257], with minor modifications. Voltage clamp recordings were carried out using ramp commands (-110 mV to +90 mV in 200 ms, 1mV/ms) applied every 5 seconds, starting 40-60 seconds prior to the introduction of any test cations (background current detection). The holding potential was -20 mV between ramps.

3.8. YO-PRO-1 permeability assay in IB3-1 cells

Fluorescence was detected using a Zeiss LSM 510 META laser scanning microscope. YO-PRO-1 (MW: 629) fluorescence was measured from single cells in the field of view (usually 20–40 cells with 20X objective). Excitation and emission wavelengths were 480 nm and 509 nm, respectively. YO-PRO-1 (1 μM) was continuously present in all solutions during agonist application. Images were captured at 0.5 Hz. YO-PRO-1 fluorescence from individual cells was averaged to obtain mean response. All experiments were performed at room temperature.

3.9. ^{45}Ca uptake assay in HEK293 cells

Radioactive uptake assays were performed 48 hours after transfection, and the uptake rates were always measured in parallel for transfected and control cells. Cells were washed twice with nominally calcium-free, modified KRH solution. Afterwards, cells were exposed for a set time to 2 μCi ^{45}Ca in KRH solution containing 100 μM cold calcium with or without zinc. Calcium uptake was stopped by rinsing the cells with ice-cold KRH-solution. Cells were lysed in 1 ml 1N NaOH overnight. The samples were mixed with scintillation liquid, and measured in a liquid scintillation counter (Packard Tri-Carb 2100 TR). Protein concentration was determined by DC Protein Assay. Changes in ^{45}Ca uptake are displayed as deviations from the basal (prior to the addition of zinc) activity ratio of non-transfected vs. transfected cells.

3.10. Data presentation

Results were presented as means ± SEM of N observations. Statistical significance was determined using paired Student’s t-test or the non-parametric rank sum t-test.

Differences were considered statistically significant when $p < 0.05$. Non-linear curve fitting was performed using the Sigma-Plot 11.0 program.

4. Results

4.1. Extracellular pH and zinc regulate cytosolic [Ca^{2+}] and CaCC activity in airway epithelial cells

4.1.1. Effects of extracellular pH on intracellular calcium concentrations in IB3-1 cells

In previous studies it was shown that modifications of the extracellular ionic environment (Na^+ and/or H^+) might influence cytosolic Ca^{2+} levels [194]. Therefore first we investigated the effects of extracellular alkalinization on $[Ca^{2+}]_i$. In the presence of Na^+ (145 mM) alkalinization of pH_o (from 7.4 to 7.9 or 8.2) did not cause significant alterations in basal $[Ca^{2+}]_i$ (NaCl pH_o 7.4: 101.7 ± 0.7 % [N=16] vs. NaCl pH_o 8.2: 101.8 ± 2.3 % [N=5] p=n.s) (Fig. 15A). In subsequent experiments, extracellular Na^+ was substituted by a non-permeant large organic cation N-methyl-D-glucamine ($NMDG^+$). At pH_o 7.4, acute removal of external Na^+ did not cause a change in basal Ca^{2+} level (NaCl pH_o 7.4: 101.7 ± 0.7 % [N=16] vs. NMDG-Cl pH_o 7.4: 101.9 ± 1.1 % [N=5] p=n.s) (Fig. 15B). However, when the pH_o was raised to 7.9 with parallel replacement of extracellular Na^+, a mild but sustained elevation in intracellular Ca^{2+} levels could be observed (NaCl pH_o 7.4: 101.7 ± 0.7 % [N=16] vs. NMDG-Cl pH_o 7.9: 133.5 ± 3.5 % [N=5] $p < 0.05$) (Fig. 15B). Raising pH_o to an even higher level (from 7.4 to 8.2) elicited a markedly greater increase in intracellular calcium levels that reached a plateau within the first 3 minutes (NaCl pH_o 7.4: 101.7 ± 0.7 % [N=16] vs. NMDG-Cl pH_o 8.2: 239.8 ± 13.3 % [N=5] $p < 0.05$) (Fig. 15B). To investigate whether the increase in $[Ca^{2+}]_i$ was due to Ca^{2+} entry, we repeated the experiments with nominally Ca^{2+}-free solutions. Under these experimental conditions cells failed to respond with an increase in $[Ca^{2+}]_i$ (3 mM $CaCl_2$: 239.8 ± 13.3 % [N=5] vs. Ca^{2+}-depleted solution: 107.6 ± 1.1 % [N=5] $p < 0.05$ at pH_o 8.2 in the presence of NMDG-Cl) (Fig. 15C). Furthermore, withdrawal of extracellular Ca^{2+} during alkalinization abolished the sustained elevation of $[Ca^{2+}]_i$ suggesting that Ca^{2+} originated from the extracellular space (Fig. 15D). In contrast to the effects of extracellular alkalinization, lowering the pH_o (from 7.4 to 6.6) in the absence of extracellular Na^+ caused a mild, but

sustained decrease in $[Ca^{2+}]_i$ (NaCl pH_o 7.4: 101.7 ± 0.7 % [N=16] vs. NMDG-Cl pH_o 6.6: 85.9 ± 2.4 % [N=5] $p < 0.05$) (Fig. 15B).

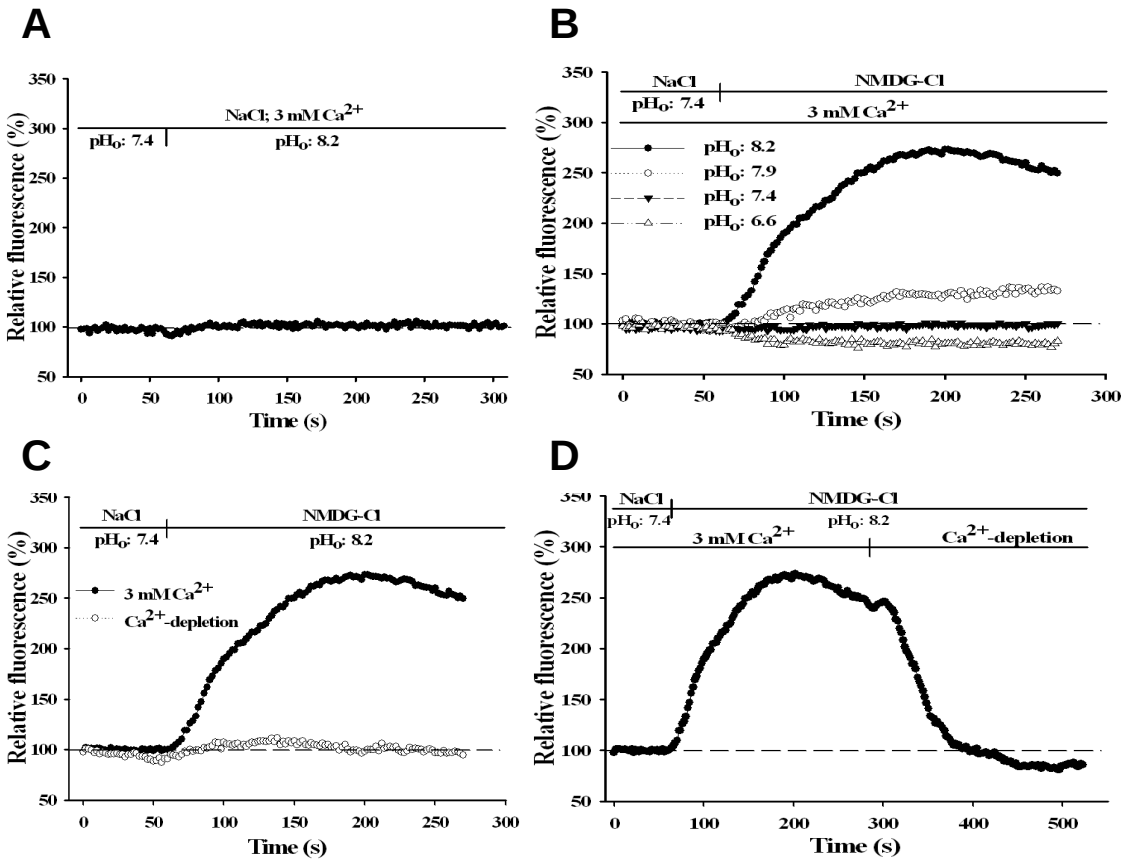

Figure 15. Representative traces showing the effects of different pH_o on relative Fluo-3 fluorescence representing $[Ca^{2+}]_i$ in IB3-1 cells. **(A)** The effect of extracellular alkalinization (pH_o 8.2) on $[Ca^{2+}]_i$ in the presence of $CaCl_2$ (3 mM). In the presence of Na^+, no change was detected in $[Ca^{2+}]_i$. **(B)** The effect of varying pH_o in the presence of $CaCl_2$ (3 mM) and following the withdrawal of Na^+. **(C)** Effect of alkalinization (pH_o: 8.2) on $[Ca^{2+}]_i$ in IB3-1 cells perfused with Na^+-free medium in the presence (3 mM) and in the absence of $CaCl_2$ (nominally Ca^{2+}-free). **(D)** The effect of removal of Ca^{2+} (from 3 mM to nominally Ca^{2+}-free) during alkalinization (pH_o: 8.2) in the absence of sodium. Each trace represents the sum of approx. 40 cells in one field of view. The fluorescence intensity of the trace prior to the application of any agonist/modification was considered as 100%. Each experiment was performed 5 times using cells from at least two different passages with similar results.

4.1.2. Effects of extracellular pH on whole-cell currents in the presence of different monovalent cations

To investigate whether the alkaline pH-induced Ca^{2+} signal could stimulate chloride efflux in these airway epithelial cells, we used the patch clamp technique in whole cell configuration. Control currents were recorded following substitution of external Na^+ by $NMDG^+$. At pH_o 8.2, we observed a slowly activating, large inward current that reached a plateau in approx. 2 min. This current was fully reversible upon resetting the pH_o to

7.4, and reversed near the equilibrium potential of Cl^- ($E_{rev.}$= -3.2 ± 0.7 mV [N=8] vs. E_{Cl^-} = -1.9 mV) (Fig. 16A-C).

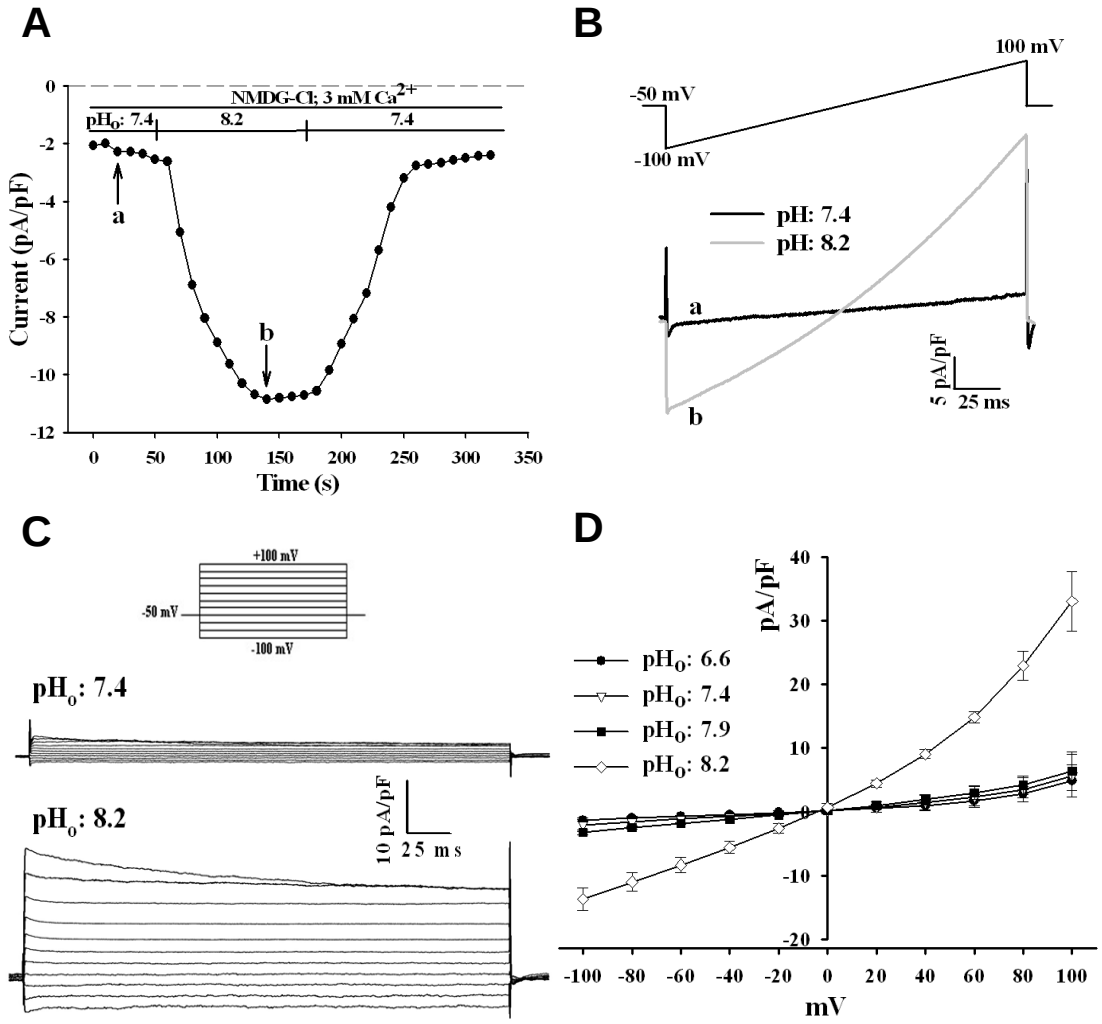

Figure 16. Alkaline pH_o-induced whole cell currents in the absence of extracellular Na^+. **(A)** Time course of inward current induced by alkalinization (pH_o: 8.2) in the presence of 3 mM $CaCl_2$, when extracellular Na^+ was substituted with $NMDG^+$. Currents were measured every 10 s at -80 mV during voltage ramps ranging from -100 to 100 mV in 200 ms. Standard pipette solution was used. **(B)** Original traces demonstrating current-voltage relationships during voltage ramps at pH_o: 7.4 and at pH_o: 8.2, measured at time points indicated in panel A (arrows). **(C)** Once steady-state current was obtained (indicated by arrows on panel A), voltage-step protocol (see materials and methods) was applied. The resultant currents are shown as representative traces. **(D)** I/V relationships showing summarized data of steady-state currents at varying pH_o (6.6, 7.4, 7.9, and 8.2) in the absence of extracellular Na^+. Data represent means ± SEM from 6-12 cells.

Following partial replacement of intracellular Cl^- with glutamate (see materials and methods), the reversal potential of the alkaline pH_o-induced current remained close to that of E_{Cl^-} (E_{rev}: -25.9 ± 1.7 mV [N=5] vs. E_{Cl^-}: -28.7 mV). These data suggest that inward currents measured at -80 mV represent chloride efflux. Moderate increase in pH_o

(7.9) did not elicit significant change in inward currents (Fig. 16D). In contrast, acidification of pH_o (6.6) resulted in a slight decrease in inward currents (Fig. 16D).

In order to show whether this stimulatory effect was not specific for $NMDG^+$, we replaced Na^+ with either $TRIS^+$ or Cs^+. Under these circumstances, alkaline pH_o (8.2) elicited a similar increase in inward current compared to that observed in the presence of $NMDG^+$, suggesting that this effect was independent of the nature and permeability features of the substituting cations (Fig. 17A). Additionally, the complete absence of Na^+ is a non-physiological condition; therefore, we tested the effects of alkaline pH_o at various extracellular Na^+ concentrations. External alkalinization did not elicit an increase in inward currents when external Na^+ concentration was near to physiological values (Fig. 17B).

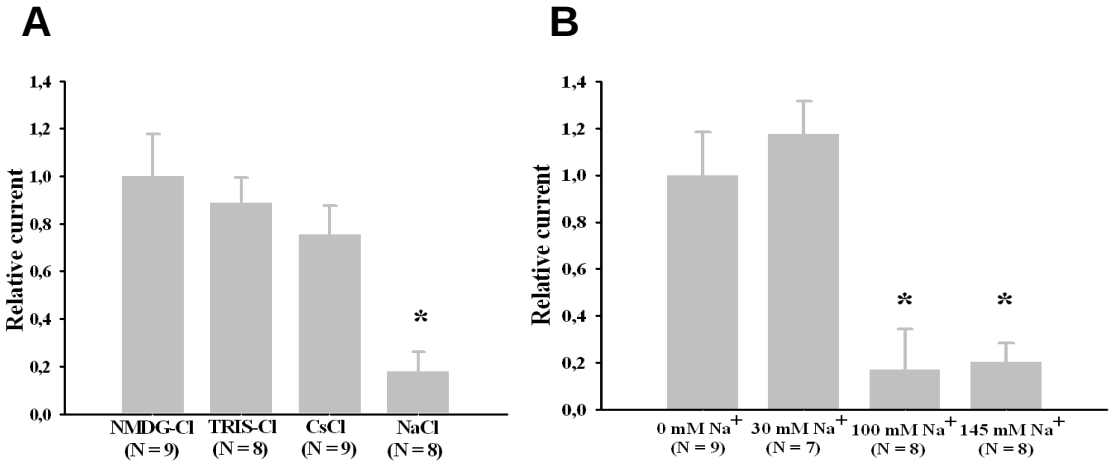

Figure 17. Alkaline pH_o-induced whole cell currents in the presence of different monovalent cations **(A)** Comparison of inward currents induced by extracellular alkalinization (pH_o: 8.2) in the presence of four different main extracellular cations, when NMDG-Cl is equimolarly replaced with TRIS-Cl, CsCl and NaCl (145 mM each). Currents are plotted relative to currents elicited in the presence of NMDG-Cl, *$p < 0.05$. **(B)** Comparison of alkalinization-induced inward currents in extracellular solutions containing different concentrations of Na^+. To maintain the constant ionic strength in the solutions, NMDG-Cl was equimolarly replaced with NaCl. Currents are plotted relative to currents elicited in the absence of Na^+, *$p < 0.05$.

4.1.3. Inward current is due to stimulation of calcium-activated chloride channels

We hypothesized that the observed Cl^- current was due to the activation of CaCCs in IB3-1 cells. The characteristic hallmark of CaCCs is the activation by intracellular Ca^{2+}. Experimentally, this can be achieved in whole cell configuration by stimulating cells with Ca^{2+}-mobilizing agonists, by Ca^{2+} ionophores such as ionomycin or by loading cells with Ca^{2+}-containing pipette solutions. Additionally, CaCC-mediated Cl^- current

can be inhibited by the intracellular inclusion of Ca^{2+} chelators (EGTA or BAPTA) or pharmacological blockers such as niflumic or flufenamic acid [258]. Therefore, the cell interior was dialyzed with pipette solution containing high (1 µM) free $[Ca^{2+}]_i$. Under these conditions we observed a significantly higher peak inward current compared to that obtained with standard (0.1 µM free $[Ca^{2+}]_i$) pipette solution (-2.1 ± 0.1 pA/pF [N=15] vs. -34.2 ± 3.5 pA/pF [N=7] $p < 0.05$ at -80 mV) (Fig. 18.). The resulting increase in current was prevented by 100 µM NFA, a potent inhibitor of CaCCs (-34.2 ± 3.5 pA/pF [N=7] vs. -4.6 ± 0.5 pA/pF [N=5] $p < 0.05$ at -80 mV) (Fig. 18.).

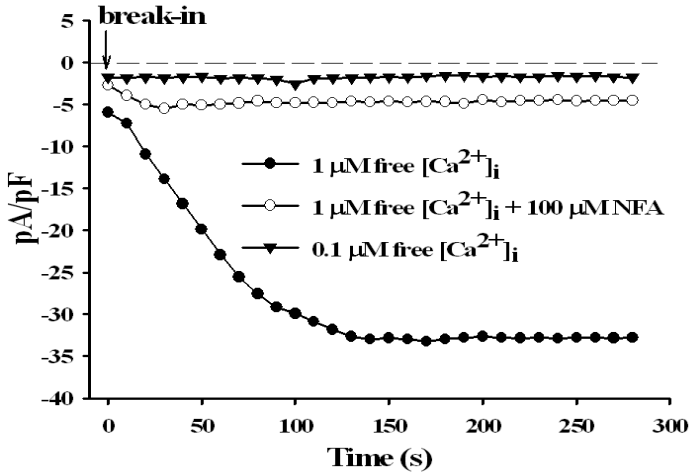

Figure 18. Demonstration of a Ca^{2+}-induced Cl^- conductance in IB3-1 cells. Time course of inward currents after cells were dialyzed with either 0.1 µM or 1 µM free $[Ca^{2+}]_i$ containing pipette solution. Cells were continuously perfused with Na^+-free control extracellular solution. In some experiments, NFA (100 µM) was added to the bath 5 min before whole cell formation (*break-in*). Currents were measured every 10 s at -80 mV during voltage ramps ranging from -100 to 100 mV in 200 ms. Representative traces are shown.

To test whether CaCCs were involved in the alkaline pH_o-induced increase of inward current, we first examined the dependency on external calcium. In NMDG-rich solution, at pH_o 8.2 the peak inward current (-11.0 ± 1.4 pA/pF [N=8] at -80 mV) was reduced when experiments were performed either in extracellular solution containing 0.1 mM Ca^{2+} (-2.1 ± 0.1 pA/pF [N=15] $p < 0.05$ at -80 mV) or by the application of 20 mM EGTA in the pipette solution (-1.1 ± 0.1 pA/pF [N=6] $p < 0.05$ at -80 mV) (Fig. 19A). These results indicate that Ca^{2+} entry from extracellular space plays a crucial role in the activation of the whole-cell inward currents in these CF airway epithelial cells.

Next, we examined whether NFA was able to inhibit the alkaline pH_o-induced inward current. As shown in Fig. 19B**,** the inward current was totally blocked by pretreatment

with 100 µM NFA, suggesting the involvement of CaCCs. In order to confirm these data, we used another inhibitor of Cl^- channels, DIDS (200 µM) which inhibited the inward current as well.

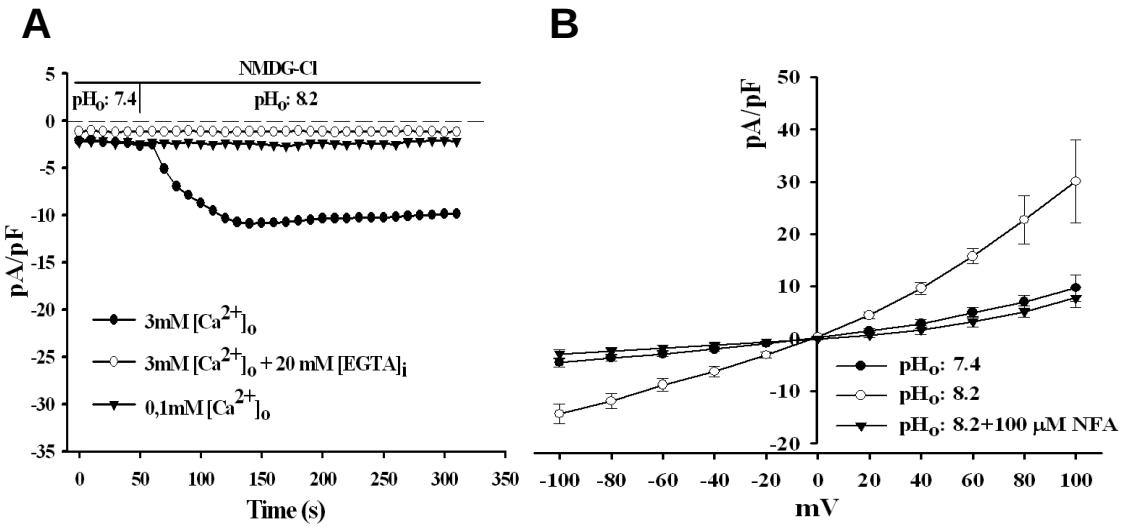

Figure 19. (A) Calcium dependency of inward currents induced by alkaline pH_o (8.2) in the absence of extracellular Na^+, but in the presence of 3 mM extracellular Ca^{2+}. Pipettes were filled either with standard or high Ca^{2+}-buffering (20 mM $[EGTA]_i$) intracellular solution. Experiments were also performed in Ca^{2+}-depleted (0.1 mM) extracellular solution (with standard pipette solution). **(B)** Summarized data showing the effect of the anion channel blocker NFA (100 µM) on the alkalinization-induced currents. Pipettes were filled with standard solution. Data represent means ± SEM from 6-12 cells.

4.1.2. Effect of zinc on intracellular calcium concentrations in IB3-1 cells

Our group has extensively investigated the effects of low micromolar Zn^{2+} (20 µM) in IB3-1 cells in the range of pH_o 7.3-7.9. We have previously found that in a Na^+-free, alkaline (pH_o 7.9) environment, Zn^{2+} elicited a sustained increase in $[Ca^{2+}]_i$, while in the presence of Na^+, zinc failed to induce changes in Ca^{2+} level regardless of pH_o [194]. Therefore, we tested Zn^{2+}-induced Ca^{2+} entry represented by the plateau phase of the Ca^{2+} signal at both pH_o 6.6 and 8.2 in the absence of Na^+. As shown in Fig. 20., at alkaline pH_o (8.2) Zn^{2+} elicited a sustained Ca^{2+} plateau, while at acidic pH_o (6.6) we observed only a transient increase in Ca^{2+} signal. These data indicate that Zn^{2+} promotes Ca^{2+} entry in a pH_o-dependent manner.

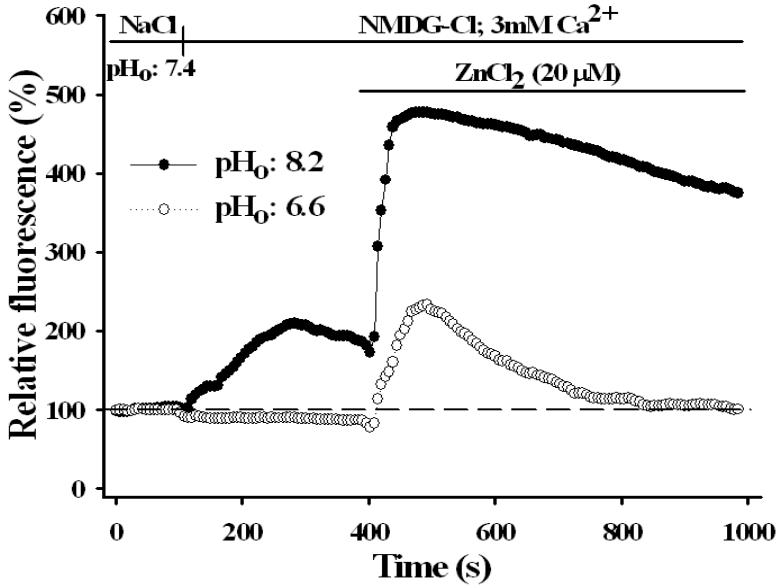

Figure 20. Representative traces showing the effect of pH_o on the Zn^{2+}-induced Ca^{2+}-signal in Na^+-free external solution. First, pH_o was changed to either 6.6 (open circles) or 8.2 (filled circles) with parallel substitution of extracellular Na^+ by $NMDG^+$ (in the presence of 3 mM $CaCl_2$). The cells were then challenged with 20 µM $ZnCl_2$ and the pattern of the Ca^{2+} signal was recorded.

4.1.5. Effects of zinc on calcium-activated chloride currents

If cytosolic [Ca^{2+}] were the only factor that determines CaCC activity, application of zinc in alkaline medium would result in large Cl^- currents. To our surprise, however, when cells were perfused with a Na^+ -free, alkaline solution in the presence of $ZnCl_2$ (20 µM), inward currents were transient and the maximal amplitude reached only approx. half the value of the current that we observed in the absence of Zn^{2+} (Fig. 21.).

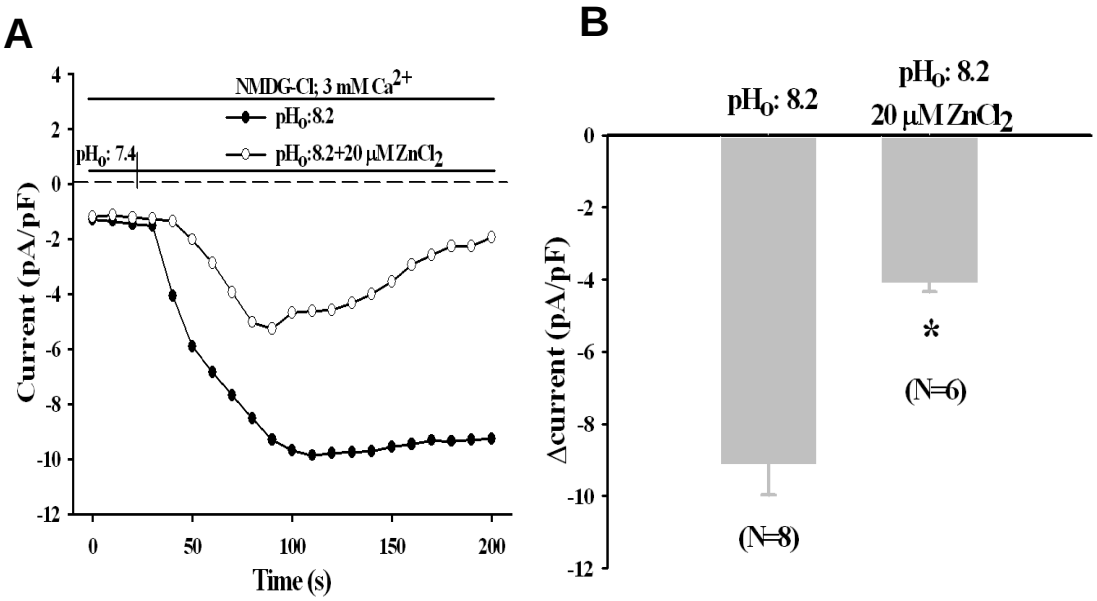

Figure 21. (A) Time course of inward currents induced either by alkalinization (filled circles) or by the simultaneous application of alkaline pH_o and 20 µM $ZnCl_2$ (open circles) in the absence of extracellular Na^+. Currents were measured every 10 s at -80 mV during voltage ramps ranging from -100 to 100 mV in 200 ms. Standard pipette solution was used. **(B)** Summarized data showing the maximal change in current amplitude detected at -80 mV during voltage ramps in the presence and absence of 20 µM $ZnCl_2$ according to results in Panel A, *$p < 0.05$.

We hypothesized that this effect of Zn^{2+} was due to direct inhibition of CaCCs. Indeed, application of Zn^{2+} (20 µM) exerted a strong inhibitory effect on steady-state currents induced by high (1 µM) free $[Ca^{2+}]_i$ containing pipette solution (Fig. 22A). Additionally, the inward current evoked by 1 µM free $[Ca^{2+}]_i$ was prevented by 5 min pretreatment with 20 µM Zn^{2+} (Fig. 22B). Taken together, these data show that although Zn^{2+} stimulates Ca^{2+} entry in airway epithelial cells it also effectively inhibits CaCCs.

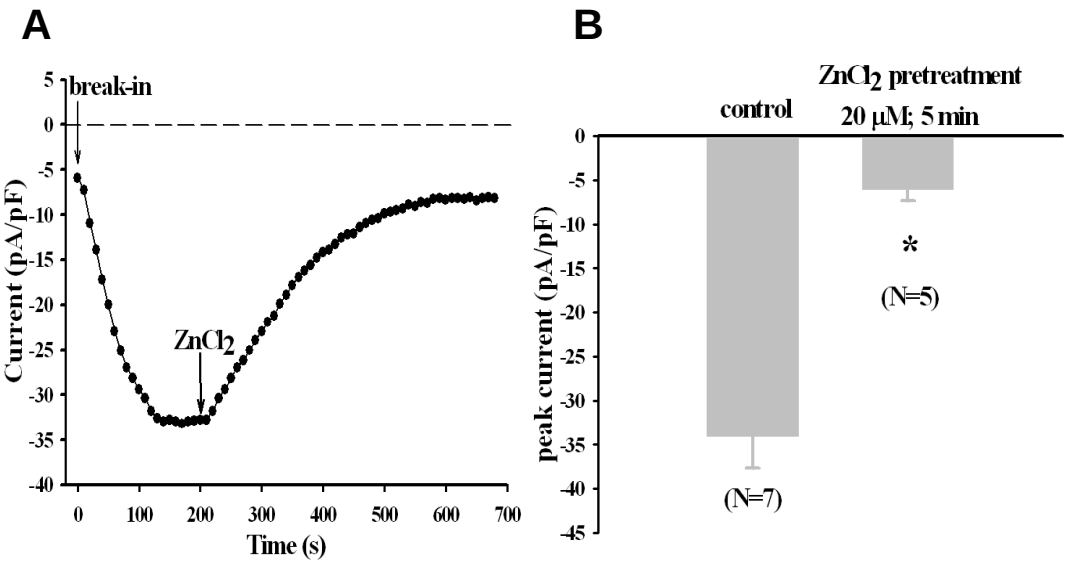

Figure 22. (A) The effect of 20 μM $ZnCl_2$ on Ca^{2+}-induced Cl^- currents induced by inclusion of 1 μM free $[Ca^{2+}]_i$ in the pipette solution. Zn^{2+} was applied at time point indicated by the arrow. Currents were measured every 10 s at -80 mV during voltage ramps ranging from -100 to 100 mV in 200 ms. **(B)** Bar graph showing the effect of pretreatment with $ZnCl_2$ (5 min, 20 μM) on peak current amplitude detected at -80 mV during voltage ramps, when pipette solution contained 1 μM free $[Ca^{2+}]_i$, *$p < 0.05$.

4.1.6. Effects of alkaline pH and zinc on cell viability

The continuous presence of alkaline pH_o, Zn^{2+} and the sustained increase in $[Ca^{2+}]_i$ may induce apoptosis of cells that can essentially be characterized by increased membrane permeability for large molecules such as the green fluorescent dye, YO-PRO-1. Therefore, we used the YO-PRO-1 uptake assay to examine the permeability properties of IB3-1 cells during exposure to high pH_o and Zn^{2+}. As it is shown in Fig. 23., neither elevations in pH_o alone, nor in concert with low micromolar (20 μM) Zn^{2+} caused a considerable increase in YO-PRO-1 fluorescence (neither cytoplasmic, nor nuclear) during the 30 min incubation time, as compared to the prompt effect of the permeabilizing agent TX-100 (Fig. 23.). These data suggest that exposure to these conditions can be well tolerated and does not lead to cell death within the investigated period.

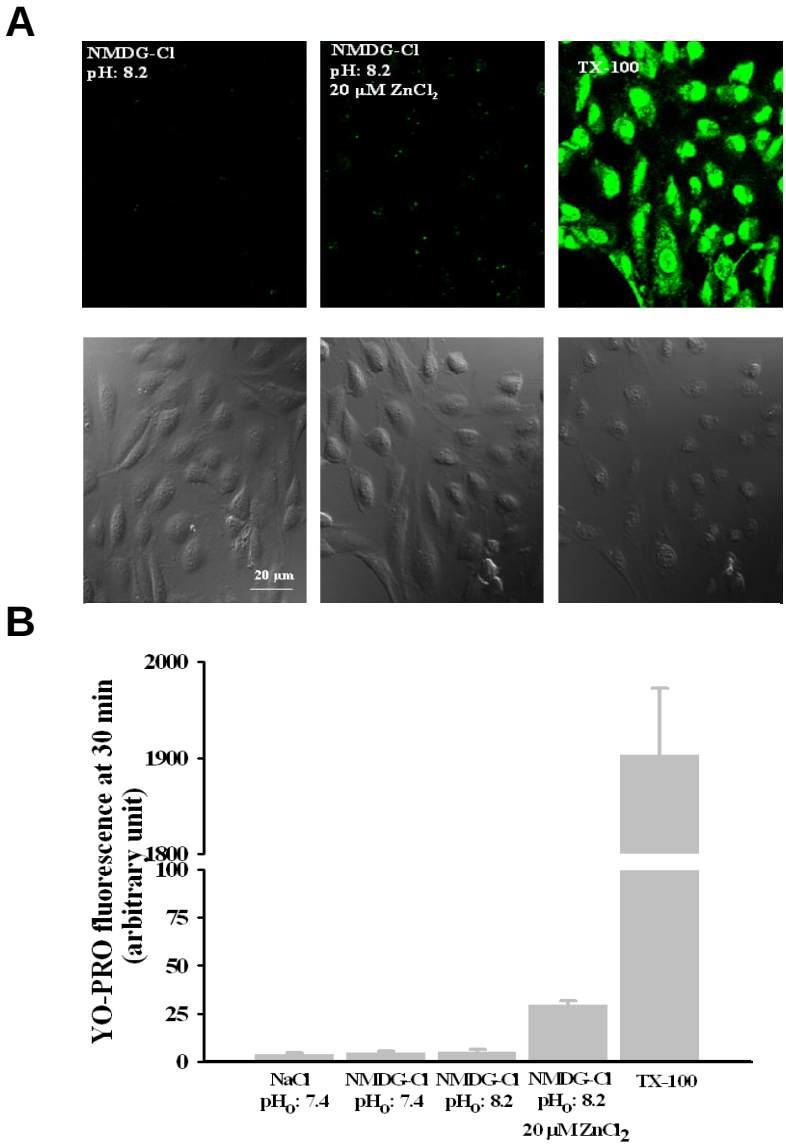

Figure 23. (A) Original images demonstrating the effect of varying extracellular conditions on the cellular uptake of YO-PRO-1. Cells were incubated in the continuous presence of YO-PRO-1 (1 µM) and 3 mM $CaCl_2$ in either Na^+-free alkaline (pH_o: 8.2) solution (*top left*), or with the simultaneous application of 20 µM $ZnCl_2$ (*top middle*) for 30 min at room temperature. The lack of YO-PRO-1 fluorescence in the cells (neither cytoplasmic, nor nuclear) indicates that the cells remain intact during our experimental conditions. *Top right* image: at the end of each experiment, 5 µl/ml of the permeabilizing agent TX-100 was added to the bath solution to initiate the entrance of YO-PRO-1 into the cells as it is confirmed by the strong nuclear labeling. *Bottom left, middle and right:* corresponding phase contrast images of the cells. **(B)** Summary of steady-state YO-PRO-1 fluorescence measured at 30 min in the presence of different extracellular conditions. Note the break and change in scale required for TX-100. Each bar represents the mean ± SEM of 4-6 experiments.

4.2. Zinc regulates and permeates human TRPV6 channels

4.2.1. Over-expression of hTRPV6 in HEK293 cells

First, we established a protein expression model to assess the permeability features of hTRPV6 channels. The presence of EYFP-hTRPV6 protein was determined by Western blot analysis. The protein lysates were probed with anti-GFP (Fig. 24A upper panel) or anti-TRPV6 (Fig. 24A lower panel) polyclonal antibodies. We observed an upper ~105 kDa band and a lower ~90 kDa band. Surface biotinylation experiments revealed that both forms of TRPV6 are present at the plasma membrane with the higher expression of the lower band (Fig. 24B) in our over-expression system. Pretreatment with PNGase F which cleaves all types of N-linked oligosaccharides resulted in a complete disappearance of both the upper and lower bands and appearance of a new more intense band ~85 kDa (Fig. 24B).

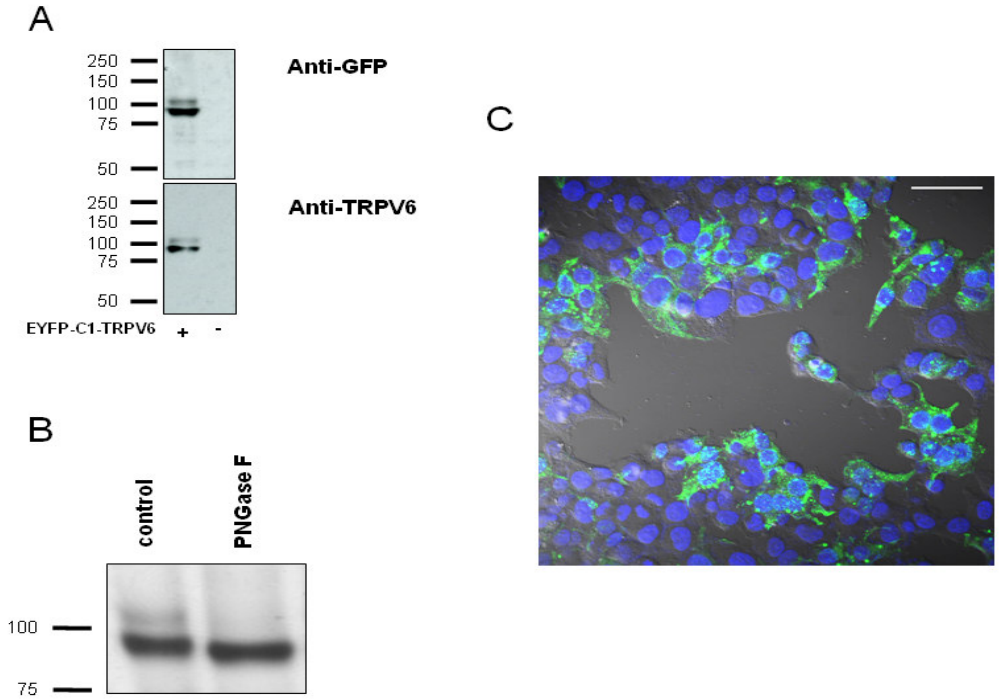

Figure 24. Expression of pEYFP-C1-hTRPV6 plasmid in HEK293 cells. **(A)** Western blot analysis using anti-GFP (top) or anti-TRPV6 (bottom) showing the expression of EYFP-hTRPV6 protein. **(B)** Deglycosylation experiments with PNGase F on surface biotinylated EYFP-hTRPV6 shows that TRPV6 is expressed in a fully glycosylated (upper band) and in an immature (lower band) form at the plasma membrane. **(C)** Representative fluorescence confocal image of HEK293 cells transfected with EYFP-TRPV6. EYFP-hTRPV6 (green), nucleus (blue). Scale bar is 50 μm.

These data suggest that the upper band is the fully glycosylated form of TRPV6 whereas the lower band represents the immature form of TRPV6. A representative immunofluorescence image shows the punctuated expression pattern of EYFP-TRPV6 overexpressed in HEK293 cells (Fig. 24C). Delineation of the plasma membrane could be observed in several cells.

4.2.2. Determination of hTRPV6 divalent cation permeability using different fluorescence dyes

When $[Ca^{2+}]_i$ was estimated with Fura-2, basal intracellular Ca^{2+} was elevated in EYFP-hTRPV6-transfected HEK cells compared to non-transfected cells (340/380 ratios: 3.227 ± 0.036 (cell number = 682) vs. 1.435 ± 0.01 (cell number = 421, Fig. 25A). When only EYFP was transfected into the cells, no difference was observed (Fig. 25B). Removal of extracellular Ca^{2+} almost completely abolished this significant difference (340/380 ratios: 1.1317 ± 0.005 vs. 1.269 ± 0.004). Re-administration of 1 mM Ca^{2+} evoked a much larger increase of $[Ca^{2+}]_i$ in EYFP-hTRPV6-transfected compared to non-transfected cells (Figs. 25A). In EYFP-transfected cells, the 1 mM Ca^{2+}-induced change was the same in both transfected and non-transfected cells (Fig. 25B).

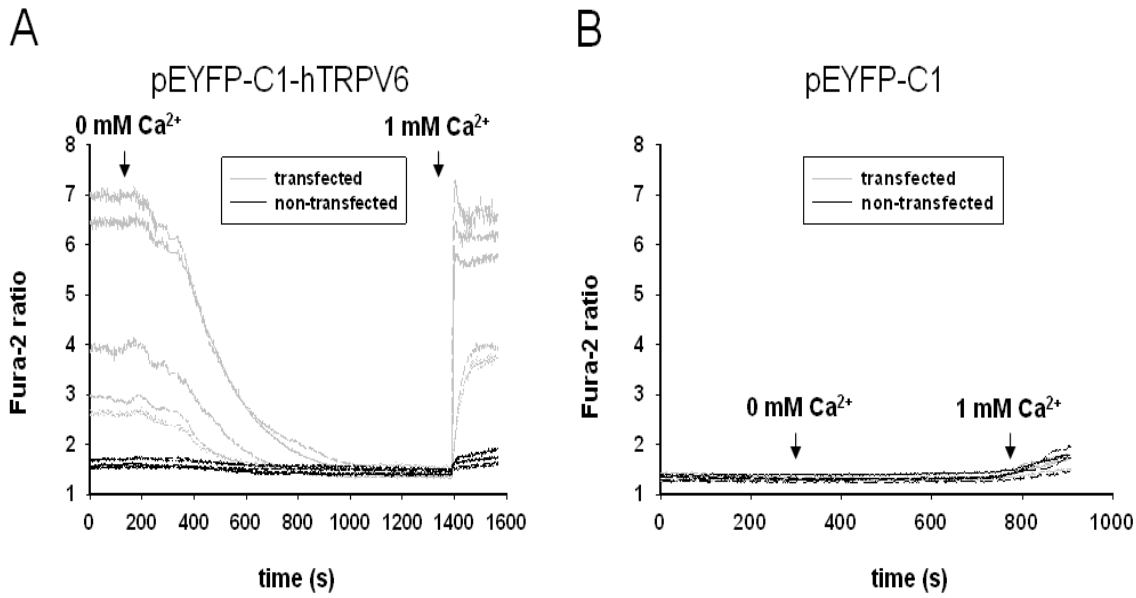

Figure 25. The expressed EYFP-hTRPV6 is fully functional as a calcium channel in HEK293 cells. Fura-2 tracings show that in EYFP-hTRPV6- **(A)** but not EYFP-expressing cells **(B)** both the basal $[Ca^{2+}]_i$ and the basal initial Ca^{2+} entry after re-administration of extracellular Ca^{2+} is significantly increased.

Next we aimed to test the permeability of TRPV6 channels for other divalent cations belonging to the calcium group elements (Ba^{2+}, Sr^{2+}). Our data show that when we substituted Ca^{2+} either with Ba^{2+} or Sr^{2+}, both divalent cations entered the cells through TRPV6 (Fig. 26A). This observation is in agreement with results from previous studies [223, 247].

Since zinc is an essential biometal of particular biological importance, we also attempted to determine whether Zn^{2+} is conducted by human TRPV6 channels. Administration of 1 mM Zn^{2+} caused a significant increase in fluorescence in TRPV6 expressing cells (Fig. 26B). For comparison, we also tested the permeation properties of TRPV6 for other members of the zinc group elements (Cd^{2+}, Hg^{2+}). These results demonstrated a greatly increased permeability to Cd^{2+} but not to Hg^{2+} in TRPV6 transfected cells (Fig. 26B).

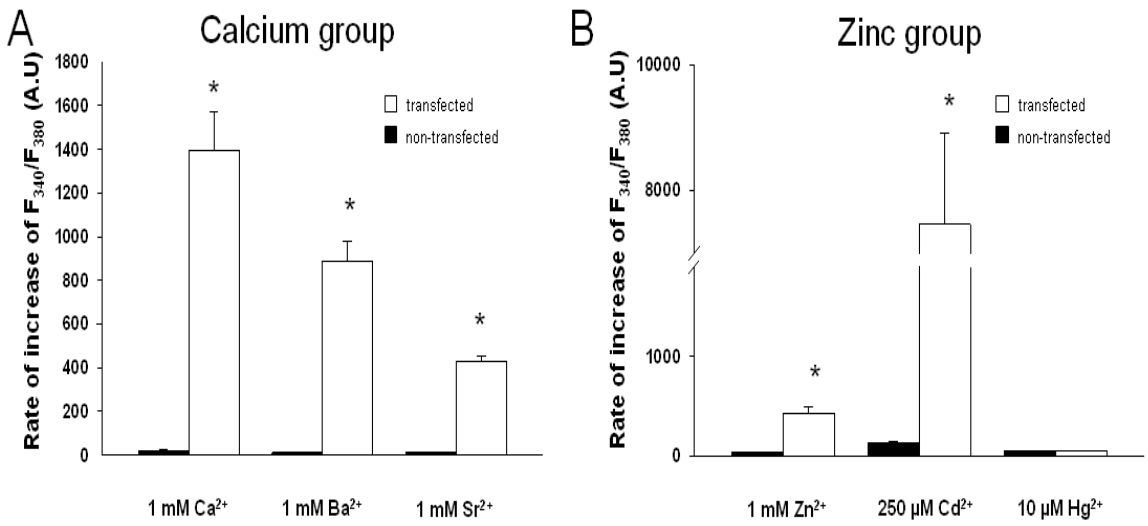

Figure 26. EYFP-hTRPV6 significantly increases the permeability of certain divalent cations in HEK293 cells. Bar graphs show the summarized data of Fura-2 calcium imaging experiments. Influx of Ca^{2+}, Ba^{2+}, and Sr^{2+} from the alkaline earth metals group **(A)**; Zn^{2+} and Cd^{2+} from group IIB **(B)**. Each group represents at least six separate experiments. $*p < 0.05$

Furthermore, we examined the effect of Ca^{2+} on Zn^{2+} influx through hTRPV6 using NewPort Green DCF, a calcium-insensitive fluorescence dye. For these measurements, we transfected HEK293 cells with a pTagRFP-C1-hTRPV6 construct to avoid the interference of EYFP and NewPort Green DCF fluorescence due to their very similar spectra. Transfection of RFP-hTRPV6 protein resulted in a punctuated distributional pattern, analogous to the pEYFP construct (see Fig. 24C in this section). Our results

showed that 1 mM Ca^{2+} significantly blocked the entry of Zn^{2+} (1 mM) through hTRPV6 (Fig. 27.).

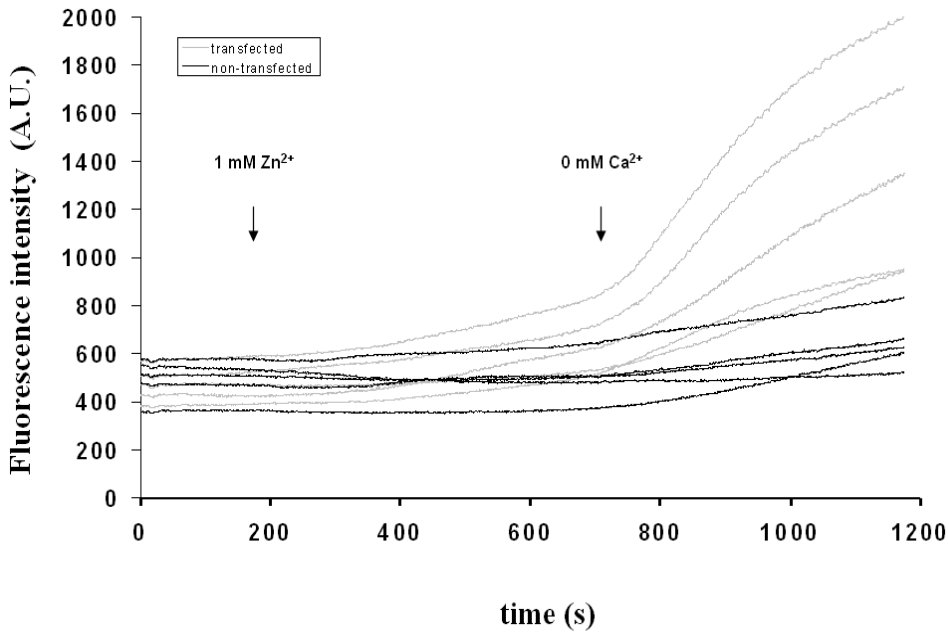

Figure 27. Effect of extracellular calcium on zinc influx mediated by hTRPV6. Representative tracings of NewPort Green DCF fluorescence intensity show that in the presence of 1 mM extracellular calcium, Zn^{2+} influx through hTRPV6 is significantly diminished.

Using Mag-Fura-2, a fluorescent dye that exhibit higher sensitivity for Zn^{2+} than Fura-2 (see methods), we tested the permeability of hTRPV6 for Zn^{2+} at low micromolar levels (1-10µM). However, we failed to detect any influx of Zn^{2+} at these concentrations (Figs. 28A and B).

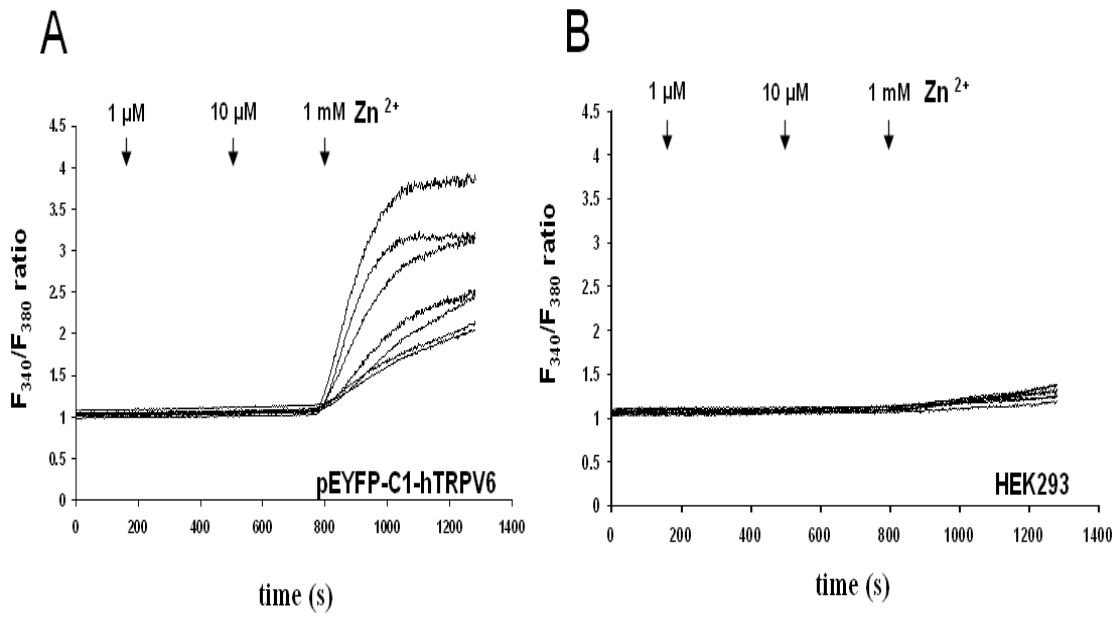

Figure 28. Representative tracings showing the effect of zinc and cadmium on Mag-Fura-2 fluorescence in pEYFP-C1-hTRPV6 expressing and non-transfected HEK293 cells. Administration of 1 mM, but neither 1 nor 10 µM Zn^{2+} induced large increase of Mag-Fura-2 ratio that was significantly more robust in hTRPV6 expressing cells compared to non-transfected cells **(A and B)**.

4.2.3. Measurement of hTRPV6 permeability properties with the patch clamp technique

To further confirm the previously obtained results with calcium and zinc, we used the patch clamp technique in whole-cell configuration. Divalent cation influx was detected by monitoring inward currents at -80 mV during voltage ramps. Initially, both EYFP-hTRPV6-transfected and non-transfected HEK293 cells were perfused with an extracellular solution lacking charge carriers (see Methods).

Supplementation of the solution with 2 mM Ca^{2+} evoked large, inwardly rectifying currents in EYFP-hTRPV6-transfected cells, while no such current was detected in non-transfected cells (Fig. 29A, B).

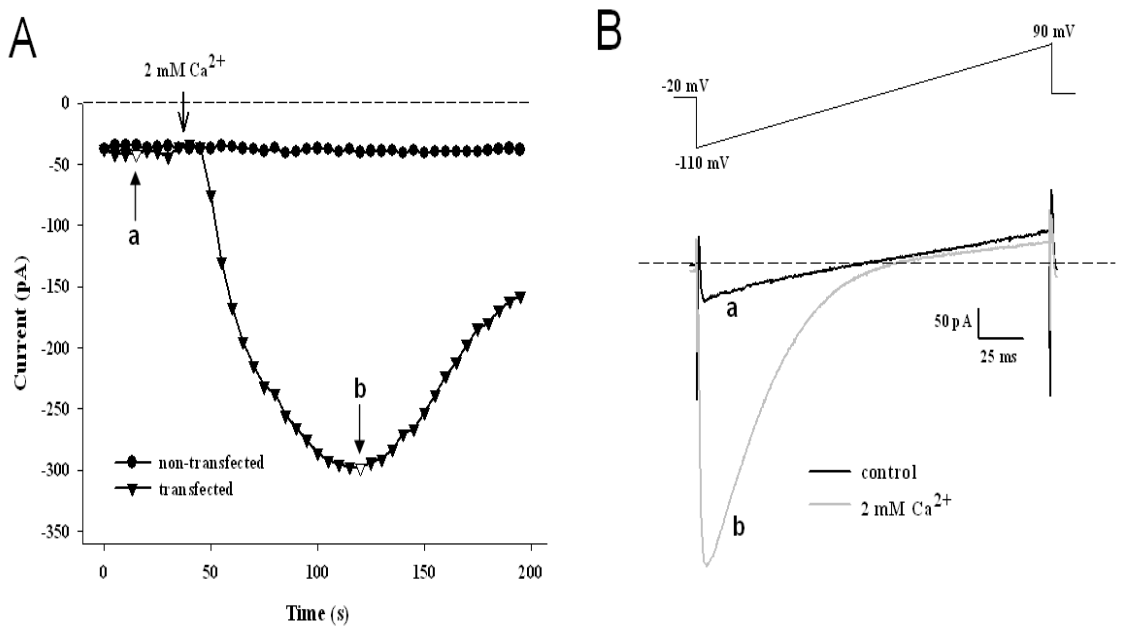

Figure 29. Inward currents obtained from EYFP-hTRPV6 expressing HEK293 cells. Currents were measured every 5 s at -80 mV during voltage ramps ranging from -110 to 90 mV in 200 ms. Cells were initially bathed in nominally divalent free solution. Test cation was administered at the time point indicated (arrow). The dashed lines represent zero current. **(A)** Time course of 2 mM Ca^{2+} evoked current that reached a peak value within 70 s and subsequently decreased until a steady-state level was reached. Only hTRPV6 expressing cells exhibited the inward current. Representative traces are shown. **(B)** Original traces demonstrating current-voltage relationship in the absence (control) and presence of 2 mM Ca^{2+}, measured at time point indicated in panel A. The Ca^{2+} current is inwardly rectifying and reverses at more positive potentials compared to control current.

Next, we found that Zn^{2+} (2 mM) produced a transient current with peak amplitude of 20-100 pA, suggesting that Zn^{2+} also permeates TRPV6 (Fig. 30A). The decay of this transient current may be due to inhibition of TRPV6 by Zn^{2+} itself. Following the transient increase in inward currents, the continuous presence of external Zn^{2+} reduced currents below control levels (Fig. 30A). This latter phenomenon is most likely due to the inhibition of basal Cl^- conductance by Zn^{2+} [259]. Cd^{2+} (2 mM) produced sustained inward currents similar to those observed in the presence of Ca^{2+} (Fig. 30B). Additionally, the Cd^{2+}-evoked current did not decay as fast as the Ca^{2+}-induced current but rather remained at a relatively high level.

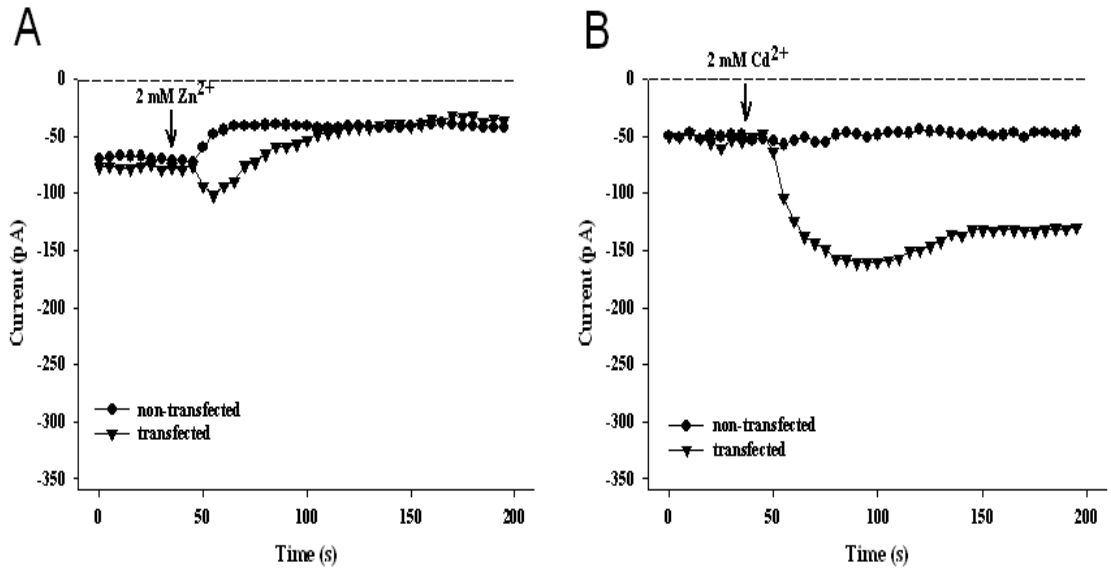

Figure 30. (A) Time course of 2 mM Zn^{2+} evoked inward current. It peaked within 30 s then decayed rapidly below control current values. Note that Zn^{2+} reduced basal inward currents in non-transfected cells suggesting that this inhibitory effect was independent of hTRPV6. Representative traces are shown. **(B)** Time course of 2 mM Cd^{2+} evoked inward current. It peaked within 50 s and subsequently decreased to a steady-state level. Representative traces are shown.

The maximal changes in current amplitudes during the experiments are summarized on Fig. 31.

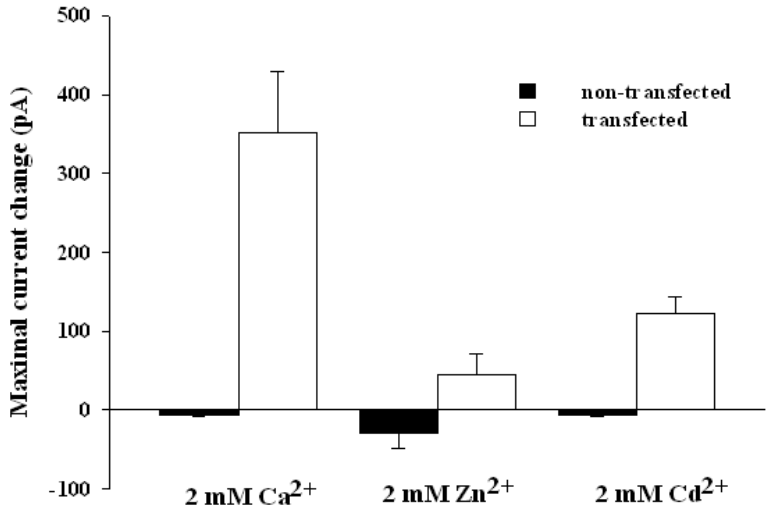

Figure 31. Summarized data showing the maximal change in current amplitude detected at -80 mV during voltage ramps in the presence of different divalent cations. Positive values represent an increase, while negative values represent a decrease in currents compared to control values. For transfected cells N = 10 (Ca^{2+}), N = 8 (Zn^{2+}), N = 6 (Cd^{2+}), and for non-transfected cells N = 4 for each test cation. Results are presented as mean ± SEM.

4.2.4. Modulation of calcium transport via hTRPV6 channels by zinc

We found that Zn^{2+} not only permeated but also modulated hTRPV6 channel activity in a biphasic manner. When we pretreated the cells with different concentrations of Zn^{2+}, high concentrations (200 and 2000 µM) inhibited, whereas low concentrations (2 and 20 µM) augmented the inward currents evoked by the administration of 2 mM Ca^{2+} (Fig. 32.). Importantly, in whole cell configuration we were not able to detect significant zinc-mediated inward current in the micromolar range (2-200 µM).

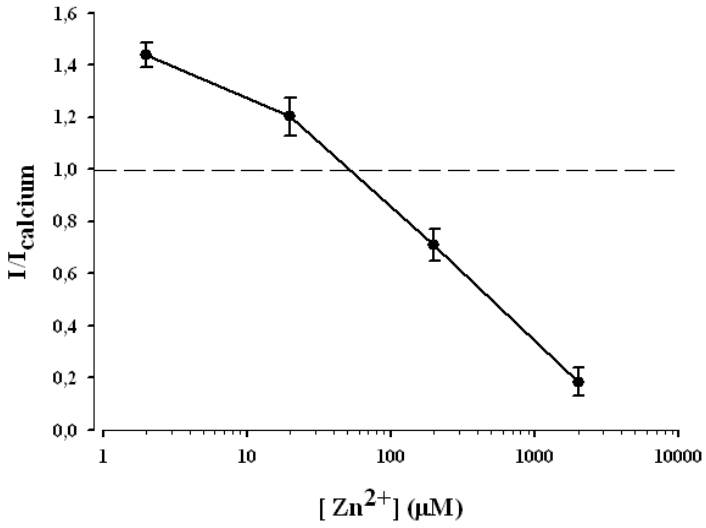

Figure 32. Inward Ca^{2+} current amplitude in TRPV6 expressing cells in the continuous presence of extracellular Zn^{2+}. In these experiments, Zn^{2+} was applied in increasing concentrations (from 2 µM to 2000 µM), prior to the addition of 2mM Ca^{2+}. Points represent mean ± SEM of 4-7 cells and are plotted relative to currents elicited in the absence of Zn^{2+} ($I_{calcium}$, dashed line) in the same cells.

To confirm our results of the electrophysiological measurements, we also used the ^{45}Ca uptake assay in the next experiments. First we established the optimal duration of ^{45}Ca uptake experiments in the cells. We found that radioactive Ca^{2+} uptake increased with time up to 10 minutes, whereupon the uptake plateaued (Fig. 33A). A two-minute incubation time was selected because the relative difference between the two groups was the largest in the increasing part of the curve at this time point.

Our data show that low concentrations of Zn^{2+} induced an increase, whereas high concentrations of Zn^{2+} inhibited ^{45}Ca uptake. These findings are in agreement with the results obtained with patch-clamp technique (Fig. 33B).

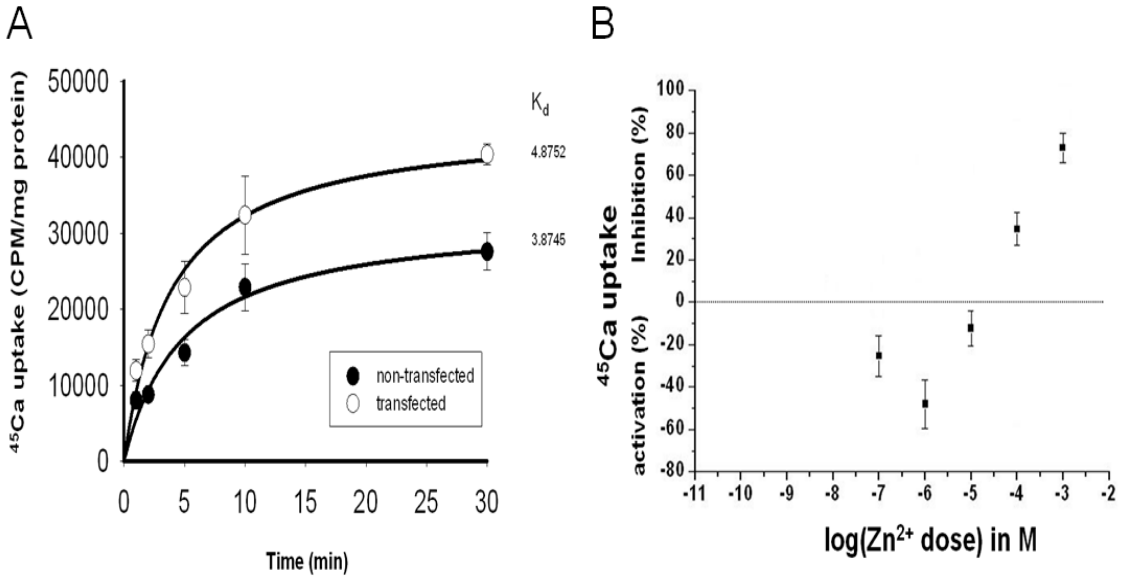

Figure 33. (A) Time course for ^{45}Ca uptake in EYFP-hTRPV6-transfected and non-transfected HEK293 cells. ^{45}Ca uptake experiments demonstrated increased Ca^{2+} uptake in EYFP-hTRPV6-expressing cells. Ca^{2+} uptake was saturated at about 10 min. For further inhibitor studies, a 2 min incubation time was chosen. (N=3) **(B)** Effect of Zn^{2+} on Ca^{2+} uptake via EYFP-hTRPV6 expressed in HEK293 cells. Summarized data shows that Zn^{2+} is a potent inhibitor of TRPV6 at high concentrations, whereas it enhanced TRPV6-mediated Ca^{2+} uptake at low concentrations.

5. Discussion

5.1. The role of zinc in epithelial chloride transport in human airways

Our group has previously shown that stimulation of human airway epithelial cells with zinc and/or ATP in an alkaline, low Na^+-containing medium ("enhanced calcium transfer solution") leads to a sustained increase in both $[Ca^{2+}]_i$ and Cl^- secretion [191, 194]. Furthermore, the same conditions induced sustained Cl^- secretion in the CF mouse nasal mucosa in vivo [194]. Results from studies using small interfering RNA technique revealed that Zn^{2+}-activated Ca^{2+} entry mechanisms mainly involve specific P2X purinergic receptor subtypes [193]. These observations suggested a possible therapeutic role for properly compiled saline aerosols supplemented with Zn^{2+} in patients with CF [260]. These interventions may increase Ca^{2+} influx from extracellular space followed by the activation of Ca^{2+}-mediated Cl^- secretion which could substitute for the lack of CFTR-mediated Cl^- transport in CF airways.

The Zn^{2+}-induced Ca^{2+} signal and ion secretion required essential modifications of the external milieu, such as a low-sodium, alkaline environment. Importantly, we have previously observed that alkalinization (from pH 7.4 to 7.9) in a sodium-free medium and prior to the addition of Zn^{2+}, caused a mild increase in basal $[Ca^{2+}]_i$ in airway epithelial cells [192, 194]. Raising external pH from 7.4 to 8.2 in physiologic saline solution caused a similar elevation in $[Ca^{2+}]_i$ in human neuroblastoma cells [261]. Additionally, in bacteria, extracellular pH and monovalent cations regulate intracellular Ca^{2+} levels through Ca^{2+} influx [262]. These observations suggested that the revealed mechanism is not unique for airway epithelial cells. These data also suggested that stimulation of Ca^{2+} entry could be achieved in CF cells without using specific purinergic agonist (ATP) and/or modulator (Zn^{2+}). Therefore our aim was to examine whether changes in external pH could alter cytosolic Ca^{2+} levels sufficiently to stimulate CaCC activity in CF airway epithelial cells. We found that in CF airway epithelial cells, alkaline pH_o (8.2) elicited Ca^{2+} entry only in Na^+-free environment. The alkaline pH_o-induced increase in $[Ca^{2+}]_i$ resulted in the activation of Ca^{2+}-dependent inward Cl^- currents. The mechanism as to how the alkaline pH_o is working is not yet clear. Extracellular pH is a well-known modulator of plasma membrane Ca^{2+} channels and

consequently the intracellular Ca^{2+} homeostasis [263]. Ca^{2+} entry can occur through voltage-dependent Ca^{2+} channels, P2X receptors, store-operated Ca^{2+} channels (SOCs), receptor-operated Ca^{2+} channels (ROC), transient receptor potential Ca^{2+} channels (TRPs) and Na^{+}/Ca^{2+} exchangers (NCX) (in reverse operation mode). With respect to their responsiveness to changes in pH_o, most of the Ca^{2+} entry mechanisms studied so far, appear to share common characteristics: extracellular acidification attenuates whereas alkalinization stimulates Ca^{2+} influx [264]. These data are in strong correlation with the early observation that transepithelial Ca^{2+} transport is inhibited in conditions associated with overproduction of acids [265]. In fact, we have found that extracellular acidification caused a mild but sustained decrease in both $[Ca^{2+}]_i$ and CaCC activity. Interestingly, in the presence of physiologic Na^{+} concentrations (145 mM), alterations in pH_o did not cause significant changes in $[Ca^{2+}]_i$. These data suggest that in airway epithelial cells, pH_o-dependent changes of Ca^{2+} homeostasis occur only in the absence of Na^{+}. Removal of extracellular Na^{+} could induce the reverse operation mode of the NCX. However, NCX was found to be insensitive to external alkalinization between 7.3 and 9.0 [266]. Furthermore, we have previously demonstrated that IB3-1 cells did not possess NCX [194]. We also asked whether increasing the extracellular pH with parallel removal of sodium could induce a significant change in intracellular pH (pH_i). Our unpublished observations suggested that in Na^{+}-free medium, increasing the external pH from 7.4 to 8.2 caused a change of pH_i less than 0.1 units. Thus, under these conditions IB3-1 cells seem to be quite “resistant” to external alkalinization. In addition, in the patch clamp experiments we used Hepes (10 mM) in the standard pipette solution which has been shown to adequately buffer pH_i following changes in pH_o [165].

Extracellular sodium may be another important regulator of Ca^{2+} entry pathways. Previous studies suggest that extracellular Na^{+} may inhibit the channels by competing with Ca^{2+} within the permeation pathway [191, 267]. In addition, Ma and his colleagues have reported that extracellular Na^{+} inhibited the P2XR-mediated Ca^{2+} influx by binding to the extracellular site on the $P2X_{cilia}$ receptor in rabbit airway ciliated cells [268]. Using different substituting cations ($NMDG^{+}$, $Tris^{+}$ and Cs^{+}) we have abolished the Na^{+}-dependent inhibition of alkaline pH_o-induced Ca^{2+} influx. Our data underline the specific role of Na^{+} in these processes. Therefore, we suggest that increasing pH_o with a parallel decrease of extracellular Na^{+} concentration effectively enhance Ca^{2+}

entry. We might speculate that changes in surface potential caused by the binding of H^+ to negative charges on the cell surface are sensed by gating mechanism of Ca^{2+} permeable channels [163, 165]. If these channels are non-selective cation channels, inhibitory effects of extracellular Na^+ could also be explained.

The sustained nature of Ca^{2+} signal induced by external alkalinization may not simply effectuate CaCC channel opening, but may also establish a favorable electrical gradient for Cl^- efflux. This might be achieved by the stimulation of Ca^{2+}-dependent K^+ channels as well as the inhibition of ENaC channels, both leading to the hyperpolarization of cell membrane potential [269]. However, sustained increases in intracellular Ca^{2+} levels might be harmful because of possible induction of apoptosis. Therefore, therapeutic approaches must be carried out in a controlled manner. We demonstrated that the effects of alkaline pH_o on Cl^- secretion are reversible upon resetting the pH to basal value (7.4). Additionally, cell viability assayed by YO-PRO-1 uptake did not change significantly, suggesting that the examined conditions can be well tolerated and does not induce significant apoptosis within the investigated period.

As it was shown, the amplitude of the alkaline pH_o-induced Ca^{2+} signal was approximately the half of that induced by zinc in sodium-free environment. Nevertheless, this alkaline pH_o-induced moderate elevation in bulk cytosolic $[Ca^{2+}]$ appeared to be sufficient to induce CaCC-mediated Cl^- efflux. We speculate that under whole-cell conditions, CaCCs may sense and react to local Ca^{2+} changes in the subplasmalemmal space rather than changes in the bulk cytosol, as it was previously suggested (see introduction) [100]. On the other hand, since CaCC activity is directly proportional to intracellular Ca^{2+}, higher Ca^{2+} levels should lead to greater increase in CaCC activity. Surprisingly we found that although Zn^{2+} enhanced significantly larger Ca^{2+} entry at alkaline pH_o, the evoked CaCC currents were small and transient compared to those observed in the absence Zn^{2+}. Therefore, the effect of Zn^{2+} on CaCC currents was in marked contrast with the effect of zinc on intracellular calcium levels. Based on these data, we hypothesized a direct interaction between zinc and the channel protein. Indeed, we could demonstrate that zinc inhibits CaCC-mediated currents in CF airway epithelial cells evoked by the inclusion of 1µM free calcium in the intracellular solution at low micromolar concentration. This finding is in agreement with recently published data, showing that CaCC activity was significantly blocked by extracellular

Zn^{2+} at low concentrations in *Xenopus* oocytes [179]. Furthermore, zinc-induced inhibition of different Cl^- channels has been shown earlier [4, 27, 30, 31]. Thus, we assume that several factors such as concentration of Zn^{2+}, composition of external solutions and the type of anion channels might determine the net effect of Zn^{2+} on Cl^- conductance. Nonetheless, based on our results we speculate that the inclusion of Zn^{2+} might be unnecessary in a sufficiently alkaline saline vehicle.

5.2. The possible role of zinc in TRPV6-mediated epithelial ion transport

TRPV6 is known to be the most highly calcium-selective member of the vanilloid transient receptor channel family. Although many studies have been conducted to investigate the role of TRPV6 in fetal and adult Ca^{2+} homeostasis, there is only scant information available about TRPV6 as a potential transporter of other divalent cations. However, there are several findings that suggest that mammalian TRPV6 can transport other cations such as Zn^{2+}, Cd^{2+}, etc. Firstly, the common ancestor of TRPV5 and 6 in fish was found to be permeable to Zn^{2+} [242, 244]. Secondly, expression of a divalent metal channel in rat and pig small intestine that transports Zn^{2+}, Ca^{2+}, Ba^{2+}, and Mn^{2+} was also reported [246]. Thirdly, increased intestinal absorption of Cd^{2+} and Zn^{2+}, as well as increased TRPV6 expression was observed in mice kept on a calcium-deficient diet [270, 271]. These data suggest that TRPV6 is permeable not only to Ca^{2+} but also to other divalent cations in the duodenum.

When we tested the expression of our tagged TRPV6 protein in HEK293 cells, we found that TRPV6 protein was expressed at the plasma membrane 48 hours after transfection. No endogenous TRPV6 was detected in non-transfected cells. We could also confirm that the TRPV6 expressed at the plasma membrane was functional, as basal $[Ca^{2+}]_i$ and basal Ca^{2+} entry measured with Fura-2 was significantly higher (70-fold difference) in transfected cells. The ^{45}Ca uptake experiments also showed that transfected cells had higher Ca^{2+} permeability but the Ca^{2+} entry was only twice that of non-transfected cells. This shows that TRPV6 was continuously open under our experimental conditions. The difference between the Fura-2 measurement and the ^{45}Ca uptake assay in terms of TRPV6 activity is probably due to an increase in Ca^{2+} buffering capacity by Fura-2, as previously suggested [272]. Fura-2 is sensitive not just to Ca^{2+} but also to other divalent cations. Importantly, we were able to demonstrate that

indeed Ba^{2+} and Sr^{2+} are transported by TRPV6, as previously reported [273]. We also tested whether elements of periodic group IIB (Zn^{2+}, Cd^{2+}, and Hg^{2+}) could be conducted by TRPV6. Zinc is an important trace element and is involved in a variety of physiological and biochemical functions. In contrast to zinc, cadmium and mercury are highly toxic to the human body. Since TRPV6 resides in the duodenal and placental epithelia, it could play an important role in zinc homeostasis and/or cadmium, mercury toxicity.

Our results with Fura-2 showed that both Zn^{2+} and Cd^{2+} but not Hg^{2+} were transported by TRPV6 overexpressed in HEK293 cells. These data suggest that hTRPV6 is permeable for Zn^{2+} and Cd^{2+} in a mammalian expression system. Using the calcium-insensitive dye, NewPort Green DFC, we aimed to test how extracellular [Ca^{2+}] affects Zn^{2+} influx through TRPV6. We observed that Zn^{2+} influx can be significantly diminished by equimolar extracellular [Ca^{2+}]. These experiments also confirmed that hTRPV6 channels are indeed permeable for Zn^{2+}. Additionally, we could not demonstrate TRPV6-dependent Zn^{2+} transport at low micromolar concentration. The negative results with Zn^{2+} could be explained with the observation that equimolar Ca^{2+} significantly diminished Zn^{2+} influx via TRPV6 and that distilled water contains Ca^{2+} in the micromolar range.

Ragozzino et al. reported that Zn^{2+} permeated nicotinic acetylcholine receptors, while blocking Na^{+} influx through the channels [39]. In fact, our data show that Zn^{2+} evoked significantly smaller currents and fluorescence signal compared to Ca^{2+} or Cd^{2+}, suggesting that, while Zn^{2+} permeates, it can also interact with TRPV6 and inhibit the channel. The transient nature of the inward Zn^{2+} current further supports the idea that Zn^{2+} ions interact with TRPV6 channels, blocking the permeation pathway.

TRP channels represent a major pathway for cation movement in non-excitable cells. Members of this ion channel family respond to various stimuli encoded within the external environment, such as temperature, osmotic conditions, pH and divalent cation concentration [274]. Regulation by external pH and divalent cations was clearly demonstrated on TRPM6 and TRPM7 channels, which are also known to be permeable for Zn^{2+} [275]. The TRPV5 channels, that are closely related to TRPV6 protein, exhibit significant sensitivity to both external and internal pH [276]. Nevertheless, it is unknown yet whether TRPV5 channels might be regulated by external divalent cations

as well. Recently it has been demonstrated that the activity of TRPM1 and TRPM2 channels is modulated by external Zn^{2+} [15, 16]. Furthermore, Zn^{2+} might also regulate Ca^{2+} uptake into cells through other entry mechanisms, such as nicotinic acetylcholine receptor channels, voltage-gated channels, or ATP-gated P2X purinergic receptor channels [39, 195, 277]. In our study, both inward Ca^{2+} current and ^{45}Ca uptake were inhibited by Zn^{2+} at high micromolar or millimolar concentration. Interestingly, Zn^{2+} at low micromolar concentration increased TRPV6-mediated Ca^{45} uptake and inward Ca^{2+} currents. These results suggest that the TRPV6 structure might contain two distinct Zn^{2+} binding sites: one activatory, high affinity and one inhibitory, low affinity. Similar phenomenon has been observed in another member of the TRP superfamily, the transient receptor potential ankyrin type 1 (TRPA1) channel [278]. Thus, we suggest that Zn^{2+} might play a pivotal role in regulation and fine tuning of TRPV6 channel-mediated transepithelial Ca^{2+} transport in various organs, such as the intestine and placenta.

These findings could be especially important for intestinal physiology. Our results suggest that hTRPV6 represents a novel mechanism through which Zn^{2+} or other dietary trace metals can be taken up into the enterocytes, particularly under low dietary Ca^{2+} conditions. Furthermore, under calcium-restricted conditions, the increased expression of duodenal TRPV6 could enhance susceptibility to heavy metal poisoning. In mice kept on a calcium-deficient diet, Cd^{2+} accumulation in the liver and intestinal expression of TRPV6 were significantly increased compared to animals on a normal diet [270, 271]. Moreover, Cd^{2+} inhibited vitamin-D_3-sensitive Ca^{2+} uptake in rat intestine when animals were kept on a low but not on a normal Ca^{2+} diet [279]. Dietary Ca^{2+} also affects intestinal absorption of heavy metals in humans. An example of chronic Cd^{2+} poisoning was the case of Itai-itai disease that affected a particularly sensitive population in the Toyama district in Japan that lived on calcium-deficient diet and consumed poisoned rice [280].

6. Conclusions

Our results indicate an important role for extracellular zinc in epithelial transport processes. Firstly, Zn^{2+} exhibits a dual effect on Ca^{2+}-dependent Cl^- channels in CF airway epithelial cells. It enhances Ca^{2+} entry at alkaline pH_o that could activate CaCCs. On the other hand, Zn^{2+} directly inhibits CaCCs resulting in reduced and transient Cl^- conductance. Furthermore we provide evidence that extracellular alkalinization per se could elicit Ca^{2+} entry and evoke Ca^{2+}-activated Cl^- conductance without the additional application of any other agonists such as ATP or Zn^{2+}. Although this effect of alkaline pH_o is strongly dependent on external Na^+ concentration, our results suggest that an optimally composed saline aerosol might have significant therapeutic effects in cystic fibrosis. Secondly, we demonstrate that Zn^{2+} regulates the function of human TRPV6, a channel essential for the absorption of Ca^{2+} from the intestines. Zn^{2+} at high (millimolar) concentrations inhibits, while at low (micromolar) concentrations enhances Ca^{2+} transport through hTRPV6 channels. These findings suggest that dietary Zn^{2+} intake might play an important role in hTRPV6 channel-mediated transepithelial Ca^{2+} transport. Furthermore, the hTRPV6 channels are also permeable for Zn^{2+} in the absence of Ca^{2+}, representing a novel pathway for Zn^{2+} absorption under calcium-restricted conditions.

7. Summary

Zinc is an important trace element that plays a fundamental role in a variety of physiological and biochemical processes. Bidirectional transport of electrolytes and water is one of the main functions of epithelial tissues in the gastrointestinal tract and in the airways. The main purpose of the present thesis was to elucidate the effect of extracellular Zn^{2+} on important epithelial transport processes, such as Cl^- secretion in cystic fibrosis (CF) airway epithelial cells and divalent metal cation transport by the intestinal Ca^{2+} transporter channel human TRPV6, respectively. Firstly, we investigated the role of Zn^{2+} in different extracellular ionic milieu on the activity of Ca^{2+}-dependent Cl^- channels in CF airway epithelial cells. Then, we tested the effect of extracellular Zn^{2+} on hTRPV6-mediated Ca^{2+} transport in transiently expressing HEK293 cells. Our results indicate that: (1) Zn^{2+} exerts a dual effect on Ca^{2+}-dependent chloride channels (CaCCs) in CF airway epithelial cells. Zn^{2+} indirectly enhanced, however directly blocked the activity of CaCCs. Nonetheless, extracellular alkalinization per se could elicit Ca^{2+} entry and evoke Ca^{2+}-activated Cl^- conductance without the application of Zn^{2+}. These findings suggest that a sufficiently alkaline, Zn^{2+}-free saline aerosol might be also beneficial for CF patients; (2) Zn^{2+} modulates hTRPV6 function in a dose-dependent manner. High concentrations of zinc inhibit, whereas low concentrations enhance Ca^{2+} transport via hTRPV6 channels. These findings suggest that dietary Zn^{2+} intake might play an important role in hTRPV6 channel-mediated transepithelial Ca^{2+} transport in the intestines. Furthermore, the hTRPV6 channels are also permeable for Zn^{2+} in the absence of Ca^{2+}, representing a novel pathway for Zn^{2+} absorption under calcium-restricted conditions.

8. Összefoglalás

A cink fontos biológiai nyomelem, mely számos élettani és biokémiai folyamatban tölt be központi szerepet. Az intesztinális, valamint légúti hámszövet alapvető funkciói közé tartozik az elektrolitok szekréciója, illetve abszorpciója. A jelen disszertáció célja az volt, hogy feltárja az extracelluláris Zn^{2+} hatását néhány fontosabb epiteliális transzportfolyamatra, így a cisztás fibrózisos (CF) légúti hámsejtek Cl^- szekréciójára, illetve a humán TRPV6, egy intesztinális Ca^{2+} csatorna divalens fémion transzportjára. Első kísérleteinkben különböző extracelluláris ionkörnyezetben vizsgáltuk a Zn^{2+} hatását Ca^{2+}-függő Cl^- csatornák aktivitására CF légúti hámsejtekben. További kísérleteinkben az extracelluláris Zn^{2+} hatását tanulmányoztuk a hTRPV6 csatornán keresztül történő Ca^{2+} transzportra, a csatornafehérjét tranziensen expresszáló HEK293 sejtekben. Eredményeink azt mutatják, hogy (1) a Zn^{2+} kettős hatást fejt ki a Ca^{2+}-függő Cl^- csatornák aktivitására CF légúti hámsejtekben. A cink alkalmazása közvetve fokozza, míg közvetlenül gátolja a Cl^- csatornák aktivitását. Ugyanakkor az extracelluláris alkalinizáció önmagában, Zn^{2+} adása nélkül is Ca^{2+} beáramlást idéz elő, mely elégséges Ca^{2+}-függő Cl^- csatornák aktiválásához. Jelen megfigyeléseink alapján feltételezhető, hogy egy megfelelően alkalikus, Zn^{2+}-mentes oldat inhalációja is kedvező hatást fejthet ki cisztás fibrózisos betegek légúti panaszaira. (2) A Zn^{2+} dózisfüggő módon modulálja a hTRPV6 csatornák funkcióját. Magas koncentrációjú cink gátolja, míg az alacsony koncentrációk fokozzák a hTRPV6 csatornákon keresztüli Ca^{2+} transzportot. Jelen eredmények arra utalnak, hogy az étrend Zn^{2+} tartalma jelentősen befolyásolhatja a vékonybélben zajló, hTRPV6 csatorna által közvetített Ca^{2+} felszívódást. Megfigyeltük továbbá, hogy Ca^{2+} hiányában a hTRPV6 csatornák Zn^{2+} számára is átjárhatóvá válnak, így feltételezhetően részt vesznek a Zn^{2+} felszívódásában kalcium-szegény étrend esetén.

9. References

1. Vallee BL and Falchuk KH: The biochemical basis of zinc physiology. *Physiol Rev*, 1993. 73(1): p. 79-118.
2. Wu FY, Huang WJ, Sinclair RB, and Powers L: The structure of the zinc sites of Escherichia coli DNA-dependent RNA polymerase. *J Biol Chem*, 1992. 267(35): p. 25560-7.
3. Harrison NL and Gibbons SJ: Zn2+: an endogenous modulator of ligand- and voltage-gated ion channels. *Neuropharmacology*, 1994. 33(8): p. 935-52.
4. Mathie A, Sutton GL, Clarke CE, and Veale EL: Zinc and copper: pharmacological probes and endogenous modulators of neuronal excitability. *Pharmacol Ther*, 2006. 111(3): p. 567-83.
5. Kuo CC, Chen WY, and Yang YC: Block of tetrodotoxin-resistant Na+ channel pore by multivalent cations: gating modification and Na+ flow dependence. *J Gen Physiol*, 2004. 124(1): p. 27-42.
6. White JA, Alonso A, and Kay AR: A heart-like Na+ current in the medial entorhinal cortex. *Neuron*, 1993. 11(6): p. 1037-47.
7. Teisseyre A and Mozrzymas JW: Inhibition of the activity of T lymphocyte Kv1.3 channels by extracellular zinc. *Biochem Pharmacol*, 2002. 64(4): p. 595-607.
8. Zhang S, Kwan DC, Fedida D, and Kehl SJ: External K(+) relieves the block but not the gating shift caused by Zn(2+) in human Kv1.5 potassium channels. *J Physiol*, 2001. 532(Pt 2): p. 349-58.
9. Noh J, Kim MK, and Chung JM: A novel mechanism of zinc block on alpha1G-like low-threshold T-type Ca2+ channels in a rat thalamic relay neuron. *Neurosci Res*, 2010. 66(4): p. 353-8.
10. Traboulsie A, Chemin J, Chevalier M, Quignard JF, Nargeot J, and Lory P: Subunit-specific modulation of T-type calcium channels by zinc. *J Physiol*, 2007. 578(Pt 1): p. 159-71.
11. Gruss M, Mathie A, Lieb WR, and Franks NP: The two-pore-domain K(+) channels TREK-1 and TASK-3 are differentially modulated by copper and zinc. *Mol Pharmacol*, 2004. 66(3): p. 530-7.

12. Kim JS, Park JY, Kang HW, Lee EJ, Bang H, and Lee JH: Zinc activates TREK-2 potassium channel activity. *J Pharmacol Exp Ther*, 2005. 314(2): p. 618-25.
13. Baron A, Waldmann R, and Lazdunski M: ASIC-like, proton-activated currents in rat hippocampal neurons. *J Physiol*, 2002. 539(Pt 2): p. 485-94.
14. Amuzescu B, Segal A, Flonta ML, Simaels J, and Van Driessche W: Zinc is a voltage-dependent blocker of native and heterologously expressed epithelial Na+ channels. *Pflugers Arch*, 2003. 446(1): p. 69-77.
15. Lambert S, Drews A, Rizun O, Wagner TF, Lis A, Mannebach S, Plant S, Portz M, Meissner M, Philipp SE, and Oberwinkler J: Transient receptor potential melastatin 1 (TRPM1) is an ion-conducting plasma membrane channel inhibited by zinc ions. *J Biol Chem*, 2011. 286(14): p. 12221-33.
16. Yang W, Manna PT, Zou J, Luo J, Beech DJ, Sivaprasadarao A, and Jiang LH: Zinc Inactivates Melastatin Transient Receptor Potential 2 Channels via the Outer Pore. *J Biol Chem*, 2011. 286(27): p. 23789-98.
17. Hosie AM, Dunne EL, Harvey RJ, and Smart TG: Zinc-mediated inhibition of GABA(A) receptors: discrete binding sites underlie subtype specificity. *Nat Neurosci*, 2003. 6(4): p. 362-9.
18. Wang TL, Hackam A, Guggino WB, and Cutting GR: A single histidine residue is essential for zinc inhibition of GABA rho 1 receptors. *J Neurosci*, 1995. 15(11): p. 7684-91.
19. Laube B, Kuhse J, and Betz H: Kinetic and mutational analysis of Zn2+ modulation of recombinant human inhibitory glycine receptors. *J Physiol*, 2000. 522 Pt 2: p. 215-30.
20. Hubbard PC and Lummis SC: Zn(2+) enhancement of the recombinant 5-HT(3) receptor is modulated by divalent cations. *Eur J Pharmacol*, 2000. 394(2-3): p. 189-97.
21. Paoletti P, Ascher P, and Neyton J: High-affinity zinc inhibition of NMDA NR1-NR2A receptors. *J Neurosci*, 1997. 17(15): p. 5711-25.
22. Rachline J, Perin-Dureau F, Le Goff A, Neyton J, and Paoletti P: The micromolar zinc-binding domain on the NMDA receptor subunit NR2B. *J Neurosci*, 2005. 25(2): p. 308-17.

23. Liu X, Surprenant A, Mao HJ, Roger S, Xia R, Bradley H, and Jiang LH: Identification of key residues coordinating functional inhibition of P2X7 receptors by zinc and copper. *Mol Pharmacol*, 2008. 73(1): p. 252-9.
24. Huidobro-Toro JP, Lorca RA, and Coddou C: Trace metals in the brain: allosteric modulators of ligand-gated receptor channels, the case of ATP-gated P2X receptors. *Eur Biophys J*, 2008. 37(3): p. 301-14.
25. Tittle RK and Hume RI: Opposite effects of zinc on human and rat P2X2 receptors. *J Neurosci*, 2008. 28(44): p. 11131-40.
26. Lorca RA, Coddou C, Gazitua MC, Bull P, Arredondo C, and Huidobro-Toro JP: Extracellular histidine residues identify common structural determinants in the copper/zinc P2X2 receptor modulation. *J Neurochem*, 2005. 95(2): p. 499-512.
27. Inagaki A, Yamaguchi S, Takahashi-Iwanaga H, Iwanaga T, and Ishikawa T: Functional characterization of a ClC-2-like Cl(-) conductance in surface epithelial cells of rat rectal colon. *J Membr Biol*, 2010. 235(1): p. 27-41.
28. Osteen JD and Mindell JA: Insights into the ClC-4 transport mechanism from studies of Zn2+ inhibition. *Biophys J*, 2008. 95(10): p. 4668-75.
29. Duffield MD, Rychkov GY, Bretag AH, and Roberts ML: Zinc inhibits human ClC-1 muscle chloride channel by interacting with its common gating mechanism. *J Physiol*, 2005. 568(Pt 1): p. 5-12.
30. Piper AS and Large WA: Single cGMP-activated Ca(+)-dependent Cl(-) channels in rat mesenteric artery smooth muscle cells. *J Physiol*, 2004. 555(Pt 2): p. 397-408.
31. Hartzell HC and Qu Z: Chloride currents in acutely isolated Xenopus retinal pigment epithelial cells. *J Physiol*, 2003. 549(Pt 2): p. 453-69.
32. Fischer H, Widdicombe JH, and Illek B: Acid secretion and proton conductance in human airway epithelium. *Am J Physiol Cell Physiol*, 2002. 282(4): p. C736-43.
33. Schwarzer C, Machen TE, Illek B, and Fischer H: NADPH oxidase-dependent acid production in airway epithelial cells. *J Biol Chem*, 2004. 279(35): p. 36454-61.

34. Decoursey TE: Voltage-gated proton channels and other proton transfer pathways. *Physiol Rev*, 2003. 83(2): p. 475-579.
35. Riera CE, Vogel H, Simon SA, and le Coutre J: Artificial sweeteners and salts producing a metallic taste sensation activate TRPV1 receptors. *Am J Physiol Regul Integr Comp Physiol*, 2007. 293(2): p. R626-34.
36. Hou S, Vigeland LE, Zhang G, Xu R, Li M, Heinemann SH, and Hoshi T: Zn2+ activates large conductance Ca2+-activated K+ channel via an intracellular domain. *J Biol Chem*, 2010. 285(9): p. 6434-42.
37. Prost AL, Bloc A, Hussy N, Derand R, and Vivaudou M: Zinc is both an intracellular and extracellular regulator of KATP channel function. *J Physiol*, 2004. 559(Pt 1): p. 157-67.
38. Jia Y, Jeng JM, Sensi SL, and Weiss JH: Zn2+ currents are mediated by calcium-permeable AMPA/kainate channels in cultured murine hippocampal neurones. *J Physiol*, 2002. 543(Pt 1): p. 35-48.
39. Ragozzino D, Giovannelli A, Degasperi V, Eusebi F, and Grassi F: Zinc permeates mouse muscle ACh receptor channels expressed in BOSC 23 cells and affects channel function. *J Physiol*, 2000. 529 Pt 1: p. 83-91.
40. Sensi SL, Canzoniero LM, Yu SP, Ying HS, Koh JY, Kerchner GA, and Choi DW: Measurement of intracellular free zinc in living cortical neurons: routes of entry. *J Neurosci*, 1997. 17(24): p. 9554-64.
41. Kerchner GA, Canzoniero LM, Yu SP, Ling C, and Choi DW: Zn2+ current is mediated by voltage-gated Ca2+ channels and enhanced by extracellular acidity in mouse cortical neurones. *J Physiol*, 2000. 528 Pt 1: p. 39-52.
42. Sheline CT, Ying HS, Ling CS, Canzoniero LM, and Choi DW: Depolarization-induced 65zinc influx into cultured cortical neurons. *Neurobiol Dis*, 2002. 10(1): p. 41-53.
43. Wagner TF, Drews A, Loch S, Mohr F, Philipp SE, Lambert S, and Oberwinkler J: TRPM3 channels provide a regulated influx pathway for zinc in pancreatic beta cells. *Pflugers Arch*, 2010. 460(4): p. 755-65.
44. Inoue K, Branigan D, and Xiong ZG: Zinc-induced neurotoxicity mediated by transient receptor potential melastatin 7 channels. *J Biol Chem*, 2010. 285(10): p. 7430-9.

45. Monteilh-Zoller MK, Hermosura MC, Nadler MJ, Scharenberg AM, Penner R, and Fleig A: TRPM7 provides an ion channel mechanism for cellular entry of trace metal ions. *J Gen Physiol*, 2003. 121(1): p. 49-60.
46. Frederickson CJ: Neurobiology of zinc and zinc-containing neurons. *Int Rev Neurobiol*, 1989. 31: p. 145-238.
47. Moran O and Zegarra-Moran O: On the measurement of the functional properties of the CFTR. *J Cyst Fibros*, 2008. 7(6): p. 483-94.
48. Verkman AS and Galietta LJ: Chloride channels as drug targets. *Nat Rev Drug Discov*, 2009. 8(2): p. 153-71.
49. Bahinski A, Nairn AC, Greengard P, and Gadsby DC: Chloride conductance regulated by cyclic AMP-dependent protein kinase in cardiac myocytes. *Nature*, 1989. 340(6236): p. 718-21.
50. Rakheja D, Xu Y, Burns DK, Veltkamp DL, and Margraf LR: Cystic fibrosis and Chiari type I malformation: autopsy study of two infants with a rare association. *Pediatr Dev Pathol*, 2003. 6(1): p. 88-93.
51. Sheppard DN and Welsh MJ: Structure and function of the CFTR chloride channel. *Physiol Rev*, 1999. 79(1 Suppl): p. S23-45.
52. Gadsby DC and Nairn AC: Control of CFTR channel gating by phosphorylation and nucleotide hydrolysis. *Physiol Rev*, 1999. 79(1 Suppl): p. S77-S107.
53. Choi JY, Joo NS, Krouse ME, Wu JV, Robbins RC, Ianowski JP, Hanrahan JW, and Wine JJ: Synergistic airway gland mucus secretion in response to vasoactive intestinal peptide and carbachol is lost in cystic fibrosis. *J Clin Invest*, 2007. 117(10): p. 3118-27.
54. Tarran R, Trout L, Donaldson SH, and Boucher RC: Soluble mediators, not cilia, determine airway surface liquid volume in normal and cystic fibrosis superficial airway epithelia. *J Gen Physiol*, 2006. 127(5): p. 591-604.
55. Mense M, Vergani P, White DM, Altberg G, Nairn AC, and Gadsby DC: In vivo phosphorylation of CFTR promotes formation of a nucleotide-binding domain heterodimer. *EMBO J*, 2006. 25(20): p. 4728-39.
56. Vergani P, Lockless SW, Nairn AC, and Gadsby DC: CFTR channel opening by ATP-driven tight dimerization of its nucleotide-binding domains. *Nature*, 2005. 433(7028): p. 876-80.

57. Aleksandrov L, Mengos A, Chang X, Aleksandrov A, and Riordan JR: Differential interactions of nucleotides at the two nucleotide binding domains of the cystic fibrosis transmembrane conductance regulator. *J Biol Chem*, 2001. 276(16): p. 12918-23.
58. Weinreich F, Riordan JR, and Nagel G: Dual effects of ADP and adenylylimidodiphosphate on CFTR channel kinetics show binding to two different nucleotide binding sites. *J Gen Physiol*, 1999. 114(1): p. 55-70.
59. Anderson MP, Gregory RJ, Thompson S, Souza DW, Paul S, Mulligan RC, Smith AE, and Welsh MJ: Demonstration that CFTR is a chloride channel by alteration of its anion selectivity. *Science*, 1991. 253(5016): p. 202-5.
60. Egan M, Flotte T, Afione S, Solow R, Zeitlin PL, Carter BJ, and Guggino WB: Defective regulation of outwardly rectifying Cl- channels by protein kinase A corrected by insertion of CFTR. *Nature*, 1992. 358(6387): p. 581-4.
61. Gabriel SE, Clarke LL, Boucher RC, and Stutts MJ: CFTR and outward rectifying chloride channels are distinct proteins with a regulatory relationship. *Nature*, 1993. 363(6426): p. 263-8.
62. Stutts MJ, Canessa CM, Olsen JC, Hamrick M, Cohn JA, Rossier BC, and Boucher RC: CFTR as a cAMP-dependent regulator of sodium channels. *Science*, 1995. 269(5225): p. 847-50.
63. Stutts MJ, Rossier BC, and Boucher RC: Cystic fibrosis transmembrane conductance regulator inverts protein kinase A-mediated regulation of epithelial sodium channel single channel kinetics. *J Biol Chem*, 1997. 272(22): p. 14037-40.
64. Naren AP, Cobb B, Li C, Roy K, Nelson D, Heda GD, Liao J, Kirk KL, Sorscher EJ, Hanrahan J, and Clancy JP: A macromolecular complex of beta 2 adrenergic receptor, CFTR, and ezrin/radixin/moesin-binding phosphoprotein 50 is regulated by PKA. *Proc Natl Acad Sci U S A*, 2003. 100(1): p. 342-6.
65. Yoo D, Flagg TP, Olsen O, Raghuram V, Foskett JK, and Welling PA: Assembly and trafficking of a multiprotein ROMK (Kir 1.1) channel complex by PDZ interactions. *J Biol Chem*, 2004. 279(8): p. 6863-73.

66. Zsembery A, Strazzabosco M, and Graf J: Ca2+-activated Cl- channels can substitute for CFTR in stimulation of pancreatic duct bicarbonate secretion. *FASEB J*, 2000. 14(14): p. 2345-56.
67. Schreiber R, Greger R, Nitschke R, and Kunzelmann K: Cystic fibrosis transmembrane conductance regulator activates water conductance in Xenopus oocytes. *Pflugers Arch*, 1997. 434(6): p. 841-7.
68. Schwiebert EM, Benos DJ, Egan ME, Stutts MJ, and Guggino WB: CFTR is a conductance regulator as well as a chloride channel. *Physiol Rev*, 1999. 79(1 Suppl): p. S145-66.
69. Kunzelmann K, Kiser GL, Schreiber R, and Riordan JR: Inhibition of epithelial Na+ currents by intracellular domains of the cystic fibrosis transmembrane conductance regulator. *FEBS Lett*, 1997. 400(3): p. 341-4.
70. Hall RA, Ostedgaard LS, Premont RT, Blitzer JT, Rahman N, Welsh MJ, and Lefkowitz RJ: A C-terminal motif found in the beta2-adrenergic receptor, P2Y1 receptor and cystic fibrosis transmembrane conductance regulator determines binding to the Na+/H+ exchanger regulatory factor family of PDZ proteins. *Proc Natl Acad Sci U S A*, 1998. 95(15): p. 8496-501.
71. Short DB, Trotter KW, Reczek D, Kreda SM, Bretscher A, Boucher RC, Stutts MJ, and Milgram SL: An apical PDZ protein anchors the cystic fibrosis transmembrane conductance regulator to the cytoskeleton. *J Biol Chem*, 1998. 273(31): p. 19797-801.
72. Wang S, Raab RW, Schatz PJ, Guggino WB, and Li M: Peptide binding consensus of the NHE-RF-PDZ1 domain matches the C-terminal sequence of cystic fibrosis transmembrane conductance regulator (CFTR). *FEBS Lett*, 1998. 427(1): p. 103-8.
73. Schwiebert EM, Egan ME, Hwang TH, Fulmer SB, Allen SS, Cutting GR, and Guggino WB: CFTR regulates outwardly rectifying chloride channels through an autocrine mechanism involving ATP. *Cell*, 1995. 81(7): p. 1063-73.
74. Matsui H, Randell SH, Peretti SW, Davis CW, and Boucher RC: Coordinated clearance of periciliary liquid and mucus from airway surfaces. *J Clin Invest*, 1998. 102(6): p. 1125-31.

75. Tarran R, Grubb BR, Gatzy JT, Davis CW, and Boucher RC: The relative roles of passive surface forces and active ion transport in the modulation of airway surface liquid volume and composition. *J Gen Physiol*, 2001. 118(2): p. 223-36.
76. Matsui H, Verghese MW, Kesimer M, Schwab UE, Randell SH, Sheehan JK, Grubb BR, and Boucher RC: Reduced three-dimensional motility in dehydrated airway mucus prevents neutrophil capture and killing bacteria on airway epithelial surfaces. *J Immunol*, 2005. 175(2): p. 1090-9.
77. Knowles MR and Boucher RC: Mucus clearance as a primary innate defense mechanism for mammalian airways. *J Clin Invest*, 2002. 109(5): p. 571-7.
78. Boucher RC: Molecular insights into the physiology of the 'thin film' of airway surface liquid. *J Physiol*, 1999. 516 (Pt 3): p. 631-8.
79. Matsui H, Davis CW, Tarran R, and Boucher RC: Osmotic water permeabilities of cultured, well-differentiated normal and cystic fibrosis airway epithelia. *J Clin Invest*, 2000. 105(10): p. 1419-27.
80. Jayaraman S, Song Y, Vetrivel L, Shankar L, and Verkman AS: Noninvasive in vivo fluorescence measurement of airway-surface liquid depth, salt concentration, and pH. *J Clin Invest*, 2001. 107(3): p. 317-24.
81. Boucher RC: Relationship of airway epithelial ion transport to chronic bronchitis. *Proc Am Thorac Soc*, 2004. 1(1): p. 66-70.
82. Tarran R, Button B, Picher M, Paradiso AM, Ribeiro CM, Lazarowski ER, Zhang L, Collins PL, Pickles RJ, Fredberg JJ, and Boucher RC: Normal and cystic fibrosis airway surface liquid homeostasis. The effects of phasic shear stress and viral infections. *J Biol Chem*, 2005. 280(42): p. 35751-9.
83. Anderson MP and Welsh MJ: Calcium and cAMP activate different chloride channels in the apical membrane of normal and cystic fibrosis epithelia. *Proc Natl Acad Sci U S A*, 1991. 88(14): p. 6003-7.
84. Cunningham SA, Awayda MS, Bubien JK, Ismailov II, Arrate MP, Berdiev BK, Benos DJ, and Fuller CM: Cloning of an epithelial chloride channel from bovine trachea. *J Biol Chem*, 1995. 270(52): p. 31016-26.
85. Boucher RC: Airway surface dehydration in cystic fibrosis: pathogenesis and therapy. *Annu Rev Med*, 2007. 58: p. 157-70.

86. Boucher RC: Regulation of airway surface liquid volume by human airway epithelia. *Pflugers Arch*, 2003. 445(4): p. 495-8.
87. Huang P, Lazarowski ER, Tarran R, Milgram SL, Boucher RC, and Stutts MJ: Compartmentalized autocrine signaling to cystic fibrosis transmembrane conductance regulator at the apical membrane of airway epithelial cells. *Proc Natl Acad Sci U S A*, 2001. 98(24): p. 14120-5.
88. Rossier BC: The epithelial sodium channel: activation by membrane-bound serine proteases. *Proc Am Thorac Soc*, 2004. 1(1): p. 4-9.
89. Myerburg MM, Harvey PR, Heidrich EM, Pilewski JM, and Butterworth MB: Acute regulation of the epithelial sodium channel in airway epithelia by proteases and trafficking. *Am J Respir Cell Mol Biol*, 2010. 43(6): p. 712-9.
90. Ji HL, Chalfant ML, Jovov B, Lockhart JP, Parker SB, Fuller CM, Stanton BA, and Benos DJ: The cytosolic termini of the beta- and gamma-ENaC subunits are involved in the functional interactions between cystic fibrosis transmembrane conductance regulator and epithelial sodium channel. *J Biol Chem*, 2000. 275(36): p. 27947-56.
91. Chambers LA, Rollins BM, and Tarran R: Liquid movement across the surface epithelium of large airways. *Respir Physiol Neurobiol*, 2007. 159(3): p. 256-70.
92. Tarran R and Boucher RC: Thin-film measurements of airway surface liquid volume/composition and mucus transport rates in vitro. *Methods Mol Med*, 2002. 70: p. 479-92.
93. Lazarowski ER, Tarran R, Grubb BR, van Heusden CA, Okada S, and Boucher RC: Nucleotide release provides a mechanism for airway surface liquid homeostasis. *J Biol Chem*, 2004. 279(35): p. 36855-64.
94. Ma HP, Saxena S, and Warnock DG: Anionic phospholipids regulate native and expressed epithelial sodium channel (ENaC). *J Biol Chem*, 2002. 277(10): p. 7641-4.
95. Kerem B, Rommens JM, Buchanan JA, Markiewicz D, Cox TK, Chakravarti A, Buchwald M, and Tsui LC: Identification of the cystic fibrosis gene: genetic analysis. *Science*, 1989. 245(4922): p. 1073-80.
96. Davis PB: Cystic fibrosis since 1938. *Am J Respir Crit Care Med*, 2006. 173(5): p. 475-82.

97. O'Sullivan BP and Freedman SD: Cystic fibrosis. *Lancet*, 2009. 373(9678): p. 1891-904.
98. Barish ME: A transient calcium-dependent chloride current in the immature Xenopus oocyte. *J Physiol*, 1983. 342: p. 309-25.
99. Hartzell C, Putzier I, and Arreola J: Calcium-activated chloride channels. *Annu Rev Physiol*, 2005. 67: p. 719-58.
100. Eggermont J: Calcium-activated chloride channels: (un)known, (un)loved? *Proc Am Thorac Soc*, 2004. 1(1): p. 22-7.
101. Huang P, Liu J, Di A, Robinson NC, Musch MW, Kaetzel MA, and Nelson DJ: Regulation of human CLC-3 channels by multifunctional Ca2+/calmodulin-dependent protein kinase. *J Biol Chem*, 2001. 276(23): p. 20093-100.
102. Sun H, Tsunenari T, Yau KW, and Nathans J: The vitelliform macular dystrophy protein defines a new family of chloride channels. *Proc Natl Acad Sci U S A*, 2002. 99(6): p. 4008-13.
103. Kunzelmann K, Milenkovic VM, Spitzner M, Soria RB, and Schreiber R: Calcium-dependent chloride conductance in epithelia: is there a contribution by Bestrophin? *Pflugers Arch*, 2007. 454(6): p. 879-89.
104. Qu Z, Wei RW, Mann W, and Hartzell HC: Two bestrophins cloned from Xenopus laevis oocytes express Ca(2+)-activated Cl(-) currents. *J Biol Chem*, 2003. 278(49): p. 49563-72.
105. Suzuki M and Mizuno A: A novel human Cl(-) channel family related to Drosophila flightless locus. *J Biol Chem*, 2004. 279(21): p. 22461-8.
106. Yang YD, Cho H, Koo JY, Tak MH, Cho Y, Shim WS, Park SP, Lee J, Lee B, Kim BM, Raouf R, Shin YK, and Oh U: TMEM16A confers receptor-activated calcium-dependent chloride conductance. *Nature*, 2008. 455(7217): p. 1210-5.
107. Schroeder BC, Cheng T, Jan YN, and Jan LY: Expression cloning of TMEM16A as a calcium-activated chloride channel subunit. *Cell*, 2008. 134(6): p. 1019-29.
108. Caputo A, Caci E, Ferrera L, Pedemonte N, Barsanti C, Sondo E, Pfeffer U, Ravazzolo R, Zegarra-Moran O, and Galietta LJ: TMEM16A, a membrane protein associated with calcium-dependent chloride channel activity. *Science*, 2008. 322(5901): p. 590-4.

109. Barro Soria R, Spitzner M, Schreiber R, and Kunzelmann K: Bestrophin-1 enables Ca2+-activated Cl- conductance in epithelia. *J Biol Chem*, 2009. 284(43): p. 29405-12.
110. Park H, Oh SJ, Han KS, Woo DH, Mannaioni G, Traynelis SF, and Lee CJ: Bestrophin-1 encodes for the Ca2+-activated anion channel in hippocampal astrocytes. *J Neurosci*, 2009. 29(41): p. 13063-73.
111. Milenkovic VM, Soria RB, Aldehni F, Schreiber R, and Kunzelmann K: Functional assembly and purinergic activation of bestrophins. *Pflugers Arch*, 2009. 458(2): p. 431-41.
112. Hartzell HC, Qu Z, Yu K, Xiao Q, and Chien LT: Molecular physiology of bestrophins: multifunctional membrane proteins linked to best disease and other retinopathies. *Physiol Rev*, 2008. 88(2): p. 639-72.
113. Rosenthal R, Bakall B, Kinnick T, Peachey N, Wimmers S, Wadelius C, Marmorstein A, and Strauss O: Expression of bestrophin-1, the product of the VMD2 gene, modulates voltage-dependent Ca2+ channels in retinal pigment epithelial cells. *FASEB J*, 2006. 20(1): p. 178-80.
114. Yu K, Xiao Q, Cui G, Lee A, and Hartzell HC: The best disease-linked Cl-channel hBest1 regulates Ca V 1 (L-type) Ca2+ channels via src-homology-binding domains. *J Neurosci*, 2008. 28(22): p. 5660-70.
115. Hwang SJ, Blair PJ, Britton FC, O'Driscoll KE, Hennig G, Bayguinov YR, Rock JR, Harfe BD, Sanders KM, and Ward SM: Expression of anoctamin 1/TMEM16A by interstitial cells of Cajal is fundamental for slow wave activity in gastrointestinal muscles. *J Physiol*, 2009. 587(Pt 20): p. 4887-904.
116. Manoury B, Tamuleviciute A, and Tammaro P: TMEM16A/anoctamin 1 protein mediates calcium-activated chloride currents in pulmonary arterial smooth muscle cells. *J Physiol*, 2010. 588(Pt 13): p. 2305-14.
117. Huang F, Rock JR, Harfe BD, Cheng T, Huang X, Jan YN, and Jan LY: Studies on expression and function of the TMEM16A calcium-activated chloride channel. *Proc Natl Acad Sci U S A*, 2009. 106(50): p. 21413-8.
118. Rock JR, O'Neal WK, Gabriel SE, Randell SH, Harfe BD, Boucher RC, and Grubb BR: Transmembrane protein 16A (TMEM16A) is a Ca2+-regulated Cl-secretory channel in mouse airways. *J Biol Chem*, 2009. 284(22): p. 14875-80.

119. Rock JR, Futtner CR, and Harfe BD: The transmembrane protein TMEM16A is required for normal development of the murine trachea. *Dev Biol*, 2008. 321(1): p. 141-9.
120. Namkung W, Phuan PW, and Verkman AS: TMEM16A inhibitors reveal TMEM16A as a minor component of calcium-activated chloride channel conductance in airway and intestinal epithelial cells. *J Biol Chem*, 2011. 286(3): p. 2365-74.
121. Kuruma A and Hartzell HC: Bimodal control of a Ca(2+)-activated Cl(-) channel by different Ca(2+) signals. *J Gen Physiol*, 2000. 115(1): p. 59-80.
122. Nilius B, Prenen J, Voets T, Van den Bremt K, Eggermont J, and Droogmans G: Kinetic and pharmacological properties of the calcium-activated chloride-current in macrovascular endothelial cells. *Cell Calcium*, 1997. 22(1): p. 53-63.
123. Arreola J, Melvin JE, and Begenisich T: Activation of calcium-dependent chloride channels in rat parotid acinar cells. *J Gen Physiol*, 1996. 108(1): p. 35-47.
124. Worrell RT and Frizzell RA: CaMKII mediates stimulation of chloride conductance by calcium in T84 cells. *Am J Physiol*, 1991. 260(4 Pt 1): p. C877-82.
125. Derichs N, Jin BJ, Song Y, Finkbeiner WE, and Verkman AS: Hyperviscous airway periciliary and mucous liquid layers in cystic fibrosis measured by confocal fluorescence photobleaching. *FASEB J*, 2011. 25(7): p. 2325-32.
126. Mall MA: Role of the amiloride-sensitive epithelial Na+ channel in the pathogenesis and as a therapeutic target for cystic fibrosis lung disease. *Exp Physiol*, 2009. 94(2): p. 171-4.
127. Mall M, Grubb BR, Harkema JR, O'Neal WK, and Boucher RC: Increased airway epithelial Na+ absorption produces cystic fibrosis-like lung disease in mice. *Nat Med*, 2004. 10(5): p. 487-93.
128. Matsui H, Grubb BR, Tarran R, Randell SH, Gatzy JT, Davis CW, and Boucher RC: Evidence for periciliary liquid layer depletion, not abnormal ion composition, in the pathogenesis of cystic fibrosis airways disease. *Cell*, 1998. 95(7): p. 1005-15.

129. Chambers LA, Constable M, Clunes MT, Olver RE, Ko WH, Inglis SK, and Wilson SM: Adenosine-evoked Na+ transport in human airway epithelial cells. *Br J Pharmacol*, 2006. 149(1): p. 43-55.

130. Myerburg MM, Butterworth MB, McKenna EE, Peters KW, Frizzell RA, Kleyman TR, and Pilewski JM: Airway surface liquid volume regulates ENaC by altering the serine protease-protease inhibitor balance: a mechanism for sodium hyperabsorption in cystic fibrosis. *J Biol Chem*, 2006. 281(38): p. 27942-9.

131. Watt WC, Lazarowski ER, and Boucher RC: Cystic fibrosis transmembrane regulator-independent release of ATP. Its implications for the regulation of P2Y2 receptors in airway epithelia. *J Biol Chem*, 1998. 273(22): p. 14053-8.

132. Tarran R, Button B, and Boucher RC: Regulation of normal and cystic fibrosis airway surface liquid volume by phasic shear stress. *Annu Rev Physiol*, 2006. 68: p. 543-61.

133. Donaldson SH and Boucher RC: Pathophysiology of cystic fibrosis. *Ann Nestle [Eng]*, 2006. 64: p. 101-9.

134. Mall M, Wissner A, Gonska T, Calenborn D, Kuehr J, Brandis M, and Kunzelmann K: Inhibition of amiloride-sensitive epithelial Na(+) absorption by extracellular nucleotides in human normal and cystic fibrosis airways. *Am J Respir Cell Mol Biol*, 2000. 23(6): p. 755-61.

135. Tarran R, Grubb BR, Parsons D, Picher M, Hirsh AJ, Davis CW, and Boucher RC: The CF salt controversy: in vivo observations and therapeutic approaches. *Mol Cell*, 2001. 8(1): p. 149-58.

136. Tarran R, Loewen ME, Paradiso AM, Olsen JC, Gray MA, Argent BE, Boucher RC, and Gabriel SE: Regulation of murine airway surface liquid volume by CFTR and Ca2+-activated Cl- conductances. *J Gen Physiol*, 2002. 120(3): p. 407-18.

137. Clarke LL, Grubb BR, Yankaskas JR, Cotton CU, McKenzie A, and Boucher RC: Relationship of a non-cystic fibrosis transmembrane conductance regulator-mediated chloride conductance to organ-level disease in Cftr(-/-) mice. *Proc Natl Acad Sci U S A*, 1994. 91(2): p. 479-83.

138. Grubb BR, Pickles RJ, Ye H, Yankaskas JR, Vick RN, Engelhardt JF, Wilson JM, Johnson LG, and Boucher RC: Inefficient gene transfer by adenovirus vector to cystic fibrosis airway epithelia of mice and humans. *Nature*, 1994. 371(6500): p. 802-6.
139. Picher M, Burch LH, Hirsh AJ, Spychala J, and Boucher RC: Ecto 5'-nucleotidase and nonspecific alkaline phosphatase. Two AMP-hydrolyzing ectoenzymes with distinct roles in human airways. *J Biol Chem*, 2003. 278(15): p. 13468-79.
140. Lazarowski ER and Boucher RC: UTP as an extracellular signaling molecule. *News Physiol Sci*, 2001. 16: p. 1-5.
141. Gilligan PH: Microbiology of airway disease in patients with cystic fibrosis. *Clin Microbiol Rev*, 1991. 4(1): p. 35-51.
142. Wat D and Doull I: Respiratory virus infections in cystic fibrosis. *Paediatr Respir Rev*, 2003. 4(3): p. 172-7.
143. Coakley RD, Grubb BR, Paradiso AM, Gatzy JT, Johnson LG, Kreda SM, O'Neal WK, and Boucher RC: Abnormal surface liquid pH regulation by cultured cystic fibrosis bronchial epithelium. *Proc Natl Acad Sci U S A*, 2003. 100(26): p. 16083-8.
144. Newport S, Amin N, and Dozor AJ: Exhaled breath condensate pH and ammonia in cystic fibrosis and response to treatment of acute pulmonary exacerbations. *Pediatr Pulmonol*, 2009. 44(9): p. 866-72.
145. Carpagnano GE, Barnes PJ, Francis J, Wilson N, Bush A, and Kharitonov SA: Breath condensate pH in children with cystic fibrosis and asthma: a new noninvasive marker of airway inflammation? *Chest*, 2004. 125(6): p. 2005-10.
146. McShane D, Davies JC, Davies MG, Bush A, Geddes DM, and Alton EW: Airway surface pH in subjects with cystic fibrosis. *Eur Respir J*, 2003. 21(1): p. 37-42.
147. Johansen PG, Anderson CM, and Hadorn B: Cystic fibrosis of the pancreas. A generalised disturbance of water and electrolyte movement in exocrine tissues. *Lancet*, 1968. 1(7540): p. 455-60.

148. Kopelman H, Durie P, Gaskin K, Weizman Z, and Forstner G: Pancreatic fluid secretion and protein hyperconcentration in cystic fibrosis. *N Engl J Med*, 1985. 312(6): p. 329-34.
149. von Eckardstein S, Cooper TG, Rutscha K, Meschede D, Horst J, and Nieschlag E: Seminal plasma characteristics as indicators of cystic fibrosis transmembrane conductance regulator (CFTR) gene mutations in men with obstructive azoospermia. *Fertil Steril*, 2000. 73(6): p. 1226-31.
150. Linsdell P, Tabcharani JA, Rommens JM, Hou YX, Chang XB, Tsui LC, Riordan JR, and Hanrahan JW: Permeability of wild-type and mutant cystic fibrosis transmembrane conductance regulator chloride channels to polyatomic anions. *J Gen Physiol*, 1997. 110(4): p. 355-64.
151. Quinton PM: Cystic fibrosis: impaired bicarbonate secretion and mucoviscidosis. *Lancet*, 2008. 372(9636): p. 415-7.
152. Paradiso AM, Coakley RD, and Boucher RC: Polarized distribution of HCO3- transport in human normal and cystic fibrosis nasal epithelia. *J Physiol*, 2003. 548(Pt 1): p. 203-18.
153. Poulsen JH, Fischer H, Illek B, and Machen TE: Bicarbonate conductance and pH regulatory capability of cystic fibrosis transmembrane conductance regulator. *Proc Natl Acad Sci U S A*, 1994. 91(12): p. 5340-4.
154. Devor DC, Bridges RJ, and Pilewski JM: Pharmacological modulation of ion transport across wild-type and DeltaF508 CFTR-expressing human bronchial epithelia. *Am J Physiol Cell Physiol*, 2000. 279(2): p. C461-79.
155. Fischer H and Widdicombe JH: Mechanisms of acid and base secretion by the airway epithelium. *J Membr Biol*, 2006. 211(3): p. 139-50.
156. Inglis SK, Wilson SM, and Olver RE: Secretion of acid and base equivalents by intact distal airways. *Am J Physiol Lung Cell Mol Physiol*, 2003. 284(5): p. L855-62.
157. Paradiso AM: ATP-activated basolateral Na+/H+ exchange in human normal and cystic fibrosis airway epithelium. *Am J Physiol*, 1997. 273(1 Pt 1): p. L148-58.
158. Dudeja PK, Hafez N, Tyagi S, Gailey CA, Toofanfard M, Alrefai WA, Nazir TM, Ramaswamy K, and Al-Bazzaz FJ: Expression of the Na+/H+ and Cl-

/HCO-3 exchanger isoforms in proximal and distal human airways. *Am J Physiol*, 1999. 276(6 Pt 1): p. L971-8.

159. Quinton PM: The neglected ion: HCO3-. *Nat Med*, 2001. 7(3): p. 292-3.
160. Park K and Brown PD: Intracellular pH modulates the activity of chloride channels in isolated lacrimal gland acinar cells. *Am J Physiol*, 1995. 268(3 Pt 1): p. C647-50.
161. Arreola J, Melvin JE, and Begenisich T: Inhibition of Ca(2+)-dependent Cl- channels from secretory epithelial cells by low internal pH. *J Membr Biol*, 1995. 147(1): p. 95-104.
162. Barnes S and Bui Q: Modulation of calcium-activated chloride current via pH-induced changes of calcium channel properties in cone photoreceptors. *J Neurosci*, 1991. 11(12): p. 4015-23.
163. Iijima T, Ciani S, and Hagiwara S: Effects of the external pH on Ca channels: experimental studies and theoretical considerations using a two-site, two-ion model. *Proc Natl Acad Sci U S A*, 1986. 83(3): p. 654-8.
164. Prod'hom B, Pietrobon D, and Hess P: Interactions of protons with single open L-type calcium channels. Location of protonation site and dependence of proton-induced current fluctuations on concentration and species of permeant ion. *J Gen Physiol*, 1989. 94(1): p. 23-42.
165. Krafte DS and Kass RS: Hydrogen ion modulation of Ca channel current in cardiac ventricular cells. Evidence for multiple mechanisms. *J Gen Physiol*, 1988. 91(5): p. 641-57.
166. Bhaskar KR, Gong DH, Bansil R, Pajevic S, Hamilton JA, Turner BS, and LaMont JT: Profound increase in viscosity and aggregation of pig gastric mucin at low pH. *Am J Physiol*, 1991. 261(5 Pt 1): p. G827-32.
167. Clary-Meinesz C, Mouroux J, Cosson J, Huitorel P, and Blaive B: Influence of external pH on ciliary beat frequency in human bronchi and bronchioles. *Eur Respir J*, 1998. 11(2): p. 330-3.
168. Allen DB, Maguire JJ, Mahdavian M, Wicke C, Marcocci L, Scheuenstuhl H, Chang M, Le AX, Hopf HW, and Hunt TK: Wound hypoxia and acidosis limit neutrophil bacterial killing mechanisms. *Arch Surg*, 1997. 132(9): p. 991-6.

169. Stoodley P, deBeer D, and Lappin-Scott HM: Influence of electric fields and pH on biofilm structure as related to the bioelectric effect. *Antimicrob Agents Chemother*, 1997. 41(9): p. 1876-9.
170. Bidani A and Heming TA: Effects of bafilomycin A1 on functional capabilities of LPS-activated alveolar macrophages. *J Leukoc Biol*, 1995. 57(2): p. 275-81.
171. Coakley RD and Boucher RC: Regulation and functional significance of airway surface liquid pH. *JOP*, 2001. 2(4 Suppl): p. 294-300.
172. Eschenbacher WL, Gross KB, Muench SP, and Chan TL: Inhalation of an alkaline aerosol by subjects with mild asthma does not result in bronchoconstriction. *Am Rev Respir Dis*, 1991. 143(2): p. 341-5.
173. Haidl P, Schönhofer B, Siemon K, and Köhler D: Inhaled isotonic alkaline versus saline solution and radioaerosol clearance in chronic cough. *Eur Respir J*, 2000. 16(6): p. 1102-8.
174. Clunes MT and Boucher RC: Front-runners for pharmacotherapeutic correction of the airway ion transport defect in cystic fibrosis. *Curr Opin Pharmacol*, 2008. 8(3): p. 292-9.
175. Wei L, Vankeerberghen A, Cuppens H, Eggermont J, Cassiman JJ, Droogmans G, and Nilius B: Interaction between calcium-activated chloride channels and the cystic fibrosis transmembrane conductance regulator. *Pflugers Arch*, 1999. 438(5): p. 635-41.
176. Knowles MR, Clarke LL, and Boucher RC: Activation by extracellular nucleotides of chloride secretion in the airway epithelia of patients with cystic fibrosis. *N Engl J Med*, 1991. 325(8): p. 533-8.
177. Kellerman D, Rossi Mospan A, Engels J, Schaberg A, Gorden J, and Smiley L: Denufosol: a review of studies with inhaled P2Y(2) agonists that led to Phase 3. *Pulm Pharmacol Ther*, 2008. 21(4): p. 600-7.
178. Grasemann H, Stehling F, Brunar H, Widmann R, Laliberte TW, Molina L, Döring G, and Ratjen F: Inhalation of Moli1901 in patients with cystic fibrosis. *Chest*, 2007. 131(5): p. 1461-6.
179. Kanjhan R and Bellingham MC: Penetratin Peptide Potentiates Endogenous Calcium-Activated Chloride Currents in Xenopus oocytes. *J Membr Biol*, 2011. 241(1): p. 21-9.

180. Machaca K and HC Hartzell: Reversible Ca gradients between the subplasmalemma and cytosol differentially activate Ca-dependent Cl currents. *J Gen Physiol*, 1999. 113(2): p. 249-66.
181. Truong-Tran AQ, Carter J, Ruffin R, and Zalewski PD: New insights into the role of zinc in the respiratory epithelium. *Immunol Cell Biol*, 2001. 79(2): p. 170-7.
182. Strand TA, Aaberge IS, Maage A, Ulvestad E, and Sommerfelt H: The immune response to pneumococcal polysaccharide vaccine in zinc-depleted mice. *Scand J Immunol*, 2003. 58(1): p. 76-80.
183. Gomez NN, Davicino RC, Biaggio VS, Bianco GA, Alvarez SM, Fischer P, Masnatta L, Rabinovich GA, and Gimenez MS: Overexpression of inducible nitric oxide synthase and cyclooxygenase-2 in rat zinc-deficient lung: Involvement of a NF-kappaB dependent pathway. *Nitric Oxide*, 2006. 14(1): p. 30-8.
184. Ho LH, Ruffin RE, Murgia C, Li L, Krilis SA, and Zalewski PD: Labile zinc and zinc transporter ZnT4 in mast cell granules: role in regulation of caspase activation and NF-kappaB translocation. *J Immunol*, 2004. 172(12): p. 7750-60.
185. Soutar A, Seaton A, and Brown K: Bronchial reactivity and dietary antioxidants. *Thorax*, 1997. 52(2): p. 166-70.
186. Truong-Tran AQ, Ruffin RE, Foster PS, Koskinen AM, Coyle P, Philcox JC, Rofe AM, and Zalewski PD: Altered zinc homeostasis and caspase-3 activity in murine allergic airway inflammation. *Am J Respir Cell Mol Biol*, 2002. 27(3): p. 286-96.
187. Richter M, Bonneau R, Girard MA, Beaulieu C, and Larivée P: Zinc status modulates bronchopulmonary eosinophil infiltration in a murine model of allergic inflammation. *Chest*, 2003. 123(3 Suppl): p. 446S.
188. Prasad AS, Fitzgerald JT, Bao B, Beck FW, and Chandrasekar PH: Duration of symptoms and plasma cytokine levels in patients with the common cold treated with zinc acetate. A randomized, double-blind, placebo-controlled trial. *Ann Intern Med*, 2000. 133(4): p. 245-52.

189. Davidson TM and Smith WM: The Bradford Hill criteria and zinc-induced anosmia: a causality analysis. *Arch Otolaryngol Head Neck Surg*, 2010. 136(7): p. 673-6.
190. Fuortes L and Schenck D: Marked elevation of urinary zinc levels and pleural-friction rub in metal fume fever. *Vet Hum Toxicol*, 2000. 42(3): p. 164-5.
191. Zsembery A, Boyce AT, Liang L, Peti-Peterdi J, Bell PD, and Schwiebert EM: Sustained calcium entry through P2X nucleotide receptor channels in human airway epithelial cells. *J Biol Chem*, 2003. 278(15): p. 13398-408.
192. Hargitai D, Pataki A, Raffai G, Füzi M, Dankó T, Csernoch L, Várnai P, Szigeti GP, and Zsembery A: Calcium entry is regulated by Zn2+ in relation to extracellular ionic environment in human airway epithelial cells. *Respir Physiol Neurobiol*, 2010. 170(1): p. 67-75.
193. Liang L, Zsembery A, and Schwiebert EM: RNA interference targeted to multiple P2X receptor subtypes attenuates zinc-induced calcium entry. *Am J Physiol Cell Physiol*, 2005. 289(2): p. C388-96.
194. Zsembery A, Fortenberry JA, Liang L, Bebok Z, Tucker TA, Boyce AT, Braunstein GM, Welty E, Bell PD, Sorscher EJ, Clancy JP, and Schwiebert EM: Extracellular zinc and ATP restore chloride secretion across cystic fibrosis airway epithelia by triggering calcium entry. *J Biol Chem*, 2004. 279(11): p. 10720-9.
195. Schwiebert EM, Liang L, Cheng NL, Williams CR, Olteanu D, Welty EA, and Zsembery A: Extracellular zinc and ATP-gated P2X receptor calcium entry channels: New zinc receptors as physiological sensors and therapeutic targets. *Purinergic Signal*, 2005. 1(4): p. 299-310.
196. Woodworth BA, Zhang S, Tamashiro E, Bhargave G, Palmer JN, and Cohen NA: Zinc increases ciliary beat frequency in a calcium-dependent manner. *Am J Rhinol Allergy*, 2010. 24(1): p. 6-10.
197. Novick SG, Godfrey JC, Pollack RL, and Wilder HR: Zinc-induced suppression of inflammation in the respiratory tract, caused by infection with human rhinovirus and other irritants. *Med Hypotheses*, 1997. 49(4): p. 347-57.
198. Linley JE, Simmons NL, and Gray MA: Extracellular zinc stimulates a calcium-activated chloride conductance through mobilisation of intracellular calcium in

renal inner medullary collecting duct cells. *Pflugers Arch*, 2007. 453(4): p. 487-95.

199. Adamson IY, Prieditis H, Hedgecock C, and Vincent R: Zinc is the toxic factor in the lung response to an atmospheric particulate sample. *Toxicol Appl Pharmacol*, 2000. 166(2): p. 111-9.
200. Barceloux DG: Zinc. *J Toxicol Clin Toxicol*, 1999. 37(2): p. 279-92.
201. Liang L, MacDonald K, Schwiebert EM, Zeitlin PL, and Guggino WB: Spiperone, identified through compound screening, activates calcium-dependent chloride secretion in the airway. *Am J Physiol Cell Physiol*, 2009. 296(1): p. C131-41.
202. Venkatasubramanian J, Ao M, and Rao MC: Ion transport in the small intestine. *Curr Opin Gastroenterol*, 2010. 26(2): p. 123-8.
203. Clarke LL and Harline MC: Dual role of CFTR in cAMP-stimulated HCO3- secretion across murine duodenum. *Am J Physiol*, 1998. 274(4 Pt 1): p. G718-26.
204. Kiela PR and Ghishan FK: Ion transport in the intestine. *Curr Opin Gastroenterol*, 2009. 25(2): p. 87-91.
205. Buresi MC, Buret AG, Hollenberg MD, and MacNaughton WK: Activation of proteinase-activated receptor 1 stimulates epithelial chloride secretion through a unique MAP kinase- and cyclo-oxygenase-dependent pathway. *FASEB J*, 2002. 16(12): p. 1515-25.
206. Oprins JC, van der Burg C, Meijer HP, Munnik T, and Groot JA: Tumour necrosis factor alpha potentiates ion secretion induced by histamine in a human intestinal epithelial cell line and in mouse colon: involvement of the phospholipase D pathway. *Gut*, 2002. 50(3): p. 314-21.
207. Köttgen M, Löffler T, Jacobi C, Nitschke R, Pavenstädt H, Schreiber R, Frische S, Nielsen S, and Leipziger J: P2Y6 receptor mediates colonic NaCl secretion via differential activation of cAMP-mediated transport. *J Clin Invest*, 2003. 111(3): p. 371-9.
208. Kaunitz JD and Akiba Y: Purinergic regulation of duodenal surface pH and ATP concentration: implications for mucosal defence, lipid uptake and cystic fibrosis. *Acta Physiol (Oxf)*, 2011. 201(1): p. 109-16.

209. Quinton PM: Physiological basis of cystic fibrosis: a historical perspective. *Physiol Rev*, 1999. 79(1 Suppl): p. S3-S22.
210. Grubb BR and Gabriel SE: Intestinal physiology and pathology in gene-targeted mouse models of cystic fibrosis. *Am J Physiol*, 1997. 273(2 Pt 1): p. G258-66.
211. Bernardi KM, Forster ML, Lencer WI, and Tsai B: Derlin-1 facilitates the retro-translocation of cholera toxin. *Mol Biol Cell*, 2008. 19(3): p. 877-84.
212. Lu L, Bao Y, Khan A, Goldstein AM, Newburg DS, Quaroni A, Brown D, and Walker WA: Hydrocortisone modulates cholera toxin endocytosis by regulating immature enterocyte plasma membrane phospholipids. *Gastroenterology*, 2008. 135(1): p. 185-193 e1.
213. Thiagarajah JR and Verkman AS: CFTR pharmacology and its role in intestinal fluid secretion. *Curr Opin Pharmacol*, 2003. 3(6): p. 594-9.
214. Gruber AD, Elble RC, Ji HL, Schreur KD, Fuller CM, and Pauli BU: Genomic cloning, molecular characterization, and functional analysis of human CLCA1, the first human member of the family of Ca2+-activated Cl- channel proteins. *Genomics*, 1998. 54(2): p. 200-14.
215. De Marco G, Bracale I, Buccigrossi V, Bruzzese E, Canani RB, Polito G, Ruggeri FM, and Guarino A: Rotavirus induces a biphasic enterotoxic and cytotoxic response in human-derived intestinal enterocytes, which is inhibited by human immunoglobulins. *J Infect Dis*, 2009. 200(5): p. 813-9.
216. Morris AP, Scott JK, Ball JM, Zeng CQ, O'Neal WK, and Estes MK: NSP4 elicits age-dependent diarrhea and Ca(2+)mediated I(-) influx into intestinal crypts of CF mice. *Am J Physiol*, 1999. 277(2 Pt 1): p. G431-44.
217. Barrett KE and Keely SJ: Chloride secretion by the intestinal epithelium: molecular basis and regulatory aspects. *Annu Rev Physiol*, 2000. 62: p. 535-72.
218. Veeze HJ, Halley DJ, Bijman J, de Jongste JC, de Jonge HR, and Sinaasappel M: Determinants of mild clinical symptoms in cystic fibrosis patients. Residual chloride secretion measured in rectal biopsies in relation to the genotype. *J Clin Invest*, 1994. 93(2): p. 461-6.
219. Mall M, Bleich M, Schurlein M, Kuhr J, Seydewitz HH, Brandis M, Greger R, and Kunzelmann K: Cholinergic ion secretion in human colon requires coactivation by cAMP. *Am J Physiol*, 1998. 275(6 Pt 1): p. G1274-81.

220. Mall M, Wissner A, Seydewitz HH, Kuehr J, Brandis M, Greger R, and Kunzelmann K: Defective cholinergic Cl(-) secretion and detection of K(+) secretion in rectal biopsies from cystic fibrosis patients. *Am J Physiol Gastrointest Liver Physiol*, 2000. 278(4): p. G617-24.

221. Kunzelmann K and Mall M: Electrolyte transport in the mammalian colon: mechanisms and implications for disease. *Physiol Rev*, 2002. 82(1): p. 245-89.

222. Hoenderop JG, Nilius B, and Bindels RJ: Calcium absorption across epithelia. *Physiol Rev*, 2005. 85(1): p. 373-422.

223. Peng JB, Chen XZ, Berger UV, Vassilev PM, Tsukaguchi H, Brown EM, and Hediger MA: Molecular cloning and characterization of a channel-like transporter mediating intestinal calcium absorption. *J Biol Chem*, 1999. 274(32): p. 22739-46.

224. Gunthorpe MJ, Benham CD, Randall A, and Davis JB: The diversity in the vanilloid (TRPV) receptor family of ion channels. *Trends Pharmacol Sci*, 2002. 23(4): p. 183-91.

225. Voets T, Janssens A, Prenen J, Droogmans G, and Nilius B: Mg2+-dependent gating and strong inward rectification of the cation channel TRPV6. *J Gen Physiol*, 2003. 121(3): p. 245-60.

226. Nilius B, Prenen J, Vennekens R, Hoenderop JG, Bindels RJ, and Droogmans G: Modulation of the epithelial calcium channel, ECaC, by intracellular Ca2+. *Cell Calcium*, 2001. 29(6): p. 417-28.

227. Nilius B, Prenen J, Hoenderop JG, Vennekens R, Hoefs S, Weidema AF, Droogmans G, and Bindels RJ: Fast and slow inactivation kinetics of the Ca2+ channels ECaC1 and ECaC2 (TRPV5 and TRPV6). Role of the intracellular loop located between transmembrane segments 2 and 3. *J Biol Chem*, 2002. 277(34): p. 30852-8.

228. den Dekker E, Hoenderop JG, Nilius B, and Bindels RJ: The epithelial calcium channels, TRPV5 & TRPV6: from identification towards regulation. *Cell Calcium*, 2003. 33(5-6): p. 497-507.

229. Niemeyer BA, Bergs C, Wissenbach U, Flockerzi V, and Trost C: Competitive regulation of CaT-like-mediated Ca2+ entry by protein kinase C and calmodulin. *Proc Natl Acad Sci U S A*, 2001. 98(6): p. 3600-5.

230. Thyagarajan B, Lukacs V, and Rohacs T: Hydrolysis of phosphatidylinositol 4,5-bisphosphate mediates calcium-induced inactivation of TRPV6 channels. *J Biol Chem*, 2008. 283(22): p. 14980-7.

231. Thyagarajan B, Benn BS, Christakos S, and Rohacs T: Phospholipase C-mediated regulation of transient receptor potential vanilloid 6 channels: implications in active intestinal Ca2+ transport. *Mol Pharmacol*, 2009. 75(3): p. 608-16.

232. van de Graaf SF, Boullart I, Hoenderop JG, and Bindels RJ: Regulation of the epithelial Ca2+ channels TRPV5 and TRPV6 by 1alpha,25-dihydroxy Vitamin D3 and dietary Ca2+. *J Steroid Biochem Mol Biol*, 2004. 89-90(1-5): p. 303-8.

233. Moreau R, Daoud G, Bernatchez R, Simoneau L, Masse A, and Lafond J: Calcium uptake and calcium transporter expression by trophoblast cells from human term placenta. *Biochim Biophys Acta*, 2002. 1564(2): p. 325-32.

234. Suzuki Y, Kovacs CS, Takanaga H, Peng JB, Landowski CP, and Hediger MA: Calcium channel TRPV6 is involved in murine maternal-fetal calcium transport. *J Bone Miner Res*, 2008. 23(8): p. 1249-56.

235. Irnaten M, Blanchard-Gutton N, and Harvey BJ: Rapid effects of 17beta-estradiol on epithelial TRPV6 Ca2+ channel in human T84 colonic cells. *Cell Calcium*, 2008. 44(5): p. 441-52.

236. Lieben L, Benn BS, Ajibade D, Stockmans I, Moermans K, Hediger MA, Peng JB, Christakos S, Bouillon R, and Carmeliet G: Trpv6 mediates intestinal calcium absorption during calcium restriction and contributes to bone homeostasis. *Bone*. 47(2): p. 301-8.

237. Kutuzova GD, Sundersingh F, Vaughan J, Tadi BP, Ansay SE, Christakos S, and Deluca HF: TRPV6 is not required for 1alpha,25-dihydroxyvitamin D3-induced intestinal calcium absorption in vivo. *Proc Natl Acad Sci U S A*, 2008. 105(50): p. 19655-9.

238. Wang X and Zhou B: Dietary zinc absorption: A play of Zips and ZnTs in the gut. *IUBMB Life*, 2010. 62(3): p. 176-82.

239. Dufner-Beattie J, Wang F, Kuo YM, Gitschier J, Eide D, and Andrews GK: The acrodermatitis enteropathica gene ZIP4 encodes a tissue-specific, zinc-regulated zinc transporter in mice. *J Biol Chem*, 2003. 278(35): p. 33474-81.

240. Wang K, Zhou B, Kuo YM, Zemansky J, and Gitschier J: A novel member of a zinc transporter family is defective in acrodermatitis enteropathica. *Am J Hum Genet*, 2002. 71(1): p. 66-73.
241. Yu YY, Kirschke CP, and Huang L: Immunohistochemical analysis of ZnT1, 4, 5, 6, and 7 in the mouse gastrointestinal tract. *J Histochem Cytochem*, 2007. 55(3): p. 223-34.
242. Qiu A and Hogstrand C: Functional characterisation and genomic analysis of an epithelial calcium channel (ECaC) from pufferfish, Fugu rubripes. *Gene*, 2004. 342(1): p. 113-23.
243. Hogstrand C, Verbost PM, Bonga SE, and Wood CM: Mechanisms of zinc uptake in gills of freshwater rainbow trout: interplay with calcium transport. *Am J Physiol*, 1996. 270(5 Pt 2): p. R1141-7.
244. Qiu A, Glover CN, and Hogstrand C: Regulation of branchial zinc uptake by 1alpha,25-(OH)(2)D(3) in rainbow trout and associated changes in expression of ZIP1 and ECaC. *Aquat Toxicol*, 2007. 84(2): p. 142-52.
245. Lu P, Boros S, Chang Q, Bindels RJ, and Hoenderop JG: The beta-glucuronidase klotho exclusively activates the epithelial Ca2+ channels TRPV5 and TRPV6. *Nephrol Dial Transplant*, 2008. 23(11): p. 3397-402.
246. Bertolo RF, Bettger WJ, and Atkinson SA: Calcium competes with zinc for a channel mechanism on the brush border membrane of piglet intestine. *J Nutr Biochem*, 2001. 12(2): p. 66-72.
247. Peng JB, Chen XZ, Berger UV, Weremowicz S, Morton CC, Vassilev PM, Brown EM, and Hediger MA: Human calcium transport protein CaT1. *Biochem Biophys Res Commun*, 2000. 278(2): p. 326-32.
248. Blanchard RK, Moore JB, Green CL, and Cousins RJ: Modulation of intestinal gene expression by dietary zinc status: effectiveness of cDNA arrays for expression profiling of a single nutrient deficiency. *Proc Natl Acad Sci U S A*, 2001. 98(24): p. 13507-13.
249. Bhutta ZA, Bird SM, Black RE, Brown KH, Gardner JM, Hidayat A, Khatun F, Martorell R, Ninh NX, Penny ME, Rosado JL, Roy SK, Ruel M, Sazawal S, and Shankar A: Therapeutic effects of oral zinc in acute and persistent diarrhea in

children in developing countries: pooled analysis of randomized controlled trials. *Am J Clin Nutr*, 2000. 72(6): p. 1516-22.

250. Berni Canani R, Buccigrossi V, and Passariello A: Mechanisms of action of zinc in acute diarrhea. *Curr Opin Gastroenterol*, 2011. 27(1): p. 8-12.

251. Berni Canani R, Secondo A, Passariello A, Buccigrossi V, Canzoniero LM, Ruotolo S, Puzone C, Porcaro F, Pensa M, Braucci A, Pedata M, Annunziato L, and Guarino A: Zinc inhibits calcium-mediated and nitric oxide-mediated ion secretion in human enterocytes. *Eur J Pharmacol*. 626(2-3): p. 266-70.

252. Lehen'kyi V, Beck B, Polakowska R, Charveron M, Bordat P, Skryma R, and Prevarskaya N: TRPV6 is a Ca2+ entry channel essential for Ca2+-induced differentiation of human keratinocytes. *J Biol Chem*, 2007. 282(31): p. 22582-91.

253. Grynkiewicz G, Poenie M, and Tsien RY: A new generation of Ca2+ indicators with greatly improved fluorescence properties. *J Biol Chem*, 1985. 260(6): p. 3440-50.

254. Simons TJ: Measurement of free Zn2+ ion concentration with the fluorescent probe mag-fura-2 (furaptra). *J Biochem Biophys Methods*, 1993. 27(1): p. 25-37.

255. Sensi SL, Yin HZ, Carriedo SG, Rao SS, and Weiss JH: Preferential Zn2+ influx through Ca2+-permeable AMPA/kainate channels triggers prolonged mitochondrial superoxide production. *Proc Natl Acad Sci U S A*, 1999. 96(5): p. 2414-9.

256. Hamill OP, Marty A, Neher E, Sakmann B, and Sigworth FJ: Improved patch-clamp techniques for high-resolution current recording from cells and cell-free membrane patches. *Pflugers Arch*, 1981. 391(2): p. 85-100.

257. Bödding M: Voltage-dependent changes of TRPV6-mediated Ca2+ currents. *J Biol Chem*, 2005. 280(8): p. 7022-9.

258. White MM and Aylwin M: Niflumic and flufenamic acids are potent reversible blockers of Ca2(+)-activated Cl- channels in Xenopus oocytes. *Mol Pharmacol*, 1990. 37(5): p. 720-4.

259. Zhu G, Zhang Y, Xu H, and Jiang C: Identification of endogenous outward currents in the human embryonic kidney (HEK 293) cell line. *J Neurosci Methods*, 1998. 81(1-2): p. 73-83.

260. Zalewski PD: Zinc metabolism in the airway: basic mechanisms and drug targets. *Curr Opin Pharmacol*, 2006. 6(3): p. 237-43.
261. Laskay G, Kálmán K, Van Kerkhove E, Steels P, and Ameloot M: Store-operated Ca2+-channels are sensitive to changes in extracellular pH. *Biochem Biophys Res Commun*, 2005. 337(2): p. 571-9.
262. Naseem R, Holland IB, Jacq A, Wann KT, and Campbell AK: pH and monovalent cations regulate cytosolic free Ca(2+) in E. coli. *Biochim Biophys Acta*, 2008. 1778(6): p. 1415-22.
263. Chen XH, Bezprozvanny I, and Tsien RW: Molecular basis of proton block of L-type Ca2+ channels. *J Gen Physiol*, 1996. 108(5): p. 363-74.
264. Ankorina-Stark I, Haxelmans S, Hirsch JR, Lohrmann E, and Schlatter E: Ca2+ entry in isolated rat cortical collecting duct is pH- and voltage sensitive. *Cell Physiol Biochem*, 1997. 7: p. 333-44.
265. Sutton RA, Wong NL, and Dirks JH: Effects of metabolic acidosis and alkalosis on sodium and calcium transport in the dog kidney. *Kidney Int*, 1979. 15(5): p. 520-33.
266. Dipolo R and Beaugé L: The effect of pH on Ca2+ extrusion mechanisms in dialyzed squid axons. *Biochim Biophys Acta*, 1982. 688(1): p. 237-45.
267. Polo-Parada L and Korn SJ: Block of N-type calcium channels in chick sensory neurons by external sodium. *J Gen Physiol*, 1997. 109(6): p. 693-702.
268. Ma W, Korngreen A, Weil S, Cohen EB, Priel A, Kuzin L, and Silberberg SD: Pore properties and pharmacological features of the P2X receptor channel in airway ciliated cells. *J Physiol*, 2006. 571(Pt 3): p. 503-17.
269. Kunzelmann K and Mall M: Pharmacotherapy of the ion transport defect in cystic fibrosis. *Clin Exp Pharmacol Physiol*, 2001. 28(11): p. 857-67.
270. Min KS, Ueda H, Kihara T, and Tanaka K: Increased hepatic accumulation of ingested Cd is associated with upregulation of several intestinal transporters in mice fed diets deficient in essential metals. *Toxicol Sci*, 2008. 106(1): p. 284-9.
271. Min KS, Ueda H, and Tanaka K: Involvement of intestinal calcium transporter 1 and metallothionein in cadmium accumulation in the liver and kidney of mice fed a low-calcium diet. *Toxicol Lett*, 2008. 176(1): p. 85-92.

272. Bodding M and Flockerzi V: Ca2+ dependence of the Ca2+-selective TRPV6 channel. *J Biol Chem*, 2004. 279(35): p. 36546-52.
273. Yue L, Peng JB, Hediger MA, and Clapham DE: CaT1 manifests the pore properties of the calcium-release-activated calcium channel. *Nature*, 2001. 410(6829): p. 705-9.
274. Venkatachalam K and Montell C: TRP channels. *Annu Rev Biochem*, 2007. 76: p. 387-417.
275. Gwanyanya A, Amuzescu B, Zakharov SI, Macianskiene R, Sipido KR, Bolotina VM, Vereecke J, and Mubagwa K: Magnesium-inhibited, TRPM6/7-like channel in cardiac myocytes: permeation of divalent cations and pH-mediated regulation. *J Physiol*, 2004. 559(Pt 3): p. 761-76.
276. Yeh BI, Kim YK, Jabbar W, and Huang CL: Conformational changes of pore helix coupled to gating of TRPV5 by protons. *EMBO J*, 2005. 24(18): p. 3224-34.
277. Magistretti J, Castelli L, Taglietti V, and Tanzi F: Dual effect of Zn2+ on multiple types of voltage-dependent Ca2+ currents in rat palaeocortical neurons. *Neuroscience*, 2003. 117(2): p. 249-64.
278. Hu H, Bandell M, Petrus MJ, Zhu MX, and Patapoutian A: Zinc activates damage-sensing TRPA1 ion channels. *Nat Chem Biol*, 2009. 5(3): p. 183-90.
279. Hamilton DL and Smith MW: Inhibition of intestinal calcium uptake by cadmium and the effect of a low calcium diet on cadmium retention. *Environ Res*, 1978. 15(2): p. 175-84.
280. Uetani M, Kobayashi E, Suwazono Y, Okubo Y, Kido T, and Nogawa K: Investigation of renal damage among residents in the cadmium-polluted Jinzu River basin, based on health examinations in 1967 and 1968. *Int J Environ Health Res*, 2007. 17(3): p. 231-42.

10. Publication list

10.1. Publications related to the thesis

Dankó T, Hargitai D, Pataki A, Hakim H, Molnar M, and Zsembery A: Extracellular alkalinization stimulates calcium-activated chloride conductance in cystic fibrosis human airway epithelial cells. *Cell Physiol Biochem*, 2011. 27(3-4): p. 401-10.

IF: 3.585

Kovacs G, **Dankó T**, Bergeron MJ, Balazs B, Suzuki Y, Zsembery A, and Hediger MA: Heavy metal cations permeate the TRPV6 epithelial cation channel. *Cell Calcium*, 2011. 49(1): p. 43-55.

IF: 3.553

10.2. Publications not related to the thesis

Hargitai D, Pataki A, Raffai G, Füzi M, **Dankó T**, Csernoch L, Várnai P, Szigeti GP, and Zsembery A: Calcium entry is regulated by Zn2+ in relation to extracellular ionic environment in human airway epithelial cells. *Respir Physiol Neurobiol*, 2010. 170(1): p. 67-75.

IF: 2.382

11. Acknowledgement

First of all, I would like to thank my supervisor Dr. Ákos Zsembery for his guidance throughout the course of my work.

I am thankful to Professor Márk Kollai and Professor Zoltán Benyó for providing me the opportunity to work at the Institute of Human Physiology and Clinical Experimental Research. I also would like to express my gratitude to all the members of the Institute for their help.

I am also thankful to our collaborators, Dr. Gergely Kovács and Professor Matthias A. Hediger (Bern, Switzerland).

I would like to acknowledge to all of my former colleagues in the Department of Pathophysiology, especially Dr. Miklós Molnár for initiating my scientific carrier.

Finally, special thanks to my family for their love, encouragement and support.